

# The Adhesion of Modified Epoxides to Fibers

*Gorbatkina Yulia Arkadievna*

*Ivanova-Mumzhieva Viktoria Georgievna*

# The Adhesion of Modified Epoxides to Fibers



# The Adhesion of Modified Epoxides to Fibers

By

Gorbatkina Yulia Arkadievna and  
Ivanova-Mumzhieva Viktoria Georgievna

**Cambridge**  
**Scholars**  
Publishing



The Adhesion of Modified Epoxides to Fibers

By Gorbatkina Yulia Arkadievna and  
Ivanova-Mumzhieva Viktoria Georgievna

This book first published 2022

Cambridge Scholars Publishing

Lady Stephenson Library, Newcastle upon Tyne, NE6 2PA, UK

British Library Cataloguing in Publication Data  
A catalogue record for this book is available from the British Library

Copyright © 2022 by Gorbatkina Yulia Arkadievna and  
Ivanova-Mumzhieva Viktoria Georgievna

All rights for this book reserved. No part of this book may be reproduced, stored in a retrieval system, or transmitted, in any form or by any means, electronic, mechanical, photocopying, recording or otherwise, without the prior permission of the copyright owner.

ISBN (10): 1-5275-8250-7

ISBN (13): 978-1-5275-8250-7

The monograph is focused on controlling interfacial strength, which is one of the substantial problems of the science of adhesion. The subject of discussion is the interfacial strength in adhesive joints in which the substrates are various fibers and the adhesives are epoxy resins modified with active diluents, rigid-chain thermoplastics, or fine fillers (in particular, nanosized fillers). The change in adhesive strength during the formation of joints (during curing) and under various operating conditions is studied. The dependence of adhesive strength on the introduced plasticizer concentration is analyzed. The existence of synergism of interfacial strength is shown; the factors responsible for the occurrence of the synergism are analyzed; the mechanisms controlling the synergism in the case of using various types of modifiers are revealed. Using the example of the activities of the adhesion research group of the Laboratory of Reinforced Plastics of Semenov Institute of Chemical Physics of the Russian Academy of Sciences, a brief historical review of the origin, development, and formation of a new direction in the science of adhesion—adhesion of polymers to fibers—is given.

The book is intended for a wide audience: researchers, teachers, students, masters, postgraduate students, and all those who are engaged in studying the surface phenomena, the physics and chemistry of polymers (primarily, epoxy resins), and the design and application of composite materials.



# TABLE OF CONTENTS

Preface .....	x
Introduction .....	xiii
List of Abbreviations .....	xviii
Principal Symbols.....	xix
Chapter One.....	1
Effect of the Nature and Amount of the Modifier on the Adhesive Strength of Epoxy–Resin Joints	
1.1. Adhesion of Epoxy Resins Modified with Active Diluents	
1.2. Adhesion of Epoxy Resins Modified with Heat-Resistant Thermoplastics	
1.3. Adhesion of Epoxy Resins Modified with Fine Mineral Fillers	
1.4. Adhesion of Epoxy Oligomers to Low-Surface Energy Solids (Materials)	
Chapter Two .....	42
Curing-Induced Changes in the Adhesion Properties of Epoxy Oligomers Modified with Thermoplastics	
Chapter Three .....	54
Adhesive Strength of Fiber–Modified Epoxy Matrix Joints under Operating Conditions	
3.1. Effect of Test Temperature	
3.2. Effect of Loading Rate on the Interfacial Strength of Fiber–Modified Epoxy Matrix Joints	
3.2.1. Interfacial Strength in Fiber–Active Diluent-Modified Epoxy Resin Systems under Quasi-Static Loading	
3.2.2. Interfacial Strength in Fiber–Heat-Resistant Thermoplastic-Modified Epoxy Resin Systems under Quasi-Static Loading and a Low-Speed Impact	



3.3. Effect of Liquid Medium on the Interfacial Strength of Polymer–Fiber Joints	
3.3.1. Changes in Adhesive Strength during Storage of Fiber–Epoxy Binder Joints in Water	
3.3.2. Strength of Polymer–Fiber Joints in Tests in Liquid Media	
3.3.2.1. Loading of Fiber–Epoxy Resin and Fiber–Heat-Resistant Thermoplastic Joints in a Liquid	
3.3.2.2. Loading of Fiber–Epoxy Resin +PSF Matrix Joints in a Liquid	
Chapter Four.....	98
Further Development of the Pull-Out Method	
4.1. On the Interpretation of Results Obtained in Studying the Adhesion of Polymers to Fibers of Different Diameters by the Pull-Out Method	
4.2. Use of Scale Dependences and Variance of Adhesive Strength in Studying the Failure of Polymer–Fiber Joints	
4.3. Electron Microscopic Study of Crack Formation and Propagation at the Binder–Fiber Interface	
In Lieu of an Afterword.....	127
Development of Studies on Adhesion at the Laboratory of Reinforced Plastics of Semenov Institute of Chemical Physics of the Russian Academy of Sciences	
Appendices .....	140
A1. Determination of the Adhesive Strength of Joints Composed of an Epoxy Matrix and a Steel Wire with a Diameter of $d \geq 100 \mu\text{m}$	
A2. Preparation of Epoxy Resin–Heat-Resistant Thermoplastic Compositions	
A3. Preparation of Epoxy Resin–Fine Filler Compositions	
A4. Measurement of the Surface Tension of Liquid Epoxy Resins	
A5. Determination of the Wettability of Cured Epoxy Resins Modified with Fluorine Compounds	
A6. Measurement of Viscosity and Contact Angles	
A7. Curing Process Investigation Procedure	
A8. Measurement of Residual Stresses	
A9. Measurement of the Temperature Dependence of the Adhesive Strength of Joints Composed of an Epoxy Matrix and a Steel Wire with a Diameter of $d \geq 100 \mu\text{m}$	
A10. Impact Loading	

References .....	151
Authors Previous Publications.....	171

## PREFACE

An extensive use of polymer composite materials, in particular, fiber-reinforced plastics, in the middle of the last century has given an impetus to the formation and rapid development of a new direction in the science of adhesion—adhesion of polymers to fibers. The use of these materials in various fields of industry and technology has been increasing every year and thereby has caused an acute necessity in the development of a scientific basis for designing composite materials.

It soon became clear that the properties of fibrous composites and their failure are determined not only by the properties of reinforcing fibers and polymer matrices, but also by the processes that occur at the fiber–matrix interface, because interfacial strength determines the possibility of stress transfer across the interface, i.e., the efficiency of using the strength of the reinforcing (fibrous) filler. To design composites with desired properties and predict changes in these properties, it was necessary to know the behavior of the adhesive strength of the components and the interfacial strength under respective conditions.

A fiber, together with the adjacent polymer layer, constitutes the unit cell of any fiber-reinforced plastic. It was these cells (or rather their models) that began to be used to determine the adhesive strength between the components of fibrous composites.

An adhesive joint is formed on the surface of a fiber immersed into an adhesive layer. The geometry of the joint is characterized by length  $l$ , which is determined by the polymer layer thickness, and area  $S$ :

$$S = \pi dl,$$

where  $d$  is the fiber diameter. The  $S$  values generally do not exceed a few square millimeters.

In the 1960s through to the 1980s, adhesion of polymers to fibers was studied in the United States, the Soviet Union, France, Finland, and—later—in Israel and Germany. At that time, an experimental and technical base for measuring the adhesive strength in polymer–fiber joints was largely founded. In those joints, the substrate was fiber segments, i.e., cylindrical objects with a small diameter (7–200  $\mu\text{m}$ ).

These "microjoints" differ from other adhesive joints in the shape and size of the specimens. It is their geometry that leads to the fact that the techniques, devices, and facilities required for preparing and testing these

joints differ from the respective techniques used to test conventional adhesive joints, in which the substrates are generally flat or slightly curved surfaces with an area of a few tens and a few hundreds of square millimeters.

It should be noted that the foundation of an experimental base for measuring the adhesive strength in fibrous filler–binder systems is a constantly evolving process. The chronology of its development coincides with the chronology of the emergence of new types of fibers and binders.

The development of methods for measuring the adhesive strength ( $\tau$ ) in polymer–fiber systems was accompanied by the accumulation of knowledge about the  $\tau$  value of various pairs and the laws governing changes in adhesive strength under various conditions for the formation and failure of joints.

This knowledge was primarily required for those who were engaged in the design and use of fibrous composite materials. For engineers and technologists, it was necessary to compare the  $\tau$  values of different pairs and know how the interfacial strength changes with a change in the temperature–time conditions for the formation of composites and in the operating conditions (with a change in temperature, loading conditions, storage, etc.). Therefore, of all the numerous factors affecting adhesive strength, those that should be known to design required materials were studied first.

As noted above, adhesion of polymers to fibers was studied in many countries; however, the studies conducted at Semenov Institute of Chemical Physics of the USSR Academy of Sciences were particularly regular and systematic. The results obtained by the early 1990s were described in two monographs:

1. Yu. A. Gorbatkina, *Adgezionnaya prochnost' v sisteme polimer- volokno*, Moscow, Khimiya, 1987.
2. Yu. A. Gorbatkina, *Adhesive Strength of Fibre–Polymer Systems*, New York–London–Toronto, Ellis Horwood, 1992.

The second book is a revised and expanded version of the first book. In particular, a chapter on adhesion of linear polymers (polyolefins and heat-resistant linear polymers, such as polysulfones, polyethersulfones, polyetherimides, and polyarylene ether ketones) to fibers was specially written for the second book. To the best of our knowledge, those two monographs still remain the only books entirely focused on the description of the basic laws governing the change in adhesive strength in joints where the substrates are fibers.

This book is a logical continuation of the two above books. It represents results obtained in studying the adhesive strength of joints composed of a fiber and a binder based on modified epoxy oligomers at the same Laboratory of Reinforced Plastics of Semenov Institute of Chemical Physics of the Russian Academy of Sciences.

The studies were conducted in collaboration with a number of institutions; the authors sincerely thank all those who participated in the studies. The authors are especially grateful to Prof. M.L. Kerber and Prof. I.Yu. Gorbunova (Chair of Technology for Processing Plastics and Elastomers, Mendeleev University of Chemical Technology of Russia). The authors also sincerely thank all those whose work and knowledge contributed to the appearance of this book.

# INTRODUCTION

This monograph is focused on studying the adhesion of modified epoxy resins to fibers. In the past two decades, these polymers have been used to design reinforced plastics exhibiting not only high strength and rigidity, but also high fracture toughness (crack resistance), impact resistance, and fairly high post-impact properties. Therefore, in those years, the structure and properties of modified epoxy matrices and composites based on them have been intensively studied.

Since epoxy resins are characterized by an advantageous combination of physicommechanical, dielectric, and chemical properties, they are commonly used in industry, in particular, in the production of reinforced plastics, adhesives, and casting compounds. However, epoxy resins in the cured state are fairly fragile substances. To eliminate this disadvantage and have the possibility of designing structural materials based on epoxy matrices with a desired set of properties, various modifiers (polymers, monomers, fine powders, etc.) are introduced into epoxy oligomers.

Until recently, the problem of crack resistance and impact resistance has been solved by modifying epoxy matrices with low-viscosity rubbers [1–7]. However, this method is fraught with a decrease in the strength and thermal characteristics of the composites. Recently, these problems have been solved by modifying epoxy matrices with flexible- and rigid-chain thermoplastics, dispersed fillers, and active diluents [8–24]. In the most recent years, blends of thermoplastics have also been used to this end [25–27]. The effect of various modifiers on the structure and properties of epoxy resins has been discussed in many reports. The least studied aspect of this problem is the adhesion of modified epoxy resins to solids.

The effect of the introduction of a modifier (minor component) on the interaction of epoxy resins with solids (particularly with fibers) is really an extremely important issue. The adhesive ability of modifiers is typically lower than that of epoxy resins: the adhesive strength of dispersed fillers to solids (with no pressure applied) is almost zero; the strength of the active diluent–solid interface is negligible; joints of heat-resistant rigid-chain thermoplastics with solids are significantly less durable than joints of epoxy resins with solids, even if the adhesive joints are formed under optimum temperature–time conditions (melt casting).

A natural question now arises of whether the introduction of a component with a lower (or even zero) adhesive ability into an epoxy binder will cause a significant decrease in the strength of the modified matrix–solid interface. For fiber-reinforced plastics, it is well known that this decrease leads (in the case of imperfect adhesion) to a deterioration in the physicomaterial characteristics of the composite material [28, 29].

This paper describes results that can provide an answer to the above question.

The measure of adhesion is shear adhesive strength  $\tau$ , which is determined by pulling a fiber out of a cured binder layer (pull-out method):

$$\tau = F/S,$$

where  $F$  is the force required to break the adhesive joint,  $S = \pi dl$  is the area of the joint (resin–fiber interfacial area),  $d$  is the fiber diameter, and  $l$  is the length of the adhesive joint (length of the fiber portion immersed into the polymer).

Composites, the adhesion of which is discussed, are based on epoxy oligomers ED-20 (counterpart of DGEBA) and ED-22. In most cases, measurements are conducted for model samples for which a steel wire with a diameter of 150  $\mu\text{m}$  is used as a support (substrate).

It is extremely convenient to use a high-strength steel wire as a substrate. The lengthwise wire diameter is constant with a high degree of accuracy; the area of the joints changes only with a change in their length  $l$ . The average load required to break the wire is 50 N (at a loading speed of 1 N/s). Therefore, steel fiber–epoxy binder joints typically undergo adhesive fracture, even if the area of the joints  $S$  achieves 1.5–2.0  $\text{mm}^2$  ( $l/d \geq 20$ –25). In the absence of samples that underwent cohesive fracture (along the fiber), the measurement accuracy for  $\tau$  increases, while the time required for conducting the experiment decreases. It is also significant that, using this substrate, it is possible to vary the area of the joints over the widest possible range.

The obtained joints were tested using adhesion meters designed at the Laboratory of Reinforced Plastics of Semenov Institute of Chemical Physics of the Russian Academy of Sciences; the adhesion meters provide measurements under quasistatic and dynamic loading at various temperatures and a constant rate of increase in the force applied to the

sample:  $F; \dot{F} = \text{const}; \dot{\tau} = \text{const}$ .

The sample preparation, testing, and measurement result processing procedures are described in detail in [30, 31]. Some necessary methodological details are given in the Appendices.

The  $\tau$  value determined in experiments depends on many factors. It was shown [28, 32, 33] that five of them can be considered as the main factors, namely, the energy of interfacial bonds, the number of these bonds, the interface imperfection, the value of residual stresses acting in the interfacial joint, and the structure of the near-surface (interfacial) layers.

To elucidate the effect of modification on the interfacial strength, it is necessary to analyze how each of the above factors changes upon the addition of a modifier (minor component) to epoxy resin. Accordingly, it is necessary to know these changes (measure them in experiments or determine them by some methods).

*The energy of bonds acting across the interface* is determined by the nature of the adhesive and the substrate.

*The number of interfacial bonds* is determined by the number of active sites on the substrate surface and the degree of involvement of these sites in the interaction with the adhesive. The last-mentioned parameter depends on the degree of wetting of the substrate by the adhesive. The higher the number of discontinuities, various defects, and air bubbles arising from interfacial wetting, the smaller the number of active sites capable of interacting with the adhesive.

*Interface imperfection* is also primarily determined by the ability of the adhesive to wet the substrate. Defects arising from poor interfacial wetting of the formed joint subsequently (upon loading) become stress concentrators, i.e., a source of decrease in the adhesive strength. Thus, from this point of view, a high degree of wetting is a necessary condition for a high interfacial strength.

*The residual stresses acting at the fiber-polymer interface* arise during the formation of the joint and the subsequent cooling of it from the formation (curing) temperature to test temperature  $T$ . They depend on the difference in the mechanical and thermal characteristics of the adhesive couple components and on the difference between the test temperature  $T$  and the glass transition temperature of the adhesive  $T_g$ , i.e., to a first approximation, on the  $\Delta T = T_g - T$  value.

*The structure of near-surface layers* determines the mechanisms of nucleation, development, and propagation of defects (cracks) responsible for the fracture of adhesive joints and, accordingly, for their interfacial strength. The structure of a polymer adhesive in the bulk and in the layers adjacent to the interface is formed during curing. In this case, one of the main questions is whether the structure of the adhesive after curing is single-phase or heterophase.



It is clear from the above that, to elucidate the dependence of the factors that determine the measured  $\tau$  value on the nature and amount of the modifier, it is necessary to study a number of characteristics of the adhesive in the liquid state, during curing, and in the solid state (after curing). It is necessary to know how the modification affects the equilibrium contact angles, which characterize the wetting ability of the adhesive; the rheological characteristics of the adhesive before and during curing, i.e., primarily, the temperature–time and concentration dependences of viscosity; the glass transition temperature of the adhesive; and the behavior of the  $\sigma$ – $\epsilon$  diagrams. These parameters can be used to determine the magnitudes of the elastic moduli, which are required for estimating the residual stresses, and detect the development of inelastic (particularly plastic) deformations in the matrix upon the addition of a modifier, data on which make it possible to discuss the fracture process in the matrices and their adhesive joints. In addition, it is necessary to know changes in the thermal expansion coefficients, which are also used in the assessment of residual stresses, and changes in the structure of the blend matrix upon the addition of a minor component. To reveal the last-mentioned changes, it is necessary to study the absorbance during curing, construct phase diagrams, and subject the structure to electron microscopy and X-ray diffraction analyses.

To the best of our knowledge, the full-range studies have not been performed for any system. The studies of the adhesion of polysulfone-modified epoxy resins were the fullest, the closest to the "ideal."

The following can be added to the above. The main aim of modification of epoxy matrices is the formation of composites with improved physicommechanical characteristics, in particular, with a higher impact resistance and crack resistance. Therefore, it is only natural that studies of the properties of matrices and the fiber–matrix interface should be combined with studies of the properties of composites based on these matrices. Only in this case it is possible to determine whether the selected type of modification is advantageous. The determination of correlations between the properties of composites and the properties of matrices (bulk and surface) provides a targeted control of the properties of the composites. This means that the studies mentioned above should be supplemented by a study of the physicommechanical characteristics of composites based on blend matrices.

However, this range of issues is beyond the scope of this manuscript, in which we confine ourselves to the description of the effect of modification on the interfacial strength and the mechanisms governing the changes caused by the modification.

These issues are discussed in Chapters 1–3. In addition, Chapter 4 describes results on the further development of the pull-out method, which is the main method used to study the interfacial strength in polymer–fiber joints.

## LIST OF ABBREVIATIONS

CNT - carbon nanotubes  
DADPS - 4,4'-diaminodiphenyl sulphone  
DMA - dynamic mechanical analysis  
DMAA - dimethylacetamid  
GEG - diethylene glycol  
FS - fluorinated surfactants  
FCNT - functionalized CNT  
PAEK - polyarylene ether ketone  
PSK - polysulphone adhesive  
PS - polysulphone  
PEI - polyetherimide  
PEPA - polyethylene polyamine  
TEAT - triethanolamine titanate  
ShF - shungite filler

## PRINCIPAL SYMBOLS

- A – surface activity of surfactants  
C – the amount of injected modifier (relative to the weight of resin)  
(concentration)  
d – fibre diameter (substrate)  
D – dispersion of adhesive strength value  
E<sub>ben</sub> – modulus of elasticity under bending  
E<sub>t</sub> – tensile modulus  
F – force required to break an adhesive joint  
G – polymer shear modulus  
k – sensitivity of the interface to the rate of application of an external load  
K – relative sensitivity of the interface to the rate of application of an  
external load  
l – adhesive joint length  
MM – molecular mass  
n – total number of test specimens  
n<sub>τ</sub> – number of joints fractured adhesively  
n<sub>σ</sub> – number of joints fractured cohesively  
Q – heat flow  
r – radius of the fibre, the adhesion of which is determined by  
S – area of adhesive joint  
S<sub>sp</sub> – specific surface area of dispersed fillers  
t<sub>c</sub> – time of cure  
t<sub>f</sub> – time during which adhesion joints are fabricated  
T<sub>f</sub> – temperature at which adhesive joints are fabricated  
W – water absorption  
α – coefficient of linear expansion  
α<sub>h</sub> – degree of resin hardening  
β – conversion of reactive groups  
G<sub>m</sub> – maximum adsorption of surfactant  
H<sub>l</sub> – limiting surfactant adsorption  
η<sub>red</sub> – reduced viscosity  
θ – contact angle  
ρ – substance density  
σ – surface tension of polymers

$\sigma_c$  – composite strength

$\sigma_{res}$  – residual stress

$\tau$  – shear adhesive strength in fibre-polymer system

$\tau_0$  – adhesion strength of control joints (not exposed to the test factor)

$\tau_t$  – adhesion strength of joints that have been in a liquid for a time  $t$

$\tau_T$  – temperature residual stresses

$\tau_{loc}$  – local adhesive strength

$\tau_{res}$  – residual stresses acting at the polymer-fibre interface

$\tau_{exp}$  – experimentally measured adhesive strength

# CHAPTER ONE

## EFFECT OF THE NATURE AND AMOUNT OF THE MODIFIER ON THE ADHESIVE STRENGTH OF EPOXY–FIBER JOINTS

### *1.1. Adhesion of Epoxy Resins Modified with Active Diluents*

Epoxy oligomers are modified with active diluents to decrease the viscosity, improve the processing characteristics of the original (liquid) compositions and increase the elasticity of the cured resins.

The commonly used active diluents are aliphatic epoxy resins, i.e., glycidic esters of polyhydric alcohols characterized by a low molecular mass, a high content of epoxy groups, and a low viscosity. They are involved in the formation of epoxy oligomers and included in their structure.

Let us consider how the adhesive ability of the ED-20 epoxy oligomer changes after modifying it with diethylene glycol diglycidyl ether DEG-1, which is a widely available and commonly used active diluent.

The variation in the strength of ED-20+triethanolamine titanate (TEAT)–steel wire joints upon the addition of DEG-1 into to the resin is shown in Fig. 1-1. Note, first of all, that the base of the studied compositions—unmodified resin ED-20—interacts with a wire to form one of the strongest (compared with other epoxy resins) interfaces (Fig. 1.1). The adhesive strength of the minor component—DEG-1—with the same wire is 30–50 times lower. However, the addition of it into the resin at concentrations of  $C \leq 50$  wt % leads to an increase in the interfacial strength, rather than to a decrease in it: the  $\tau$ – $S$  curve of the ED-20+TEAT system is localized below the  $\tau$ – $S$  curves of the ED-20+TEAT+DEG-1 systems for joints of all sizes. Figure 1.1 shows this effect for an adhesive containing 50 wt % DEG-1. (All adhesive strength values given in this chapter were obtained at room temperature and a loading rate of  $\dot{F} = 1$  N/s).

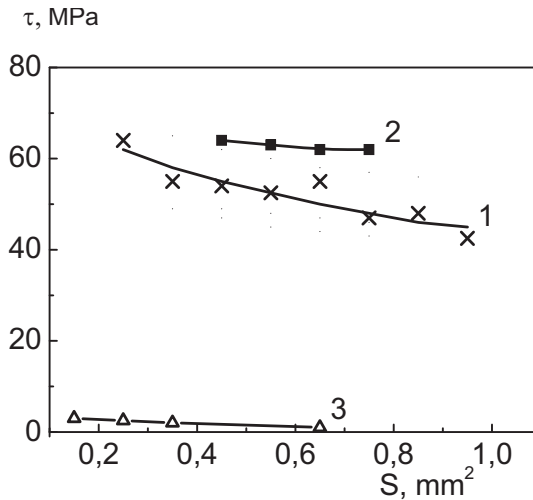


Fig. 1-1. Dependence of adhesive strength  $\tau$  on the area of joints  $S$  for ED-20+TEAT+DEG-1-steel wire systems ( $d = 150 \mu\text{m}$ ) at various DEG-1 concentrations in the matrix ( $C$  (%): (1) 0, (2) 50, and (3) pure DEG-1). Data on plotting the  $\tau$ - $S$  curves are given in A1.

The same figure (Fig. 1-1) clearly shows that the  $\tau$  values depend on the size of the joint; they monotonously and nonlinearly decrease with increasing  $S$ . This decrease in  $\tau$  is a common phenomenon. It is observed for joints of thermosetting and thermoplastic polymers with fibers of any nature and any diameter, if the measurements were conducted at temperatures  $T$  below the glass transition temperature of the polymer  $T_g$ :  $T < T_g$ . It is known [30, 31, 34–46] that the behavior of the dependence represents a nonuniform distribution of tangential stresses—both external (applied) and “internal” residual (primarily thermally induced) stresses existing in the joints before their loading and, as was noted in the Introduction, arising during the preparation of the specimens and their cooling to test temperature  $T$ —at the fiber–polymer interface.

With an increase in the amount of the active diluent introduced into the matrix, the  $\tau(S)$  dependence becomes less pronounced; this relationship seems only natural. In fact, the DEG-1 diethylene glycol used to modify the epoxy matrix has a plasticization effect: the introduction of it leads to a decrease in  $T_g$  (Fig. 1-2). Since the interfacial residual stress value is proportional, to a first approximation, to  $\Delta T = T_g - T$  (in our case  $T \approx 20^\circ\text{C}$ ), with a decrease in  $T_g$ , the  $\Delta T$  value becomes lower, the residual

stresses decrease, and their distribution becomes more uniform. It is this factor that leads to a more gently sloping  $\tau$ – $S$  dependence.

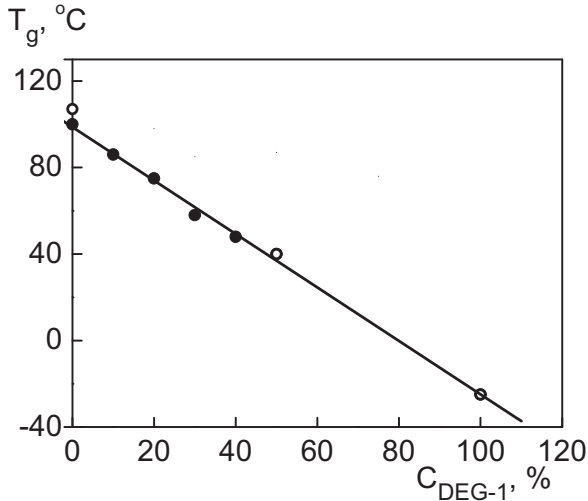


Fig. 1-2. Variation in glass transition temperature  $T_g$  after modifying the ED-20 epoxy resin with diethylene glycol diglycidyl ether DEG-1. The  $T_g$  values are determined: (•) from thermomechanical curves and (o) by the DSC method.

The concentration dependence of the adhesive strength of the studied joints (at  $l/d \geq 6$ ) is described by a curve with a weakly pronounced maximum (Fig. 1-3), which is observed at a diluent content of 40–50%. The increase in the  $\tau$  values at the maximum (relative to the adhesive strength of the unmodified resin) is 15–20%. Figure 1-3 also shows the concentration dependence recorded after introducing the DEG-1 active diluent into the ED-16 epoxy resin cured at room temperature with polyethylene polyamine (PEPA); the  $\tau$ – $C$  dependence is also described by a curve with a maximum, and the maximum is also observed at large amounts of the diluent (~40 wt %).

Thus, the plasticization of the ED-20 resin, which exhibits a high adhesive ability, with diethylene glycol, which is a component with an extremely low adhesive ability, does not decrease the adhesive strength in joints with fibers; in a certain concentration range, the plasticization even increases this parameter. In other words, upon the introduction of the DEG-1 active diluent into ED-20, the synergistic effect of adhesive strength is observed.



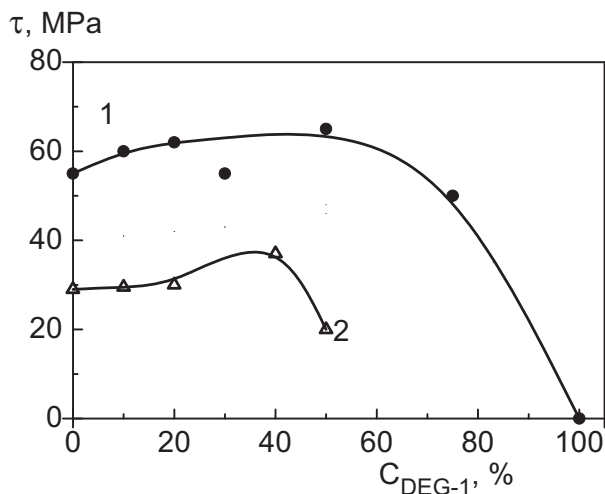


Fig. 1-3. Dependence of adhesive strength  $\tau$  of modified epoxy binder–steel wire joints ( $d = 150 \mu\text{m}$ ) on the amount of the DEG-1 active diluent:

(1) ED-20+TEAT+DEG-1 at  $S = 0.55 \text{ mm}^2$  ( $l/d \approx 7.5$ ) and

(2) ED-16+PEPA+DEG-1 at  $S = 0.95 \text{ mm}^2$  ( $l/d \approx 13$ ).

The following question now arises: what are the causes of this effect? To answer it, we will consider how factors responsible for the measured adhesive strength value change during plasticization.

DEG-1 is an active diluent capable of incorporating into the polymer chain. The use of it does not change the nature of the bonds acting at the adhesive–fiber interface. The introduction of DEG-1 leads to an extremely effective decrease in viscosity ( $\eta$ ): upon the addition of 20% DEG-1 into the ED-20 resin, the  $\eta$  values decrease by almost 2 orders of magnitude (Fig. 1-4).

A decrease in viscosity accelerates the spreading of the compositions over the surface of solids and contributes to a decrease in the interfacial imperfection. However, the wetting ability of the unmodified ED-20 resin is fairly high; for example, the equilibrium contact angles  $\theta$  formed by ED-20 on glass fibers do not exceed  $12^\circ$ . Modifying leads to as low decrease in  $\theta$  as  $2^\circ$ <sup>1</sup>. Therefore, the resin–fiber contact areas in all ED-20+TEAT+DEG-1 systems can be considered the maximum possible and

<sup>1</sup> The measurements were conducted by the Shcherbakov–Ryazantsev method [47, 48]; the  $\theta$  values were calculated from the parameters of small droplets deposited directly on the fibers.

almost identical. This means that the modifying of the ED-20 oligomer with the DEG-1 active diluent should not lead to an increase in the number of bonds established at the interface during curing and a significant decrease in the interfacial imperfection. Accordingly these factors cannot be responsible for an increase in the adhesive strength.

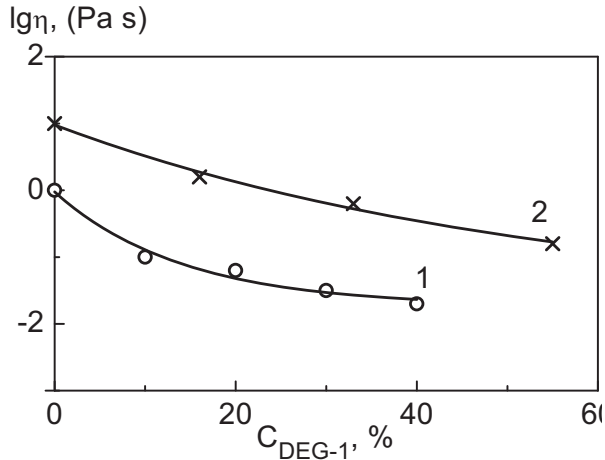


Fig. 1-4. Dependence of the logarithm of viscosity  $\lg \eta$  of epoxy compositions on amount  $C$  of the introduced active diluent: (1) ED-20+DEG-1+TEAT and (2) ED-16+DEG-1+TEAT.

The ED-20+DEG-1+TEAT systems do not undergo phase separation during curing and remain single-phase after curing at any DEG-1 concentration. This finding is evidenced by the almost linear decrease in the glass transition temperature upon the introduction of diethylene glycol into ED-20 (Fig. 1-2), the study of the thermal degradation of cured polymers [49], and the transparency of the cured specimens. Therefore, there is no reason to attribute the increase in the measured adhesive strength values to a change in the structure and properties of the near-surface layers and, hence, to a change in the failure mechanisms.

Thus, the key factor determining the change in  $\tau$  upon modifying should apparently be considered the change in the residual stresses  $\tau_{\text{res}}$  existing at the interface. As noted above, the  $\tau_{\text{res}}$  value is proportional, to a first approximation, to the difference  $\Delta T = T_g - T$ , which, in the case under consideration, where all measurements were conducted at room temperature, decreases with an increase in the amount of DEG-1 introduced into the resin. Accordingly, the  $\tau_{\text{res}}$  values should decrease, and

their distribution should become more uniform; it is these effects that were observed in experiments (Fig. 1-1).

A decrease in  $\tau_{\text{res}}$  leads to a gradual increase in the adhesive strength of the joint of the studied compositions with fibers (Fig. 1-3) to fairly large  $C$  values of  $\cong 50$  wt %.

However, a decrease (narrowing) of the  $\Delta T$  range also means that the measurement temperature approaches the glass transition temperature of the binder, while the adhesive strength decreases (similar to the cohesive strength of the polymers).

When the DEG-1 content in the ED-20+DEG-1+TEAT system achieves 50 wt %, the glass transition temperature approaches room temperature. At higher DEG-1 concentrations, the compositions are in the rubberlike state and the adhesive strength values above  $T_g$  decrease by several dozen times.

Thus, upon modifying the ED-20 epoxy oligomer with the DEG-1 active diluent, the maximum in the concentration dependence of the adhesive strength arises from the plasticization of the epoxy binder. Plasticization leads to the following: first, a decrease in the interfacial residual stresses and, second, the approximation of the measurement temperature to the region of transition of the binder from the glassy state to the rubberlike state. The superposition of these two competing processes leads to the appearance of a maximum in the concentration dependence of the adhesive strength and the synergistic effect of the interfacial strength.

## ***1.2. Adhesion of Epoxy Resins Modified with Heat-Resistant Thermoplastics***

The modifying of epoxy resins with heat-resistant thermoplastics, which is commonly used at present, provides the formation of polymer blends exhibiting a high crack and impact resistance without deteriorating their heat resistance. Polysulfones (PSFs) [10–15, 50–57], polyethersulfones [16, 17, 58–60], polyether ketones [61, 62], polyetherimides (PEIs) [8, 9, 63–69], and other thermoplastics are added to epoxy resins [70–83]. The maximum amount of the introduced thermoplastic usually does not exceed 20–25%, because thermoplastics significantly increase the viscosity of epoxy compositions; at a higher content of thermoplastics in the blend, they become unprocessable.

In the initial state, rigid-chain linear polymers are solid substances that exist in the form of powders, granules, films, etc. To provide the formation of adhesive joints with solids (particularly fibers), thermoplastics should

be converted into a melt capable of wetting the surface of the substrate. Without applying pressure, this effect can be achieved only at fairly high temperatures and fairly long contact times between the adhesive and the substrate.

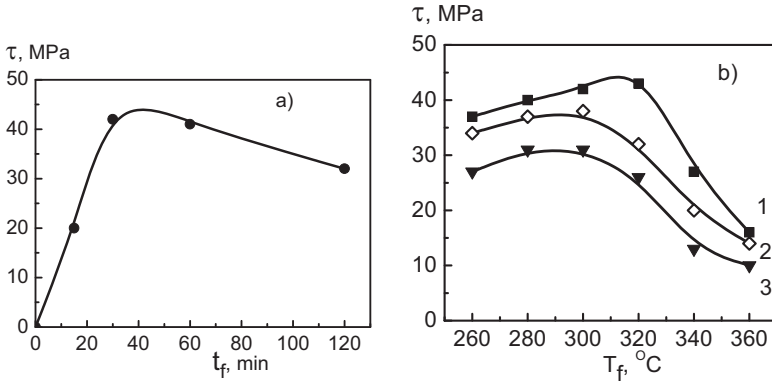


Fig. 1-5. Effect of (a) time  $t_f$  and (b) temperature  $T_f$  of formation on the adhesive strength of PSF–steel wire joints (wire diameter of  $d = 150 \mu\text{m}$ ): (a)  $T_f = 300^\circ\text{C}$  and  $S = 0.55 \text{ mm}^2$  and (b)  $t_f = 1 \text{ h}$  and  $S = (1) 0.55, (2) 0.75, (b) \text{ and } (3) 1.05 \text{ mm}^2$ .

A typical example is shown in Fig. 1-5. Here, the interfacial strength of PSF–steel wire pairs under different temperature–time conditions for the formation of adhesive joints is shown. It is evident that, for this couple, joints with maximum interfacial strengths can be formed at temperatures of 300–320°C and contact times of 30–60 min. Below 260°C, a high-quality interface (without pores and discontinuities) cannot be formed for the following reasons: a homogeneous polymer melt is not formed below this temperature; wetting, which is a necessary condition for adhesion, does not occur; and, accordingly, bonds between the fiber and the polymer are hardly formed.

In the case of using epoxy resin–PSF blends as matrices of fibrous composites, they are usually cured at temperatures of 160–200°C. In this case, fiber–epoxy resin bonds are formed at the interface; as follows from the above, fiber–PSF bonds cannot be formed. The same is true of other epoxy resin–heat-resistant thermoplastic blends (epoxy resin–PEI, epoxy resin–poly(arylene ether ketone) (PAEK), etc.).

Thus, to modify epoxy resins with rigid-chain thermoplastics, the component added to the resin should exhibit adhesive ability that is really

close to zero under the temperature–time conditions used to cure the epoxy resins.

Accordingly, to use epoxy resin–heat-resistant thermoplastic blends as binders in the production of reinforced plastics (primarily those based on continuous fibrous fillers), it was necessary to elucidate the laws governing the change in their adhesive properties during modifying and the mechanisms that control them.

Figures 1-6 and 1-7 show the effect of the modifying of epoxy resin with a typical representative of heat-resistant rigid-chain thermoplastics—PSF PSK-1—on the interfacial strength of the ED-20 resin–steel wire joints. It is evident (Fig. 1-6) that the scale dependences of the adhesive strength  $\tau$ – $S$  of epoxy resin–PSF blends are described, as usual, by monotonically descending curves. The addition of PSF leads to an increase in the interfacial strength; moreover, in the studied concentration range, the increase is nonmonotonic: the  $\tau$  values of the 5% epoxy resin–PSF blends are very close to the  $\tau$  values of the unmodified resin, and the curve describing the  $\tau$ – $S$  dependence for the blend with 20% PSK-1 is close to the curve of the 10% blend. The maximum amount (20 wt %) of the introduced modifier is limited to the viscosity of the resulting polymer blend and the possibility of preparing joints with a well-formed interface, which is associated with the viscosity.

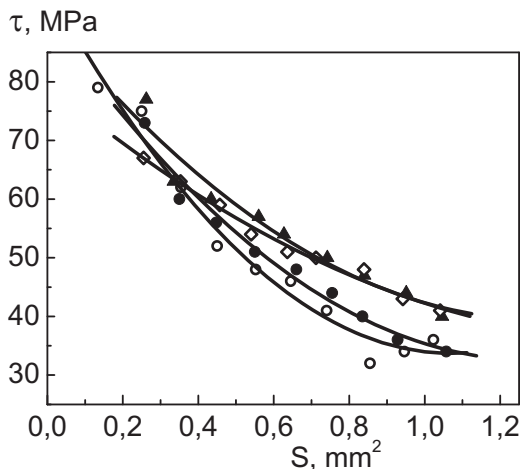


Fig. 1-6. Dependence of adhesive strength  $\tau$  on the area of joints  $S$  for ED-20+TEAT+PSK-1–steel wire systems ( $d = 150 \mu\text{m}$ ) on the PSK-1 content in the matrix ( $C$ , %): (○) 0, (●) 5, (▲) 10, and (◇) 20. Conditions for the preparation and curing of blends are given in A2.

The nonmonotonic change in adhesive strength is clearly seen in Fig. 1-7: the concentration dependences of  $\tau$  of ED-20+PSK-1+TEAT–steel wire joints are described by curves with a maximum. The behavior of the  $\tau$ – $C$  curves is almost independent of the specimen size ( $l/d \geq 6$ –8). In all the cases, a maximum is observed after the addition of 10–12% PSK-1 into the matrix; the increase in  $\tau$  values at the maximum achieves 25–40% (relative to the value of the unmodified ED-20 resin).

Thus, the addition of small amounts of rigid-chain linear PSF PSK-1 to the ED-20 epoxy resin leads to the occurrence of the synergistic effect of adhesive strength: in a certain concentration range, the adhesive ability of the resulting blend is higher than the adhesive ability of the sum of the components.

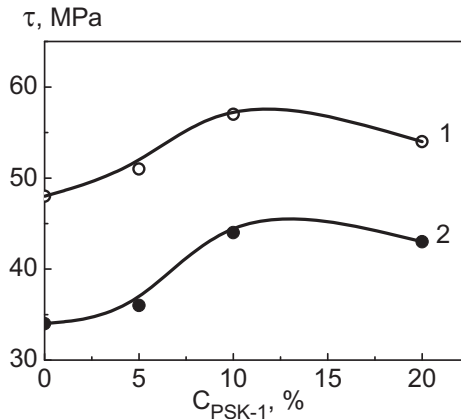


Fig. 1-7. Dependence of adhesive strength  $\tau$  in the ED-20+TEAT+PSK-1–steel wire system ( $d = 150 \mu\text{m}$ ) on the PSK-1 modifier concentration  $C$ . Area of adhesive joints  $S = (1) 0.55$  and  $(2) 0.95 \text{ mm}^2$ .

The modifying of ED-20 with PSF makes it possible to prepare binders providing the same high adhesion to fibers as in the case of modifying the resin with the DEG-1 active diluent, i.e., binders, whose adhesive ability is not inferior to that of the best epoxy compositions (see Figs. 1-1 and 1-6).

Earlier, it was repeatedly shown [28, 30, 31, 85–87] that, if the change in the adhesive strength under the action of a particular factor is determined mostly by the matrix, then the relationships established in the case of using a steel wire as a substrate are preserved for adhesion to fibers of a different chemical nature (with a high surface energy). The results obtained for the studied blends confirm these conclusions.

Figures 1-8 and 1-9 show the effect of the amount of the introduced PSF on the interfacial strength for blends interacting with glass and polyamide (capron) fibers (dependences are obtained from the  $\tau$ - $S$  curves similar to those shown in Fig. 1-6); the figures suggest that the nature of the fiber significantly affects the strength level of the resulting joints. Epoxy resin-PSF blends form extremely strong joints with glass fibers; these joints are not inferior to joints with a steel wire (if the  $\tau$  values are measured for specimens of comparable geometry, see Table 1-1). In the joints with polyamide fibers, the adhesive strength is significantly lower than that with steel and glass fibers. Apparently, this fact is attributed to the lower surface energy of capron fibers.

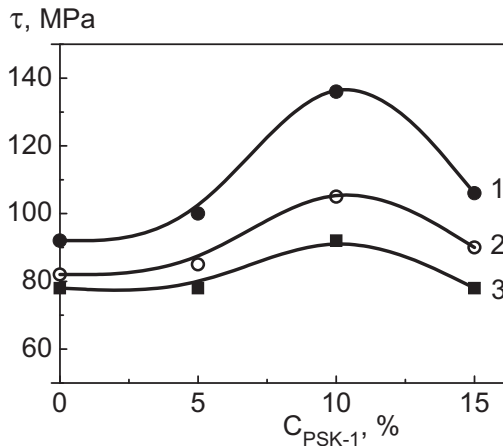


Fig. 1-8. Dependence of adhesive strength  $\tau$  in the ED-20+TEAT+PSK-1-glass fiber system ( $d = 13\text{--}30 \mu\text{m}$ ) on the PSK-1 modifier concentration  $C$ . Area of adhesive joints  $S = (1) 2 \times 10^{-3}$ , (2)  $3 \times 10^{-3}$ , and (3)  $4 \times 10^{-3} \text{ mm}^2$ . The loading rate is  $10^{-3} \text{ N/s}$ .

**Table 1-1. Geometric dimensions of the joints (at  $l/d \cong 7$ ) and the adhesive strength of the ED-20+TEAT-fiber systems**

Fibers	Fiber diameter $d, \mu\text{m}$	Length of joint $l, \mu\text{m}$	Area of joint $S, \text{mm}^2$	$\tau, \text{MPa}$
Steel	150	1000	0.55	50
Glass	$\sim 30$	200	0.01	55
Polyamide (capron)	200	1400	0.95	10

All the characteristic features observed for adhesion to steel fibers are preserved during the interaction with glass and polyamide fibers: upon the addition of PSF to ED-20, the adhesive strength in a concentration range of 5–20% increases; that is, the synergistic effect of adhesive strength occurs; the  $\tau$  values pass through a maximum, which is observed at  $C = 8–12\%$ ; the increase in adhesive strength at the maximum achieves 25–40% (Figs. 1-8 and 1-9, Table 1-2).

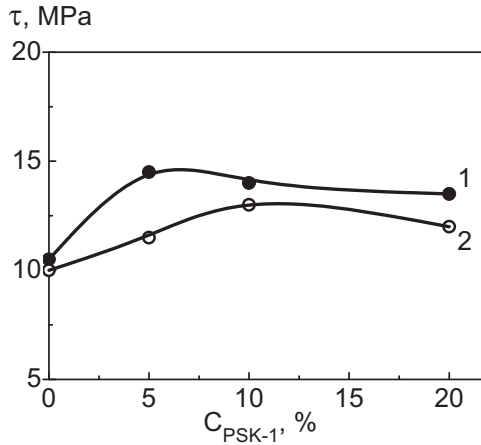


Fig. 1-9. Dependence of adhesive strength  $\tau$  in the ED-20+TEAT+PSK-1–capron fiber system ( $d = 200 \mu\text{m}$ ) on the PSK-1 modifier concentration  $C$ . Area of adhesive joints  $S = (1) 0.95$  and (2)  $1.05 \text{ mm}^2$ .

**Table 1-2. Increase in adhesive strength in the case of using epoxy resin–rigid-chain thermoplastic blends as adhesives**

Epoxy resin	Curing agent	Modifier	$C_{\text{max}}, \%^{**}$	Studied concentration range, %	$\Delta\tau/\tau_0, \%^{***}$
ED-20	TEAT	PSK-1 $M = 60\ 000$	10-12	0–25	25–40
ED-20	TEAT	Ultem-1000	15	0–15	25–30
ED-20	DADPS*	PAEK-21	15	0–15	25–35
ED-22	DADPS	PAEK-21	30	0–30	60–80
ED-22	DADPS	PAEK-22-21	30	0–30	50–80

\*Diaminodiphenyl sulfone. \*\* $C_{\text{max}}$  is the modifier concentration at which the maximum of adhesive strength  $\tau_{\text{max}}$  was obtained.

\*\*\* $\Delta\tau/\tau_0 = (\tau_{\text{max}} - \tau_0)/\tau_0$ ,  $\tau_0$  is the  $\tau$  value for joints with unmodified epoxy resin; the  $\Delta\tau/\tau_0$  value depends on the sizes of the adhesive joint.



Neither the nature of the fiber, nor the fiber diameter, nor the area of adhesive joints changes the behavior of the concentration dependence of the interfacial strength. All these data suggest that it is the matrix that is associated with the fundamental changes in the adhesive strength.

The replacement of one amine curing agent (TEAT) with another (DADPS) does not change the behavior of the concentration dependence either (see Fig. 1-10).

In the case of using compositions cured with DADPS, the interfacial strength in joints with fibers is usually slightly lower than that in joints with compositions cured with TEAT. This fact is apparently attributed to the higher level of residual stresses arising (all other conditions being equal) at the interface in the case of using more heat-resistant matrices (cured with DADPS).

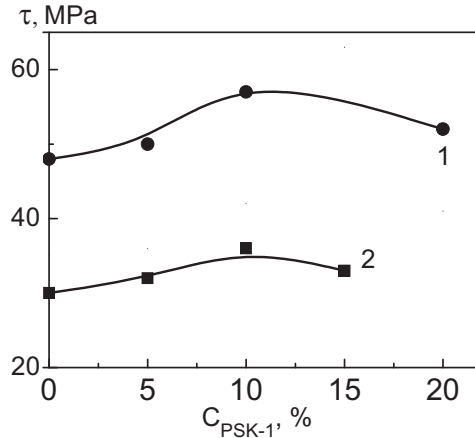


Fig. 1-10. Concentration dependences of the adhesive strength of epoxy resin+PSF-steel fiber joints ( $d = 150 \mu\text{m}$ ). Joint formation conditions:  $180^\circ\text{C}$  and 6 h. The area of the joints is  $S = 0.55 \text{ mm}^2$ . Curing agents: (1) TEAT and (2) DADPS.

However, the pattern of change in the adhesive strength of epoxy resin – PSF blends cured with DADPS remains the same: the synergism of the strength is observed, and all the main features discussed in detail above are clearly visible in analyzing the  $\tau$ – $S$  and  $\tau$ – $C$  curves. In the case of using another epoxy resin—ED-22—as the matrix component, all the laws governing the change in the interfacial strength for during the adhesion of the ED-22+PSK-1+TEAT and ED-22+PSK-1+DADPS blends to the fibers do not differ from those observed for blends based on the ED-20 oligomer (see Fig. 3-33).

Thus, not only the replacement of the nature and geometry of the substrate and one amine curing agent with another, but also the replacement of one main (epoxy) component of the matrix with another does not change the pattern of change in the adhesive strength as a function of the amount of the introduced modifier. The chemical nature of the components of the joint determines only the quantitative value of the observed effect. (Note that it is the similarity of the curves describing the dependence of interfacial strength on the studied factor that justifies the possibility of estimating the adhesion ability of polymer matrices in experiments with a steel wire, which is very methodologically convenient).

Let us now consider how the nature of the introduced thermoplastic affects the interfacial strength. Figures 1-11 and 1-12 show typical scale and concentration dependences of adhesive strength in the case of modifying the ED-20 oligomer with the Ultem 1010 PEI. The observed picture does not completely coincide with that described above for epoxy resin–PSF adhesives. Although the shape of the  $\tau$ – $S$  curves is the same as that of the PSF-modified systems (see Fig. 1-6), the higher the percentage of PEI, the higher the  $\tau$ – $S$  curves lie; are localized; that is, in the case of modifying with PEI, the adhesive strength increases monotonically. This is clearly seen in Fig. 1-12. A maximum in the concentration dependence cannot be achieved, because, upon the introduction of this modifier, the viscosity of the compositions increases so significantly that it is very difficult to obtain specimens with a well-formed interface at concentrations of  $C \geq 15$ –20 wt %.

In the case of curing the epoxy resin–PEI compositions with TEAT instead of DADPS, the adhesive strength of the modified compositions at  $C > 10$  wt % is also higher than  $\tau$  of the unmodified resin (see Fig. 1-12); that is, for the ED-20+PEI+TEAT system, the synergistic effect of adhesive strength is also observed. A maximum in the  $\tau$ – $C$  curve cannot be achieved for the same reasons as for the blends cured with DADPS. However, in the case of modifying the ED-20 resin with PEI, it can also be stated that the  $\tau$ – $C$  dependence is described by a curve with a maximum.

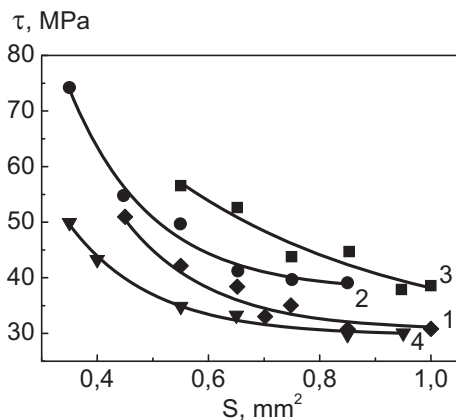


Fig. 1-11. Dependence of adhesive strength  $\tau$  on the area of joints  $S$  for the ED-20+DADPS+Ultem 1010–steel wire system ( $d = 150 \mu\text{m}$ ) at the different amounts of PEI in the matrix  $C$  (%): (1) 10, (2) 15, (3) 20, and (4) 0.

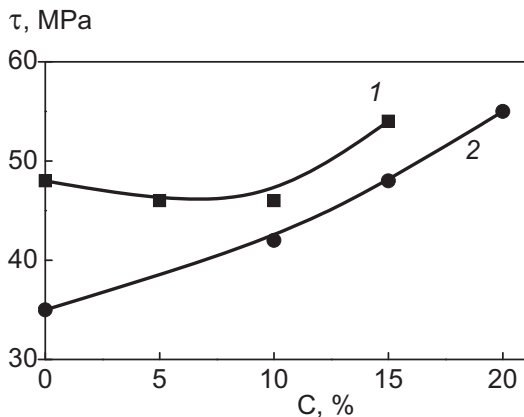


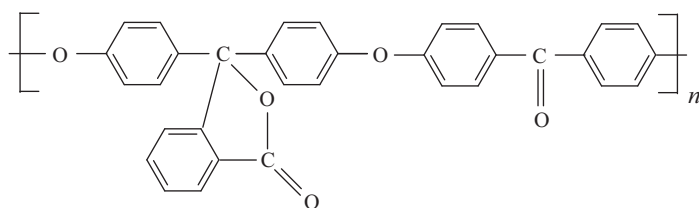
Fig. 1-12. Concentration dependences of the adhesive strength of the epoxy resin+PEI–steel wire joints ( $d = 150 \mu\text{m}$ ) at  $S = 0.55 \text{ mm}^2$ : (1) ED-20+TEAT+Ultem 1010 and (2) ED-20+DADPS+ Ultem 1010.

Apparently, the above statement holds true in all cases where the addition of a component with a lower adhesive ability than that of the modified matrix provides the occurrence of the synergistic effect of adhesive strength (it increases in a certain concentration range). In fact, at extremely high modifier concentrations, the adhesive strength will be determined by the adhesive ability of the modifier. Since this ability is

lower than that of the unmodified resin (at  $C = 0$ ), in this case, the  $\tau$ – $C$  dependence should be represented by a curve with a maximum.

The most thermostable and heat-resistant thermoplastics used to modify epoxy resins are PAEKs. These polymers with different molecular masses and chemical structures were synthesized at Nesmeyanov Institute of Organoelement Compounds of the Russian Academy of Sciences.

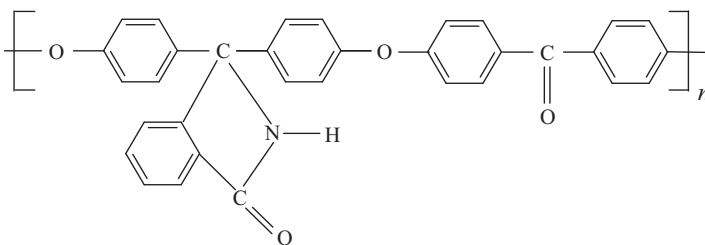
PAEK-21 is a thermoplastic transparent cardo homopolymer of dark yellow to reddish brown color, which is synthesized by the polycondensation of 4,4'-difluorobenzophenone with 3,3-bis-(4'-hydroxyphenyl)phthalide in *N,N*-dimethylacetamide (DMAA) in the presence of  $K_2CO_3$  [88, 89]:



PAEK-21

Monolithic polymer specimens in the form of film pieces with a thickness of 300–400  $\mu\text{m}$  or foamed flakes were prepared by solution casting onto a substrate. Depending on the polycondensation conditions, PAEK-21 specimens with different molecular masses were prepared. In this book, PAEK-21 specimens with different intrinsic viscosities were studied:  $\eta_{\text{int}} = 0.39 \text{ dL/g}$  (PAEK-21N) and  $\eta_{\text{int}} = 0.68 \text{ dL/g}$  (PAEK-21V).

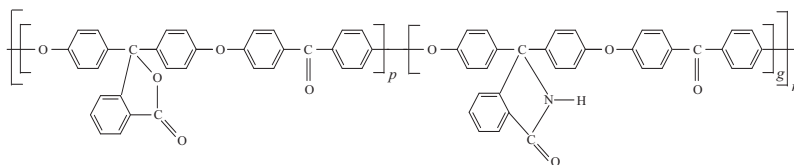
PAEK-22 is a homopolymer based on 4,4'-difluorobenzophenone and phenolphthalein imide containing phthalimide groups; it is isolated in the form of a white dispersed powder [90]:



PAEK-22

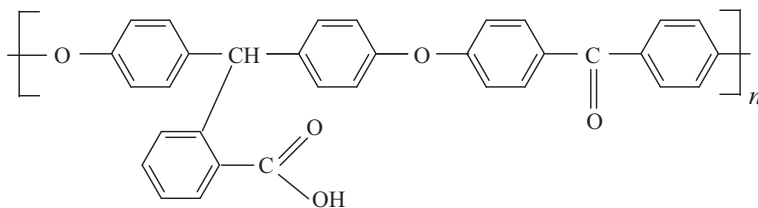
PAEK-22-21 is a copolymer based on 4,4'-difluorobenzophenone and a blend of 3,3-bis-(4'-hydroxyphenyl)phthalide and 3,3-bis-(4'-hydroxyphenyl)phthalimidine containing phthalide and phthalimide groups in a ratio of 0.75 : 0.25.

The copolymer is a transparent film with a thickness of 200–300  $\mu\text{m}$  or light brown foamed flakes synthesized by solution casting using a solution in chloroform.



PAEK-22-21

PAEK-41 is a homopolymer based on 4,4'-difluorobenzophenone and phenolphthalein containing active carboxyl groups; it has the form of a white fine powder [91]:



PAEK-41

At room temperature, all PAEKs are soluble in chloroform and diethylene glycol and insoluble in water. Some of PAEKs are soluble in ED-22 under heating to 115–120°C; during heating, some PAEKs react to form partially crosslinked structures.

Some characteristics of the studied PAEKs are listed in Table 1-3; conditions for combining PAEKs with epoxy oligomers and the curing regime of the adhesive joints are shown in Table A2-1. It was possible to measure the adhesive strength to fibers only for those of PAEKs that were made in the form of films. It was found that the adhesive strength is extremely low: for the PAEK-21–steel wire joints, it is as low as 2–6 MPa at any molecular mass of the polymer. PAEK-21 does not contain reactive groups. The adhesive ability of PAEK-22-21, which contains a small

amount of phthalimide groups, is slightly higher: it is 10–15 MPa (see Table 1-3 and Fig. 1-13).

It was impossible to estimate the adhesive properties of the powdered PAEK-22 and PAEK-41, because it was impossible to obtain a homogeneous melt of these polymers and form joints with a high-quality interface.

**Table 1.3. Some characteristics of the used PAEKs\***

PAEK	$M \times 10^{-3}$	Intrinsic viscosity $\eta_{\text{intr}}$ , dL/g (solvent)	Incipient melting point, °C
PAEK-21N	29	0.39 (CHCl <sub>3</sub> )	210**
PAEK-21V	73	0.66 (CHCl <sub>3</sub> )	235***
PAEK-22	–	0.56 (DMAA)	260
PAEK-22-21	36	0.48 (DMAA)	215–220**, 240***
PAEK-41	–	0.40 (DMAA)	215

\*According to [92]. \*\*Punch load is  $P = 1000 \text{ N/m}^2$ . \*\*\*Punch load is  $P = 10 \text{ N/m}^2$ .

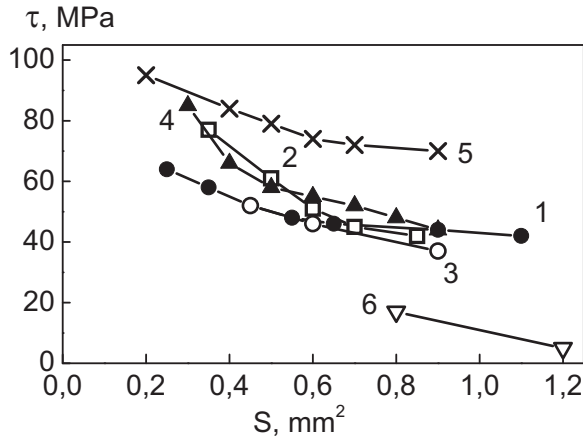


Fig. 1-13. Dependence of adhesive strength  $\tau$  on the area of joints  $S$  for ED-22+DADPS+PAEK-22-21–steel wire systems ( $d = 150 \mu\text{m}$ ) at the different amounts of the PAEK-22-21 modifier in the matrix: (1) 0, (2) 5, (3) 10, (4) 15, and (5) 30 wt %; (6) “pure” PAEK-22-21.

Figure 1-13 shows typical scale dependences of the adhesive strength of epoxy resin+PAEK–fiber joints. For all the studied pairs, with an increase in  $S$ , the  $\tau$  values decrease monotonically and nonlinearly, as was also observed for epoxy resin–PSF and epoxy resin–PEI blends.

Thus, in the case of using a new class of adhesives—thermoset–thermoplastic blend matrices,— the shape of the scale dependence of the adhesive strength in joints with fibers remains the same as in the case of using thermosetting and thermoplastic polymers [30, 31]. This fact not only suggests that this dependence is typical and dominant, but also shows that, for the most diverse systems, the same physical causes (primarily, the nonuniformity of the interfacial stress field) form the basis for this dependence.

In the case of modifying the ED-22 resin with PAEK-22-21 (Fig. 1-13), the  $\tau$ – $S$  curves corresponding to concentrations of 5–15 wt % lie very close to each other; only upon the introduction of 30 wt % of the modifier, the  $\tau$ – $S$  curve rises up. This means that the adhesive strength begins to increase considerably upon the introduction of ~30% of the thermoplastic, which is clearly seen in Figs. 1-13 and 1-14 and Table 1-2. In this case, the increase in the adhesive strength is 60–80% (depending on the geometry of the joint).

For joints in which the adhesive is the ED-22 resin modified with PAEK-21N, the adhesive strength changes similarly with an increase in the minor component concentration (see Fig. 1-14). In either case, with an increase in the concentration to 30%, the adhesives lose their transparency after curing. Apparently, during curing, epoxy resin–PAEK blends undergo phase separation.

The concentrations of the other PAEKs in the ED-22 resin, at which the joints were formed, did not exceed 10 wt %. At this content of PAEK-21V and PAEK-41, the adhesive strength increased as low as by 10–15% (Fig. 1-14). In this case, the adhesives remain transparent; that is, in these cases, the blends apparently do not undergo phase separation during curing.

As in the case of modifying epoxy oligomers with PEIs, an extreme point in the concentration dependence of adhesive strength in epoxy resin+PAEK–fiber systems was not observed. However, since the adhesive ability of PAEK is significantly lower than that of epoxy resins (Fig. 1-12), it can be assumed that, with an expansion of the minor component concentration range, the  $\tau$ – $C$  dependence will be a dependence with a maximum.

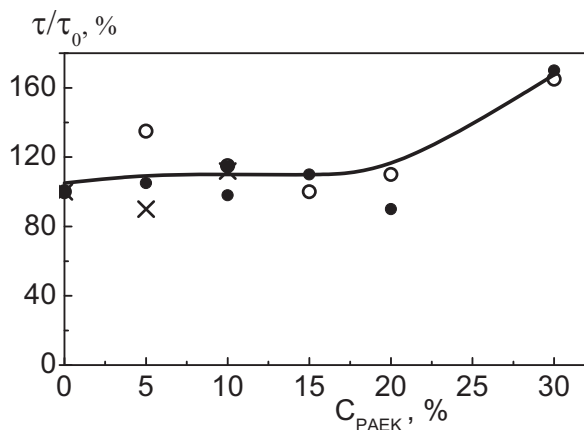


Fig. 1-14. Increase in the adhesive strength in the ED-22+DADPS+PAEK–steel wire systems ( $d = 150 \mu\text{m}$ ): (o) PAEK-21N, (●) PAEK-22-21, (x) PAEK-41, and (■) PAEK-21V; the contact area is  $S = 0.6 \text{ mm}^2$ ;  $\tau_0$  is the adhesive strength in the case of using the unmodified ED-22 resin as the adhesive.

Let us now consider factors that can be responsible for an increase in the interfacial strength in the case of modifying epoxy oligomers with heat-resistant thermoplastics. As in the discussion of the effect of an active diluent, let us determine how each of the main factors responsible for the measured adhesive strength value changes upon the introduction of a thermoplastic.

Since the adhesive ability of thermoplastics is lower than that of epoxy resin, the replacement of some interactions by other (if any) cannot lead to an increase in the  $\tau$  values.

The viscosity of the compositions abruptly increases with an increase in the amount of the modifier. Thus, at a curing temperature ( $180^\circ\text{C}$ ) for the ED-20 resin, it is  $2 \times 10^{-3} \text{ Pa s}$ ; after the addition of 20 wt % PSK-1 or PEI, it is  $180 \times 10^{-3}$  and  $200 \times 10^{-3} \text{ Pa s}$ , respectively; that is, it increases by almost 2 orders of magnitude; the spreading rate decreases, and the contact angles increase (see also Table 2-1 and A3). Therefore, the introduction of a thermoplastic cannot increase the number of bonds formed at the interface during curing and decrease the interfacial imperfection, which is primarily determined by the ability of the adhesive to wet the substrate. This means that these factors cannot be responsible for an improvement of the adhesion between the epoxy blend matrix and the fibers.

The residual stress value depends, all other conditions being equal, on the elastic modulus values and the thermal expansion coefficients of the



components; upon the introduction of 20 wt % of a thermoplastic (e.g., PSK-1 or PEI) into ED-20, these parameters vary only slightly (see Table 1-4). Upon the introduction of PAEK-21V, the change in these parameters is somewhat stronger. A slight decrease in residual stresses cannot provide a considerable increase in the interfacial strength, although it can contribute to a certain increase in this parameter. Therefore, residual stresses cannot be considered as the main factor governing the interfacial strength in thermoplastic-modified epoxy resin–solid joints.

The next factor responsible for the  $\tau$  value is the structure of the near-surface (interfacial) layers. The nucleation and formation of defects responsible for failure and propagation of cracks occur in these layers; that is, the failure mechanisms of adhesive joints depend on the structural and morphological organization of these layers. The structure of the near-surface layers is formed during the curing of the joints and depends on the phase separation processes that occur during curing.

**Table 1.4. Physicomechanical properties of epoxy resin–PSF adhesives [87]**

	PSF concentration, wt %				
	0	5	10	15	100
Glass transition temperature $T_g$ , °C	93	97	99	100	
Linear expansion coefficient, $\alpha \times 10^6$ , deg <sup>-1</sup> at $T = 60\text{--}85^\circ\text{C}$ at $T = 135\text{--}175^\circ\text{C}$	72 176	69 168	70 180	72 168	48 55
Density $\rho$ , kg/m <sup>3</sup>	1220	1190	1170	1150	1210
Tensile strength $\sigma_t$ , GPa	74	74	78	59	82
Tensile modulus $E_t$ , GPa	3.0	2.6	3.2	2.9	2.8
Flexural modulus $E_f$ , GPa	3.4	3.35	3.4	3.2	2.8
Shear strength $\tau_{sh}$ , MPa	51	53	54	55	58

The evolution of the structure of epoxy resin–heat-resistant thermoplastic blends with an increase in the introduced thermoplastic concentration was studied in detail using the example of epoxy resin–PSF blends [15, 91]. It was found that epoxy resin–thermoplastic blends, which are completely miscible in a wide temperature range before curing, undergo phase separation during curing. The pattern of phase separation depends on the amount of the thermoplastic introduced into the ED-20 epoxy oligomer. Compositions containing 5 wt % PSF form matrix–inclusion structures: individual “islands” (particles) of the thermoplastic

are dispersed in the epoxy resin. The addition of 10–15% PSF leads to the formation of larger and more intricately organized regions of the thermoplastic in the epoxy resin and the formation of a structure with the so-called “cocontinuous” phases. At an even higher modifier content, phase inversion is observed. The structure of the matrices in the near-surface layers is similar to their structure in the bulk; however, it is enriched in epoxy resin. Therefore, it is reasonable to expect that the mechanisms governing the failure of blends in the bulk act at the interface as well.

An increase in the crack-tip plastic zone upon the addition of a thermoplastic should lead to an increase in the energy required for crack formation and propagation, an increase in the mechanical characteristics of the blend, and an increase in the adhesive strength. A change in the crack propagation path during the interaction of the crack with the second-phase particles should contribute to the occurrence of the same effects; that is, the synergism of adhesive strength observed for the studied epoxy resin–thermoplastic blends can be primarily attributed to a change in the failure process with a change in the blend composition and a change in the pattern of crack formation and propagation in the near-surface layers (interface).

The decrease in the adhesive strength at fairly large amounts of the thermoplastic (obvious in the case of modifying with PSK-1 and expected in the case of the introduction of PEI or PAEK) is most probably caused by an increase in the concentration of the phase exhibiting a lower adhesive ability than that of epoxy resins.

Thus, an increase in the amount of the thermoplastic increases the plasticity of the matrix, changes the mechanism of crack formation and propagation in the near-surface layers, and decreases residual stresses; as a consequence, the interfacial strength increases. However, an increase in the concentration of the component exhibiting a lower adhesive ability than that of epoxy resins contributes to a decrease in the adhesive strength. The superposition of these two processes leads to the occurrence of a maximum in the concentration dependence of the adhesive strength.

### ***1.3. Adhesion of Epoxy Resins Modified with Fine Mineral Fillers***

To control the physicomechanical characteristics of polymers (and reduce their cost), the introduction of fine mineral fillers into them is commonly used. In the 21st century, significant attention is paid to the use of nanofillers and, accordingly, the study of their effect on the properties of polymers [93–109]. However, the modifying of polymers with

dispersed fillers as a method to control the strength of the polymer–solid interface has not yet been considered. This fact is apparently attributed to the intuitive idea that this modifying of a polymer can only decrease the interfacial strength in joints of the polymer with solids. In fact, the adhesive strength of the particles of mineral fillers to solid substrates is almost zero, as that of any solids contacting without applying an external pressure. In addition, the points of contact of the particles with a solid surface can become sites of stress concentration and sites of formation of dangerous defects responsible for degradation. As a consequence, it would seem that, upon the addition of fine mineral powders to polymers, the strength of the polymer–solid interface should decrease.

However, it was found [110, 111] that the introduction of mineral fillers into polyolefins can lead not only to a decrease in adhesive strength  $\tau$  in filled polymer–fiber joints, but also to an increase in it: in some cases, the dependence of  $\tau$  on filler concentration  $C$  was described by a curve with a maximum. The theoretical and practical importance of the observed effect necessitated a comprehensive study of the effect. First of all, it was necessary to clarify whether a similar effect is observed in the case of using crosslinked polymers as the adhesives.

The results described in the previous section show that the presence of small amounts of a thermoplastic, which forms a separate phase composed of submicrometer-sized organic particles in epoxy resin, in the bipolymer matrix frequently provides an improvement in the adhesive strength of the matrix to fibers. The following question now arises: how will the modifying of epoxy oligomers with small inorganic particles affect the adhesive ability of the oligomers?

Below, it is discussed how the strength of the fiber–binder interface changes upon the introduction of micrometer-sized, submicrometer-sized, and nanosized particles (Aerosil, alumina, clay, carbon black, a shungite filler (SF), nanotubes) into epoxy resins. The composition and some characteristics of the fillers are listed in Tables 1-5–1-7.

Figure 1-15 shows typical  $\tau$ – $S$  curves for original (unfilled) and dispersion-filled epoxy binders.

It is evident that, at any filler concentration  $C$ , an increase in the size of the joint causes a monotonic decrease in the adhesive strength (breaking load monotonically nonlinearly increases). The behavior of the curves remains almost unchanged after the addition of the filler; this fact suggests that, after this modifying, the residual stresses vary only slightly.

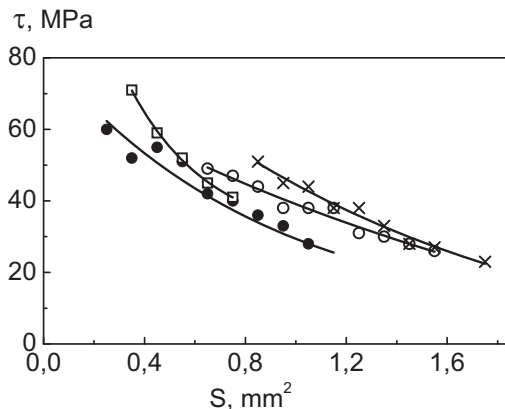


Fig. 1-15. Dependence of the adhesive strength of ED-22+TEAT+SF–steel wire joints with a diameter of 150 μm on the size of the joints. Shungite content (relative to the weight of ED-22): (●) 0, (o) 10, (x) 20, and (◻) 30%.

**Table 1.5. Characteristics of dispersed fillers**

	Aerosil (A-380)	Industrial carbon black (UM-66)	Nanotubes (MWNTs)*
Density, kg/m <sup>3</sup>	2200	1600	1600
Bulk density, kg/m <sup>3</sup>	50	300	86
Particle sizes			
Diameter, nm	5–15	70–130	40–60
Length, μm	–	–	5–15
Chemical purity	–	–	≥95
Specific surface area, m <sup>2</sup> /g	340–420	150–175	40–70
Ash content, at most, %	–	–	1
Weight fraction of silica, %	99.9		

\*Multiwalled nanotubes.

The concentration dependences of the adhesive strength observed upon the introduction of various mineral powders into epoxy resin [104, 113] are shown in Fig. 1-16.

It is evident that, by introducing fine fillers into epoxy resins, it is possible to increase the adhesive strength of the adhesive–substrate systems. The observed effect does not depend either on the shape of the particles or on their size. Adhesive strength increases after the addition of nanosized round Aerosil particles, after the introduction of flat submicron-

sized  $\text{Ca}^{++}$ -montmorillonite particles, and after the addition of cylindrical particles of  $\alpha\text{-Al}_2\text{O}_3$  and  $\theta\text{-Al}_2\text{O}_3$  nanocrystalline fibers.

**Table 1.6. Characteristics of nanostructured alumina powders [94] (average diameter and average length of the particles is 4–6 and 30–40  $\mu\text{m}$ , respectively)**

Treatment temperature, °C	750	900	1200
Phase composition	$\gamma$	$\theta$	$\alpha$
Bulk density*, $\text{kg}/\text{m}^3$	460	480	540
Pycnometric density**, $\text{kg}/\text{m}^3$	2940	3230	3750
Specific surface area, $\text{m}^2/\text{g}$	111	96–98	18
Average crystallite size, nm	8.2	9–11	55

\*Weight of 1 unit volume ( $1 \text{ cm}^3$  or  $1 \text{ m}^3$ ), State Standard GOST 27801-93.

\*\*Determined according to GOST–2211-90, except for the liquid medium, which was hexane.

**Table 1.7. Composition (wt %) and some physicochemical properties of SFs [112]**

Parameter	SF-1	SF-3	SF-5
C	98–99	28–32	2.1–4.4
$\text{SiO}_2$	–	57–66.2	92.8–95.9
$\text{Al}_2\text{O}_3$	–	3.2–4.45	0.11–0.79
$\text{TiO}_2$	–	0.16–0.3	0.02
$\text{Fe}_2\text{O}_3+\text{FeO}$	–	1.0–2.3	0.1–0.9
MgO	–	0.4–0.8	0.37
CaO	–	0.07–0.3	–
$\text{K}_2\text{O}$	–	0.8–1.6	0.18
$\text{Na}_2\text{O}$	–	0.11–0.3	0.1
MnO	–	0.01–0.02	0.013
NiO	1.0	–	–
CoO	0.022	–	–
$\text{Cr}_2\text{O}_3$	0.068	–	–
$\text{V}_2\text{O}_5$	1.0	–	–
CuO	0.032	–	–
S	0.4–0.8	0.2–0.7	0.2–0.5
$\text{H}_2\text{O}$	0.4–1.0	0.2–0.5	0.1–0.3
$d$ , $\mu\text{m}^*$	4–40	2–8	1–20
pH**	5.6–6.5	4.69–5.20	6.0–6.7
$S_{\text{sp}}$ , $\text{m}^2/\text{g}^{***}$	14–30	30–50	30–40

\*Particle diameter. \*\*pH of aqueous suspensions. \*\*\*Specific surface area.

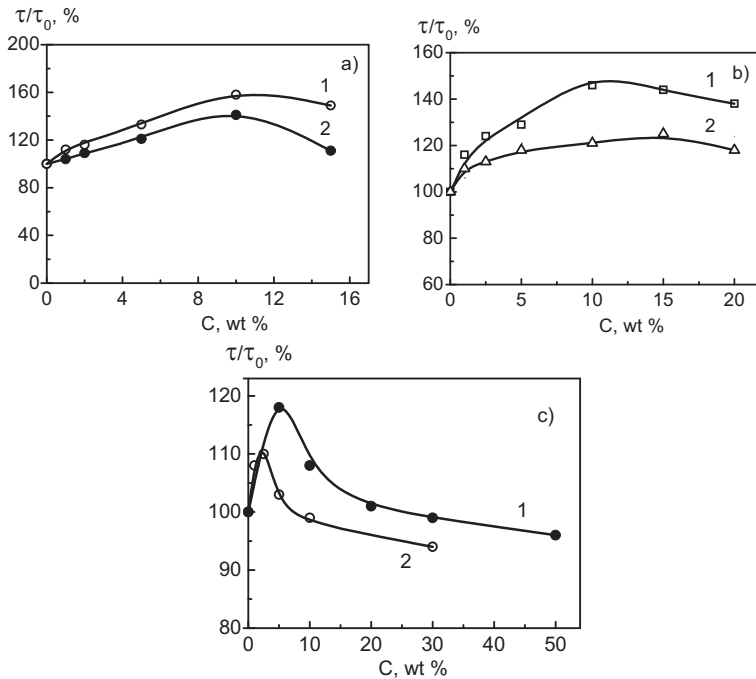


Fig. 1-16. Concentration dependences of adhesive strength  $\tau$  of dispersion-filled epoxy binder–steel wire joints ( $d = 150 \mu\text{m}$ ) in relative units;  $\tau_0 = \tau$  at  $C = 0$ : (a) ED-20+TEAT+aerosil,  $S = (1) 0.45$  and  $(2) 0.55 \text{ mm}^2$ ; (b) ED-22+TEAT+Ca<sup>++</sup>-montmorillonite,  $S = (1) 0.45$  and  $(2) 0.65 \text{ mm}^2$ ; and (c) ED-22+TEAT+Al<sub>2</sub>O<sub>3</sub>:  $(1) \theta\text{-Al}_2\text{O}_3$  and  $(2) \alpha\text{-Al}_2\text{O}_3$ ,  $S = 0.55 \text{ mm}^2$ .

The nanocrystalline alumina (Al<sub>2</sub>O<sub>3</sub>) fibers used in the work were prepared by impregnating hydrated cellulose fibers with an aluminum chloride solution [114, 115]. Depending on the heat treatment conditions, alumina was obtained in various crystalline forms ( $\gamma$ ,  $\theta$ , and  $\alpha$  phases). The resulting oxide fibers were ground in a drum with porcelain balls and sieved into fractions. The ground and sieved nanocrystalline fibers were white powders with elongated (approximately cylindrical) particles with a diameter of 4–6  $\mu\text{m}$  and a length of 30–40  $\mu\text{m}$ . Some of their characteristics are given in Table 1-6.

It is evident from Fig. 1-16 that, in all cases, the  $\tau$ – $C$  dependences are described by curves with a more or less clearly pronounced maximum; that is, in all cases, the synergistic effect of adhesive strength is observed. The behavior of the curves hardly changes with a change in the  $S$  value,

i.e., with a change in the sizes of the joints. The position of the maximum (filler concentration providing a maximum interfacial strength value) is different for different fillers. Upon the introduction of Aerosil and clay, the maximum is achieved at  $C = 10$  and  $12$  wt %, respectively; for aluminas, at  $2.5$  and  $5.0$  wt %. The increase in the  $\tau$  values at the maximum (compared with the unfilled matrix) is approximately the same— $20$ – $30\%$ —upon the addition of all the fillers.

Figures 1-17 and 1-18 show the concentration dependences of adhesive strength upon the introduction of carbon-containing fillers (industrial carbon black (soot), schungite, carbon nanotubes (CNTs)) into epoxy oligomers [116, 117]. It is evident that the addition of two of the fillers improves (in a certain concentration range) the adhesive strength: the  $\tau$ – $C$  dependences, as in the case of introduction of mineral fillers, are described by curves with a maximum. Upon the addition of industrial carbon black no. 66 (electroconductive carbon material UM-66) or no. 76 (technical carbon UM-76), the maximum is observed at  $C = 2$  wt % (Fig. 1-17a). The two carbon fillers provide a nearly identical increase in the interfacial strength at the above concentration: the ascending branches of the  $\tau$ – $C$  curves almost coincide for the two types of carbon black. Upon the achievement of a maximum, the  $\tau$  values of the systems filled with carbon black no. 66 abruptly decrease: event at  $C = 2.5$  wt %, the adhesive strength is lower than that in the unmodified resin–substrate joints. For the ED-20+TEAT+carbon black no. 76 systems, the  $\tau$  values decrease quite gradually upon the achievement of a maximum. It is not improbable that, in the case of modifying the composition with carbon black no. 66, the abrupt decrease in the  $\tau$ – $C$  curves upon the achievement of a maximum is attributed to an imperfect stirring of the binder during the introduction of the fillers.

The maximum increase in adhesive strength, as in the case of introducing other fillers into epoxy resin, is  $20$ – $40\%$  (relative to  $\tau$  values in joints with the unmodified resin).

Figure 1-17b shows the adhesive strength variation in the case of using schungite as the filler [109].

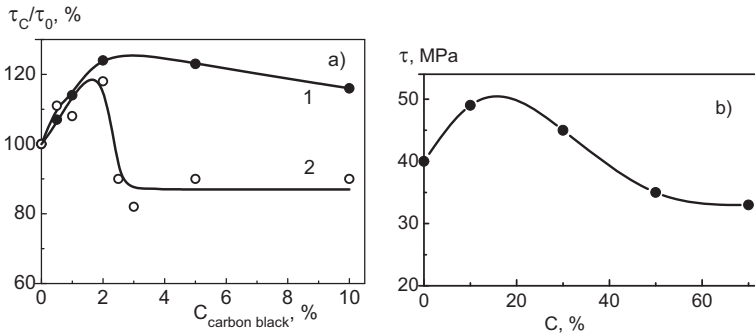


Fig. 1-17. Concentration dependences of adhesive strength  $\tau$  of dispersion-filled epoxy resin–steel wire joints ( $d = 150 \mu\text{m}$ ): (a) D-22+TEAT+carbon black: (1) carbon black no. 66 and (2) carbon black no. 76,  $S = 0.45 \text{ mm}^2$ ,  $\tau_0 = \tau$  for  $C = 0$  and (b) ED-22+TEAT+schungite,  $S = 0.65 \text{ mm}^2$ .

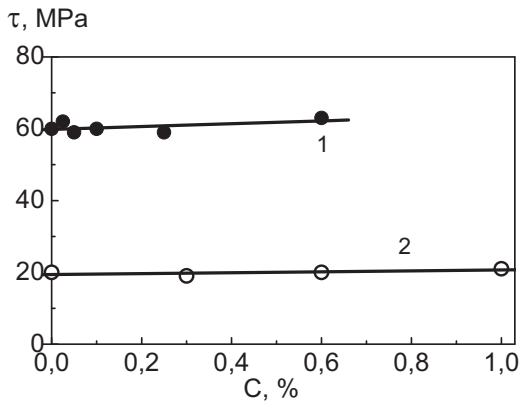


Fig. 1-18. Concentration dependence of adhesive strength  $\tau$  of CNT-filled epoxy resin–steel wire joints ( $d = 150 \mu\text{m}$ ): (1) ED-20+TEAT+functionalized CNTs (FCNTs),  $S = 0.4 \text{ mm}^2$  and (2) ED-20+PEPA+CNTs (MWCNT-40-60),  $S = 0.55 \text{ mm}^2$ .

The SF is a representative of the so-called unconventional fillers. It is prepared by grinding schungite rocks [118–120]. This mineral has a complex composition, the main components of which are noncrystalline carbon with a metastable structure, aluminosilicates, and quartz; in addition, it contains small amounts of metal oxides. The carbon content in schungites of various types varies in a range of 2.5–98 wt % (see Table 1-7). Ground schungite is highly miscible with polar and nonpolar polymers.



The particles of this filler have a unique mosaic surface structure with alternating mineral and carbon regions, which opens up wide possibilities for modifying it [120]. The explored reserves of schungite rocks in the territory of Russia are estimated at hundreds of millions of tons [118–120]. The introduction of schungites into polymers is responsible for many of their useful properties (e.g., electrical conductivity). Therefore, in recent years, the properties of schungites and the polymers filled with them have been intensively studied.

The particles of the used SF were porous spheres with an average diameter of 4  $\mu\text{m}$ .

It is evident from Fig. 1-17b that the introduction of an SF into epoxy resin can provide an increase in the adhesion strength of the resin–fibers system. With an increase in the SF content, the adhesive strength changes nonmonotonically: the  $\tau$ – $C$  curve passes through a maximum. The highest adhesive strength is provided by matrices containing 10–20% SF. The increase in the adhesive strength at the maximum achieves  $\sim 20\%$ . The  $\tau$  values of the modified epoxy resin decrease below the adhesive strength values of the unfilled resin only after the addition of 35 wt % of the filler.

A joint consideration of the described results and the data of [110, 111] suggests that SFs can be effectively used as a tool to increase the adhesion between an adhesive and a solid (fiber) in the case of using both linear (polyolefins) and crosslinked polymers (epoxy resins) as the adhesives; this finding provides still more evidence of the efficiency of this natural carbon-containing mineral.

The modifying of epoxy oligomers with CNTs with both untreated and treated surfaces did not lead to an increase in the adhesive ability of the compositions: typical results are shown in Fig. 1-18. It is evident that, in the case of addition of FCNTs to ED-20, the adhesive strength in the joints with a steel wire remains constant.

There are many indications in the literature that an improvement in the properties of CNT-modified epoxy resins is observed at low amounts (tenths or even hundredths of a percent of the weight of the main component) of CNTs (see, e.g. [121]). In the case under discussion, 0.0125–0.6 wt % FCNTs was added to the binder. However, it is not improbable that, to improve the adhesion of the ED-20+TEAT+CNT binder to the substrate, the amount of introduced nanotubes should be increased.

Note that all compositions whose adhesion to a steel wire is shown in Figs. 1-16, 1-17a, and 1-17b were cured with TEAT. In the case of the "hot" curing of epoxy resins, this tertiary aromatic amine provides a high adhesion to solid surfaces (exhibiting a fairly high surface energy). As

noted above, the  $\tau$  values increased by 20–30% relative to this high initial level. In the case of modifying the ED-20 resin with CNTs, it was also studied how the interfacial strength changes during the curing of the ED-20 resin with PEPA, which is an aliphatic amine used in the "cold" curing of epoxy resins. The interfacial strength in the ED-20+PEPA–steel wire joints is significantly lower than that in the ED-20+TEAT–the same wire joints (see Fig. 1-18). However, in this case, it was also found that the addition of CNTs to the ED-20 resin does not change the adhesive ability of the resin. The question of why the modifying of epoxy resins with nanotubes does not lead to the occurrence of the synergistic effect of interfacial strength still remains open.

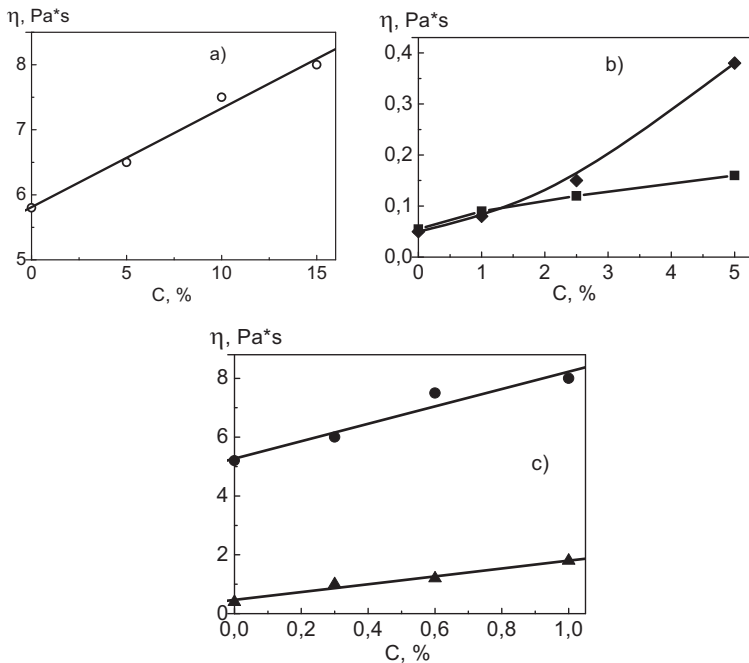


Fig. 1-19. Dependence of the viscosity of the ED-20 epoxy oligomer on (a) the schungite concentration in it at 20°C, (b) the concentration of (♦) Aerosil A-380 and (■) carbon black UM-66 at 80°C, and (c) the L-MWNT40-60 concentration at (●) 20 and (▲) 50°C.

In interpreting the mechanisms governing the synergism of adhesive strength, it is of interest to compare the effects of the modifying of epoxy resins with fine fillers and heat-resistant thermoplastics on the main factors responsible for the measured  $\tau$  value. The studied mineral powders are modifiers that hardly interact with fibers and slightly increase the viscosity of the epoxy compositions (Fig. 1-19).

The introduction of a filler leads to a change in the physicomaterial characteristics of the polymer, in particular, to an increase in elastic modulus  $E$  of the polymer and a decrease in the coefficient of linear expansion  $\alpha$ . As a consequence, the thermally induced residual stresses acting at the fiber–matrix interface can change, because both an increase in the elastic modulus and a decrease in the coefficient of expansion of the matrix lead to their decrease. As a result, the adhesive strength value measured in experiments can increase. However, as was noted in the discussion of the  $\tau$ – $S$  curves in Fig. 1-15, in the studied systems, the residual stresses vary only slightly upon the introduction of dispersed fillers; therefore, they cannot significantly increase the adhesive strength values.

Thus, the main factor responsible for the change in adhesive strength upon filling, as well as upon modifying with thermoplastics, is the structure of the near-surface layers, i.e., the layers in which crack formation and failure processes occur.

Dispersion-filled epoxy matrices before and after curing are two-phase systems, unlike bipolymer epoxy matrices, which are single-phase before curing and can become two-phase after curing. An increase in the percentage of a dispersed filler does not lead to a qualitative change in the structure of the interfacial layers. This feature also makes epoxy matrices modified with mineral powders different from epoxy resins modified with thermoplastics, in which the thermoplastic phase exists in the form of a dispersion of organic particles at  $C \leq 10\%$  and in the form of larger and more complex cocontinuous structures at  $C \geq 10$ – $20\%$ . The introduction of fine mineral powders does not increase the plasticity of the matrices, whereas the addition of thermoplastics is accompanied by an increase in the plasticity of the epoxy compositions. Therefore, a change in the  $\tau$  values in dispersion-filled epoxy resins can be associated only with the defect (crack) nucleation process in the presence of particles of the second phase and with a change in the crack propagation path upon encountering the particles. The presence of dispersed particles exhibiting mechanical properties different from those of the polymer (resin) in the resin (adhesive) can lead to a change in the failure process of the adhesive joint. Upon encountering an obstacle (particle) in the propagation path, the crack

can slow down propagation, stop it, change the path to move around this obstacle, undergo branching, etc. All these effects slow down the failure process and, ultimately, lead to an increase in  $\tau$ . Apparently, this factor is the fundamental cause of the increase in the interfacial strength. In addition, the increase in the  $\tau$  values for dispersion-filled matrices is less than that for matrices modified with thermoplastics, where the adhesive strength can also increase owing to the occurrence of significant plastic deformations at the tip of the propagating crack.

The decrease in the adhesive strength (after passing a maximum) is apparently attributed to an increase in the interface damage probability with an increase in the number of particles, which leads to the nucleation of defects contributing to failure at the fiber–matrix interface and in the near-surface layers; that is, as in the case of modifying with thermoplastics, a decrease in  $\tau$  values is associated with an increase in the minor component concentration.

Thus, using fine fillers, it is possible not only to decrease the strength of fiber–epoxy matrix joints, but also to increase it, which means that this type of modifying can also be regarded as a method to control the adhesive strength.

To summarize, the following should be stated. We have seen that, in the case of using any modifying method, the synergism of adhesive strength in modified epoxy matrix–fiber joints is frequently observed. The frequent occurrence of the synergistic effect indicates the existence of a common fundamental cause that underlies the phenomenon and governs it.

The totality of the currently available experimental data suggests that the occurrence of the synergistic effect is inextricably associated with the structural organization of the near-surface layers (interphase). The structure of these layers determines the development of the failure processes of the adhesive joints that occurs in the layers. The degradation process can be conventionally divided into three stages: nucleation, development (subcritical growth), and “catastrophic” propagation of the dangerous defect (crack) responsible for failure. The development of each of the stages depends on the structure of the interphase formed during curing. Therefore, one of the main questions now is how the type and amount of the modifier affect the structure of the cured epoxy resin and whether the structure of the adhesive after curing is homogeneous or heterogeneous.

If the polymer structure after curing remains homogeneous (epoxy resin–modifier blend does not undergo phase separation during curing), then all three stages of crack development in the modified polymer occur essentially under the same conditions as in the case of the unmodified

resin. This is the case with the modifying of epoxy oligomers with active diluents, which are incorporated into the polymer network during curing and do not form a separate phase. In this case, it is not reasonable to expect any considerable change in the interfacial strength. It is 15–20%; it is associated with the plasticizing effect of the modifier (with a decrease in the glass transition temperature and interfacial residual stresses).

If the structure of the cured adhesive is heterogeneous, then various versions of the development of the failure process can take place depending on the heterogeneity pattern.

If the polymer structure is a continuous phase of the main (epoxy) component, in which a small amount of modifier particles is distributed (as is the case of introducing a small amount of dispersed mineral fillers or heat-resistant thermoplastics into oligomer), then the first two stages of crack development—nucleation and subcritical growth—can occur under nearly the same conditions as those in the unmodified resin: it may be that the crack does not “feel” the filler. However, the third stage—crack propagation—occurs, generally speaking, in a different way than it does in the unmodified resin. The propagating crack can encounter a particle (obstacle) in its path. As discussed above, this event can lead to an increase in the interfacial strength. Experiments confirm that, in a certain concentration range, the interfacial strength increases. However, in this case, the increase in the  $\tau$  values is small, namely, up to 20–30% (relative to the original resin).

If the introduced minor component forms fairly long intricately organized structures after curing (e.g., cocontinuous structures in the case of modifying with heat-resistant thermoplastics) in epoxy resin (base of the composition), then the nucleation and subcritical growth of a dangerous defect (crack) can occur in the presence of a polymer phase exhibiting plasticity at the tip of the propagating crack.

Crack propagation can also include the passage through this phase. In this case, the crack development and propagation consume more energy than in a homogeneous polymer or in a polymer with a small amount of modifier particles. Accordingly, in this case, the modifying is most effective. The increase in the interfacial strength is also maximal. In some cases, the  $\tau$  values (at an optimum concentration) increased by 50–80% (Table 1-2, Fig. 1-14).

Thus, in the proposed picture, the main cause of the occurrence of the synergism of adhesive strength in fiber-modified epoxy matrix joints is a change in the structure of the near-surface layers (interphase) and, as a consequence, a change in the mechanisms governing the failure process.

#### ***1.4. Adhesion of Epoxy Oligomers to Low-Surface Energy Solids (Materials)***

Epoxy resins are characterized by a fairly high adhesion to glass, steel, and other materials with a high surface energy exceeding many tens of millijoules per square meter ( $\text{mJ}/\text{m}^2$ ). Therefore, they are effectively used in all kinds of adhesive joints, compounds, and composite materials. However, epoxy adhesives cannot provide a high adhesive strength in interaction with materials whose surface energy is low (less than  $40 \text{ mJ}/\text{m}^2$ ). This finding is primarily attributed to the fact that they poorly wet these surfaces because of a fairly high intrinsic surface tension  $\sigma$ . On average, the  $\sigma$  values of most epoxy resins lie in a range of  $45 \pm 5 \text{ mN}/\text{m}$ . Therefore, compositions based on epoxy resins cannot spread over surfaces whose surface tension is less than the above values. A method to improve the wetting and, accordingly, increase the adhesion to low-energy surfaces is to decrease the surface tension of epoxy compositions. To this end, surfactants are commonly used [122].

Substances whose molecules are asymmetric and contain one or more hydrophilic groups and one or more hydrophobic radicals are frequently used as surfactants in aqueous media. This structure, which is referred to as diphilic, determines the surface adsorption activity of surfactants, i.e., their ability to concentrate on interfacial surfaces and change their surface properties. Surfactants are generally used in aqueous or aqueous–organic media (oil dispersions, emulsions of lubricants in water); they are used significantly less frequently in organic or low-polarity media. A necessary condition for the manifestation of surface-active properties in low-polarity media is the diphilic nature of the surfactants used, i.e., the presence of oleophilic and oleophobic parts in them. An example of these compounds is provided by organosiloxanes, which have Si–O–Si bonds—molecule backbone—in the structure; these bonds impart oleophobicity to the molecule, while lateral organic radicals impart oleophilicity to it [123].

The most active surfactants for organic media are compounds containing terminal fluorinated moieties. These compounds, which exhibit an extremely low surface tension  $\sigma$  ( $6\text{--}25 \text{ mN}/\text{m}$ ) [124], are capable of abruptly decreasing the surface tension of hydrocarbon joints even if they are taken in negligible concentrations (approximately 1–2 wt %) [120]. Thus, the addition of 1% of a partially fluorinated surfactant—pentadecafluorodecanol  $\text{C}_7\text{F}_{15}(\text{CH}_2)_3\text{OH}$ —to ethylene glycol leads to a more than twofold decrease in the  $\sigma$  value of ethylene glycol, namely, from 43.6 to 21.1  $\text{mN}/\text{m}$  [125].

This feature of organofluorine surfactants gave grounds to believe that they can be used to improve the adhesion of epoxy binders to low-energy surfaces.

This assumption has been first verified in [127, 128].

The studies were conducted using the ED-20 epoxy oligomer and employing PEPA as the curing agent.

The fluorine-containing surfactants (F-surfactants) were ethers of fluorine-containing telomeric alcohol and glycidol and a specimen of hydroxypropylated fluorine-containing telomeric alcohol 1,1,7-trihydrofluoropentanol. The structural formulas of the organofluorine compounds and some of their characteristics are given in Table 1-8.

**Table 1-8. Structure and characteristics of organofluorine compounds [122]**

Compound no.	Chemical formula	$\sigma$ , mN/m	$\rho$ , kg/m <sup>3</sup>
1	$\text{H}(\text{CF}_2\text{CF}_2)_3\text{CH}_2\text{OH}$	25.2	1750
2	$\text{H}(\text{CF}_2\text{CF}_2)_5\text{CH}_2\text{O}[\text{CH}(\text{CH}_3)\text{CH}_2\text{O}]_{12}\text{CH}(\text{OH})\text{CH}_3$	28.3	1267
3	$\text{CH}_2\text{-CHCH}_2\text{OCH}_2(\text{CF}_2\text{CF}_2)_3\text{H}$ O	28.2 (20°C) 26.2 (50°C)	1608

Compound no. 3 (Table 1-8) not only satisfies the basic requirement, i.e., structure diphilicity, but also, being a reactive compound, can be involved in the curing of epoxy resin. The copolymerization capacity is a very important characteristic of reactive F-surfactants, because their adsorption at interfaces is a dynamic process, which can be “frozen” during polymerization (curing).

Figure 1-20 shows experimental curves characterizing the change in the surface tension of the ED-20 epoxy oligomer at the air–liquid interface as a function of the fluorine compound concentration. The shape of the  $\sigma$ – $C$  curve of compound no. 1 indicates the absence of any significant surface activity for it. However, the epoxy ether based on it (compound no. 3), which has a diphilic structure, exhibits significant surface activity. At a concentration of 0.01 mol/L for compound no. 1, the surface tension of the epoxy oligomer decreases less than by 2 mN/m, whereas at the same concentration of compounds nos. 2 and 3, the decrease in the surface tension of ED-20 is 12 and 17 mN/m.

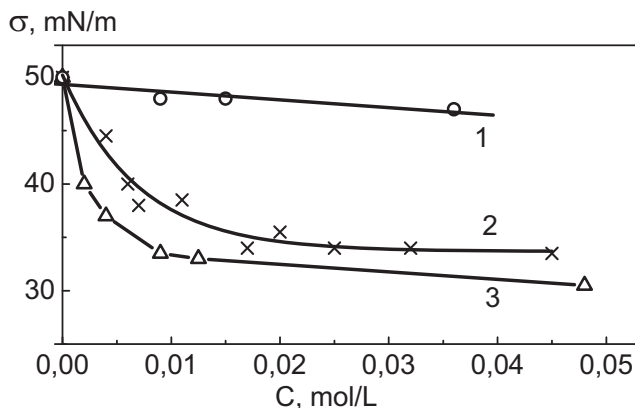


Fig. 1-20. Surface tension in the ED-20 epoxy resin–F-surfactant system; the numbers of the curves correspond to the numbers of compounds in Table 1-8. The measurement temperature is 50°C. The measurement procedure is given in A4.

Concentration dependences of surface tension ( $\sigma$ – $C$  curves) can be used to determine a number of thermodynamic parameters of surfactants, for example, their surface activity ( $A$ ) and maximum adsorption ( $\Gamma_m$ ). Quantitatively, the surface activity of surfactants is characterized by the value

$$A = \lim_{C \rightarrow 0} \frac{d\sigma}{dC}.$$

The  $A$  values for the studied compounds, which were determined by extrapolating the  $\sigma$ – $C$  curves to  $C = 0$  (Fig. 1-20), are listed in Table 1-9. They confirm the conclusion that compound no. 3 exhibits the highest surface activity.

**Table 1-9. Thermodynamic parameters of fluorine compounds [127]**

Thermodynamic parameters	Fluorine compounds		
	no. 1	no. 2	no. 3
$A^*$ , (mN L)/(m mol)	50	1500	5700
$G_m \times 10^4$ , mol/m <sup>2</sup>	–	19	22.5
$C_m \times 10^2$ , mol/L	–	2	5

\*According to Fig. 1-19.



The amount of F-surfactants adsorbed at the interface with a liquid epoxy oligomer (G) can be calculated using the Gibbs equation:

$$G = \left(-\frac{1}{RT}\right) \frac{d\sigma}{d\ln C},$$

where  $R$  is the universal gas constant and  $T$  is the measurement temperature.

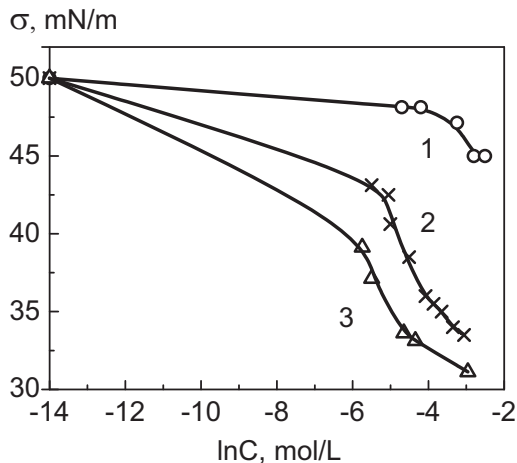


Fig. 1-21. Surface tension of the ED-20 epoxy resin-F-surfactant system in the  $\sigma$ - $\ln C$  coordinates; the numbers of the curves correspond to the numbers of compounds in Table 1.9. The measurement temperature is 50°C.

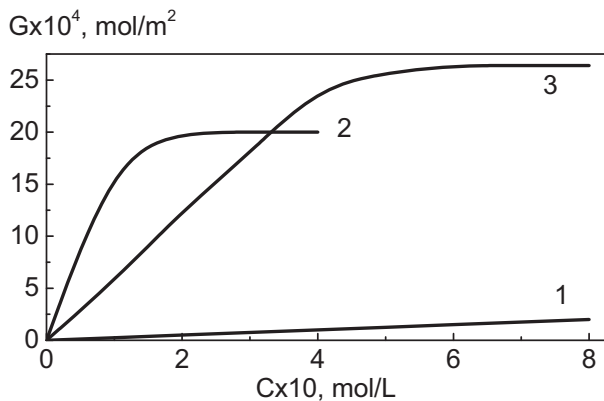


Fig. 1-22. Gibbs adsorption isotherms in the  $G$ - $C$  coordinates (according to Fig. 1-21).

Surface tension isotherms plotted in the  $\sigma$ – $\ln C$  coordinates are shown in Fig. 1-21, whereas Fig. 1-22 shows Gibbs adsorption isotherms calculated from the  $\sigma$ – $\ln C$  curves using the Gibbs equation. The initial curvilinear portion of the isotherms (Fig. 1-22) corresponds to a decrease in surface tension during the adsorption of surfactant molecules at the interface; in this case, adsorption  $G$  increases (Fig. 1-22). At the point of transition from the curvilinear to rectilinear portion of the  $\sigma$ – $\ln C$  isotherm, a maximum adsorption  $G = G_m = \text{const}$  is achieved. Portions with a constant  $G = G_m$  value are clearly visible in the adsorption isotherms (Fig. 1-22). It is known that the point of transition to the horizontal portion of the  $\sigma$ – $\ln C$  isotherm corresponds to either the solubility limit of the surfactant or the achievement of a critical micelle concentration. Upon the achievement of this concentration, the surface tension cannot decrease.

Upon the achievement of a maximum adsorption, the entire surface of the liquid is occupied by surfactant molecules sorbed on it. The further addition of the surfactant to the modified liquid (in the case under consideration, to the ED-20 epoxy oligomer) does not lead to a decrease in the surface tension at the liquid–air interface; therefore, it is inappropriate.

It should be borne in mind that a further increase in the amount of the F-surfactant leads to the formation of a heterophase system consisting of ED-20 and micelles of the F-surfactant.

The determination of the concentration providing a maximum constant  $G = G_m$  value means the determination of the maximum amount of the surfactant that should be introduced into a given substance at a given temperature. It is clearly seen from Figs. 1-20 and 1-22 that the maximum concentrations required for modifying the ED-20 oligomer with the studied compounds do not exceed 0.02–0.05 mol/L. Values of maximum adsorption  $G_m$  and maximum concentrations  $C_m$  are listed in Table 1-9.

The use of organofluorine compounds containing a reactive group in the carbon moiety structure makes it possible not only to decrease the surface tension of the liquid epoxy oligomer, but also to “fix” molecules of these compounds at the interfaces during curing. This factor provides a change in the surface properties of not only liquid compositions, but also cured compositions. The presence of a layer modified with an F-surfactant on the surface of the cured epoxy resin was confirmed by the measurement of the contact angles of this surface with water.

The contact angles of the unmodified cured ED-20 resin with water were 65°–67°. Measurements of  $\theta$  on the surface of the cured resin modified with compounds nos. 2 and 3 were conducted twice: immediately after curing and after surface treatment with the Freon 113 solvent. The measurement results are shown in Fig. 1-23.

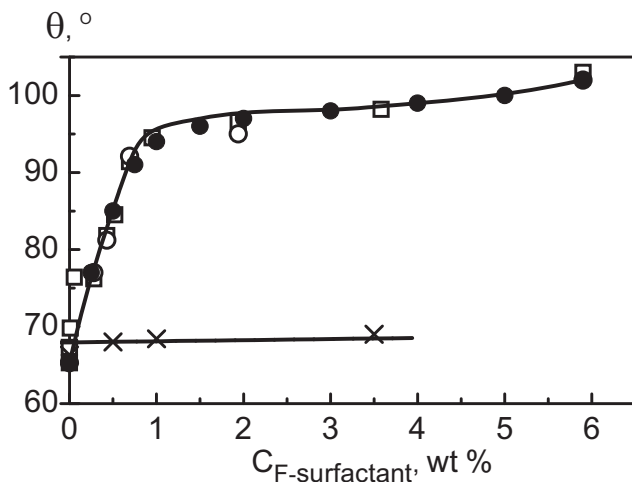


Fig. 1-23. Dependence of contact angles  $\theta$  formed by water droplets on the surface of the cured ED-20 resin modified with an F-surfactant on the amount ( $C$ ) of the introduced F-surfactant: (x, □) compound no. 1 and (•, o) compound no. 3. The  $\theta$  values were determined (•, □) immediately after the curing of the samples and (x, o) after surface treatment with Freon 113. The measurement procedure is given in A5.

It is evident that the introduction of an F-surfactant into epoxy resin leads to an increase in the contact angles formed by water droplets. The chemical structure of fluorine-containing radicals does not affect the pattern of the increase: upon the addition of both compound no. 1 (without reactive groups) and compound no. 3 (containing reactive groups), the  $\theta$  values are almost identical. This fact suggests that, in the two cases, the same groups (moieties)—apparently, the terminal fluoroalkyl radicals—emerge to the interface with air in the cured resin.

However, the chemical structure of F-surfactants introduced into epoxy oligomers significantly affects the bonding between fluorine compound and the resin during curing. The data of Fig. 1-23 show that only reactive surfactants (fluorine compound no. 3) remain on the surface of the specimens after solvent treatment. Inert surfactants bound to the surface only via weak adsorption forces are readily removed from the surface: after treatment with Freon, at any concentration of introduced fluorine compound no. 1, the contact angles are equal to the  $\theta$  values measured on the surface of the unmodified resin.

The results obtained in studying the thermodynamic characteristics of reactive F-surfactants show that compound no. 3, which is hereinafter

referred to as FG-3, exhibits the highest surface activity. It is this compound that was used to verify the hypothesis that the use of F-surfactants can increase the adhesive strength for epoxy compositions interacting with materials whose surface energy is lower than 35–40 mJ/m<sup>2</sup>. Adhesive strength was studied using the ED-20+PEPA+FG-3 compositions in joints with a hollow organic fiber poly(4-methylpentene-1) (P4MP-1). The surface energy of it is 25–28 mJ/m<sup>2</sup>. The amount of introduced FG-3 was 0.16, 0.34, 0.6, and 2 wt %. Measurements of the geometric parameters of the fiber (Fig. 1-24) showed that the average outer and inner diameter of the fiber is 60 and 45  $\mu\text{m}$ , respectively, and the average fiber wall thickness is approximately 7.5  $\mu\text{m}$ .

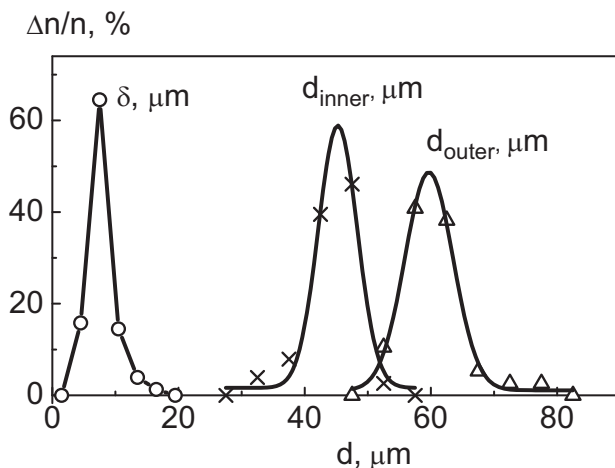


Fig. 1-24. Distribution curves for the outer and inner diameters and wall thickness  $\delta$  of the P4MP-1 fiber.

The results obtained in studying the adhesion of the ED-20 resin modified with the FG-3 surfactant to P4PM1 fibers are shown in Figs. 1-25 and 1-26. It is evident that, for both the unmodified and modified resins, the  $\tau$ – $S$  dependence is described by a monotonically decreasing nonlinear function; that is, neither the nature of the fiber nor the modifying method affects the behavior of the scale dependence of adhesive strength; for the new class of joints, this dependence preserves the usual shape.

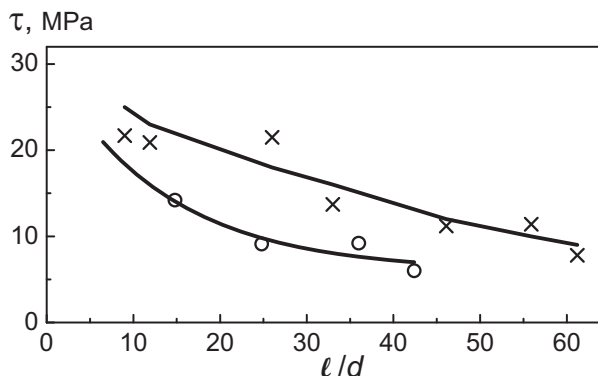


Fig. 1-25. Dependence of adhesive strength in the ED-20+PEPA+FG-3-P4MP-1 fiber system on the scale factor. The amount of FG-3: (o) 0 and (x) 0.34 wt %.

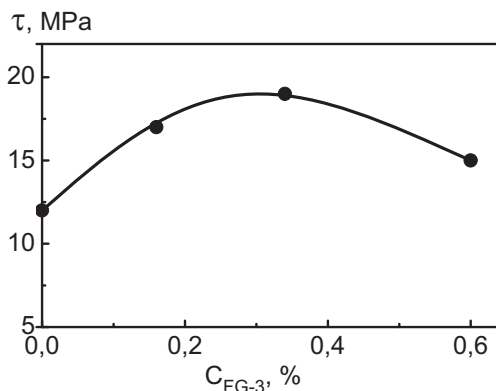


Fig. 1-26. Dependence of adhesive strength in the ED-20+PEPA+FG-3-P4MP-1 fiber system on the amount of introduced FG-3;  $l/d \approx 25$ .

The dependence of the adhesive strength on the amount of the modifier introduced into ED-20 (Fig. 1-26) is described by a curve with a maximum, which corresponds to the introduction of 0.3 wt % FG-3. The increase in the adhesive strength at the maximum is  $\sim 50\%$ . However, it should be noted that the adhesive strength of the unmodified ED-20 resin-P4PM-1 fiber system is low; the increase in  $\tau$  values is considerable relative to these low adhesive strength values.

Data on the dependence of the adhesive strength in the ED-20+PEPA+FG-3-P4MP-1 fiber system on the amount of introduced FG-3 (Fig. 1-26) are in good agreement with the results of studying the

maximum concentration of surfactants: the maximum in the concentration dependence of adhesive strength is observed at a concentration of 0.3 wt %, which is close to the value of  $C_m = 5 \times 10^{-2}$  mol/L (see above), which corresponds to 0.26 wt %.

An improvement in the wetting of the studied fiber upon modifying the ED-20 epoxy oligomer with a low surface energy compound increases the actual contact area between the adhesive and the substrate; it is this factor that provides an increase in the number of bonds acting across the interface and an increase in the adhesive strength.

The modifying of oligomers with surfactants significantly differs from the various types of bulk modifying discussed in the previous sections. The use of this method changes all factors responsible for the measured adhesive strength value. The presence of a surfactant at the interface can change the nature of the bonds acting across the interface, their number, and the interfacial imperfection. It does not change the bulk properties of the polymer (glass transition temperature, elastic modulus  $E$ , coefficients of thermal expansion  $\alpha$ ); however, it can change the structure and texture of the near-surface layers. A change in the first three factors contributes to an increase in the adhesive strength. In the case under discussion, a change in the last two factors contributes to a decrease in the adhesive strength.

Since the introduction of a surfactant should not significantly change the bulk properties of the polymer, it would seem that it should not affect the interfacial residual stress value. In fact, the maximum possible value of these stresses (proportional to the difference between the values of elastic moduli and coefficients of linear thermal expansion of the matrix and the fiber) remains unchanged. However, with an increase in the adhesive strength, the level of stresses transferred from the binder to the fiber, in particular, residual stresses, increases.

A change in the structure of the near-surface layers, which becomes heterogeneous after the introduction of a surfactant in an amount exceeding the critical micelle concentration (see above), will apparently also contribute to an increase in the stresses actually acting at the interface.

As a consequence, the  $\tau$ – $C$  dependence is described by a curve with a maximum. Thus, the data confirm the assumption that the introduction of F-surfactants into epoxy resin can improve the adhesion of this resin to low surface energy solids. It was found that, in this case, a quite significant increase in adhesive strength can be obtained. For the studied system, it was 50%.

Apparently, the proposed method for controlling the adhesive strength is one of the most natural methods, because it is aimed at improving the wetting, which is a necessary condition for high adhesion.

## CHAPTER TWO

# CURING-INDUCED CHANGES IN THE ADHESION PROPERTIES OF EPOXY OLIGOMERS MODIFIED WITH THERMOPLASTICS

Adhesive bonds between a substrate and an adhesive are formed during the formation of a joint.

Below, we discuss the bond formation process in systems where the adhesives are epoxy oligomers modified with heat-resistant thermoplastics and the substrates are fibers.

These studies are useful for both elucidating the adhesion mechanism and directionally controlling the interfacial strength. The main aim of these studies is to find an answer to the following questions: how does the presence of a thermoplastic in the adhesive affect the curing process and what are the laws that govern the variation in adhesive properties in the presence of these modifiers?

The described results were obtained in studying the curing of adhesives based on the ED-20 epoxy oligomer cured with DADPS and modified with the following three heat-resistant thermoplastics: PSF PSK-1, PEI Ultem 1010, and PAEK. The composition of the compositions, the conditions for their preparation and curing, and a brief description of the research methods are given in the Appendix (see A2, A6, A7, and A8).

A necessary (albeit insufficient) condition for the formation of a strong adhesive bond is a proper wetting of the substrate with the polymer. The effect of thermoplastic modifiers on the wetting of glass plates with an epoxy oligomer during curing can be determined from the results shown in Table 2-1. It is evident that contact angles ( $\theta$ ) formed by droplets of an unmodified ED-20 resin with a curing agent on a glass plate at 180°C at the droplet deposition time are 29°, i.e., fairly high. The addition of thermoplastics to the resin leads to an increase in these values: at a weight fraction of modifiers of 20%, the  $\theta$  value increases to 52°–53°.

The  $\theta$  values listed in Table 2-1 do not characterize the wetting ability of the studied compositions, because these values refer to a nonequilibrium contact angle. However, it is these values and the kinetics of their variation

that are important for a correct presentation and understanding of the processes that occur during the formation of adhesive joints.

It is fundamentally impossible to measure equilibrium contact angle  $\theta_{\text{equil}}$  during curing, because immediately after the deposition of a droplet onto a substrate, along with the spreading of the droplet (which should lead to the formation of an equilibrium contact angle), there occurs a network formation process (curing process); the viscosity increases, and the spreading rate decreases. After the completion of the curing process, the  $\theta$  values of the studied systems were lower than the initial values by as little as a few degrees ( $3^{\circ}$ – $7^{\circ}$ ). The difference in the initial and “final” contact angle values does not depend on the nature and amount of the introduced modifiers; that is, it does not depend on the viscosity exhibited by the studied systems before the onset of the curing process (viscosity values are also listed in Table 2-1).

**Table 2-1. Viscosity and contact angle values of ED-20+DADPS+thermoplastic compositions before the onset of the curing process and after the completion of the process at a temperature of 180°C\* [133]**

Composition	Initial viscosity, Pas	Contact angles			
		Before the onset of the curing process (at $t \cong 0$ )		After the completion of the curing process	
		$\theta, ^{\circ}$	$\cos\theta$	$\theta, ^{\circ}$	$\cos\theta$
ED-20 + DADPS	0.002	29	0.87	25	0.90
ED-20 + DADPS + 10 % PSK-1	0.024	43	0.73	40	0.76
ED-20 + DADPS + 10 % Ultem 1010	0.038	35	0.82	28	0.88
ED-20 + DADPS + 20 % PSK-1	0.182	53	0.60	49	0.65
ED-20 + DADPS + 20 % Ultem 1010	0.202	52	0.61	48	0.66

\*Each  $\theta$  value is the result of averaging of ten measurements.

It is evident that, with an increase in the content of any of the modifiers, the viscosity of the binder significantly increases (by about two orders of magnitude), particularly in the case of using PEI. The fact that



the change in  $\theta$  during curing (at  $180^\circ\text{C}$ ) does not depend on the initial viscosity of the compositions is apparently attributed to the extremely high rate of the network formation process and a slight effect of the introduced modifiers on this rate. Thus, the presence of thermoplastics worsens the wetting of a solid (glass) surface with the ED-20 resin at the deposition time; however, it has little effect on the variation in  $\theta$  during curing.

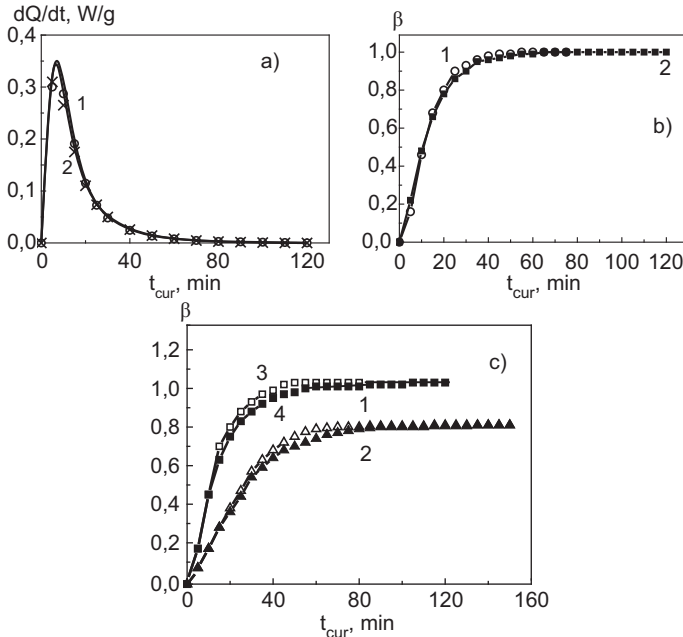


Fig. 2-1. Variation in (a) heat flow  $dQ/dt$  and (b, c) reactive group conversion  $\beta$  during the isothermal curing of the ED-20 resin modified with thermoplastics: (a, b) ED-20+DADPS (1) and ED-20+DADPS+10% PAEK (2) at a curing temperature of  $180^\circ\text{C}$ ; (c) ED-20+DADPS (1, 3) and ED-20+DADPS+10% PSK-1 (2, 4) at a curing temperature of (1, 2)  $160^\circ\text{C}$  and (3, 4)  $180^\circ\text{C}$ .

Figure 2-1 shows typical curves representing the kinetics of the isothermal curing of the studied compositions at  $160$ – $190^\circ\text{C}$  [134, 135]. The curves were recorded by differential scanning calorimetry (DSC), which is the most commonly used method for studying the curing of reactive oligomers. According to Fig. 2-1, the introduction of 10 wt % of a heat-resistant thermoplastic has a negligible effect on the kinetics of the structure formation process: the unmodified and modified epoxy resins are characterized not only by identical shapes of the  $dQ/dt$ – $t_{cur}$  and  $\beta$ – $t_{cur}$  curves,

but also by similar  $dQ/dt$  and  $\beta$  values at any curing time  $t_{\text{cur}}$ . However, it should be noted that, upon the introduction of PSF PSK-1 into ED-20, a certain slowdown in the curing process is observed in the initial portion.

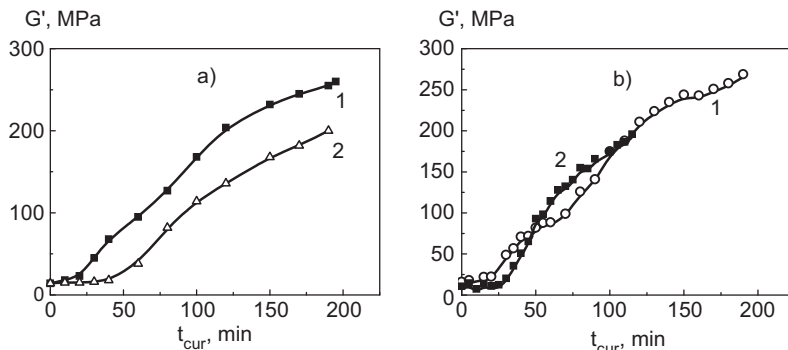


Fig. 2-2. Variation in the shear modulus during the isothermal curing of the thermoplastic-modified ED-20 resin at 180°C: (a) ED-20+DADPS (1) and ED-20+DADPS+10%PSK-1 (2); (b) ED-20+DADPS (1) and ED-20+DADPS+10%PAEK (2).

The decrease in the cure rate recorded by both methods is most probably attributed to the fact that the introduction of a thermoplastic component leads to an increase in the viscosity of the reaction mixture and, in addition, a decrease in the reactive group concentration owing to the “dilution” of the cured composition (epoxy oligomer) with the thermoplastic.

A typical curve of variation in the glass transition temperature of epoxy resin–PSF blends in the first hours of curing is shown in Fig. 2-3; Table 2-2 lists the glass transition temperatures of the studied systems cured at different temperatures to the cure depth that is maximal at each of these temperatures.

With an increase in the curing temperature of the composition,  $T_g$  increases. This fact is apparently attributed to the higher depth of occurrence of the curing process. In addition, it is evident that the introduction of PSF leads to a slight decrease in the  $T_g$  value of the composition at a curing temperature of 160°C, while the introduction of PAEK increases this parameter. According to [129–131],  $T_g$  values can be used as a measure of the degree of curing of the material.

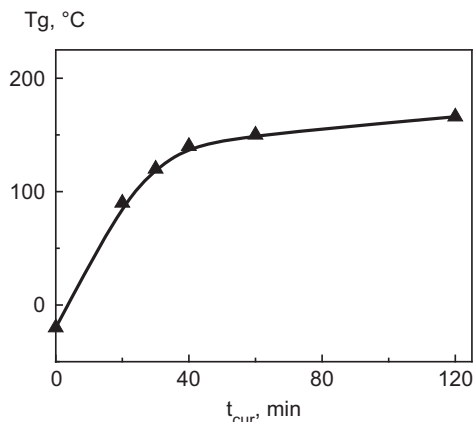


Fig. 2-3. Variation in the glass transition temperature of the ED-20+DADPS composition at the isothermal curing at 180°C.

**Table 2-2. Effect of the curing temperature on the glass transition temperatures of unmodified and modified epoxy compositions\***

Composition	Curing temperature, °C							
	160		170		180		190	
	$T_g$ , °C TM A	$T_g$ , °C DM A	$T_g$ , °C TM A	$T_g$ , °C DM A	$T_g$ , °C TM A	$T_g$ , °C DM A	$T_g$ , °C TM A	$T_g$ , °C DM A
ED-20+DADPS	171	175	179	174	185	190	196	195
ED20+DADPS+ 10%PSK-1	164	165	174	172	190	185	199	194
ED20+DADPS+10 %PAEK	174	175	173	180	198	200	–	–

\*The glass transition temperatures were determined as follows: TMA, from thermomechanical curves; DMA, from the  $tg\delta$  maximum.

However, Table 2-2 shows that the glass transition temperatures  $T_g$  of the unmodified and modified compositions can differ by 10–13°C, while the levels of conversion determined by the DSC method are close (Fig. 2-1).

The temperature dependences of  $tg\delta$  of cured polymers containing PSK-1 exhibit two maxima; this fact suggests that the system underwent phase separation [134].

Comparison of the data in Table 2-2 shows that the use of PAEK as a modifier of the ED-20 oligomer provides the formation of epoxy compositions exhibiting a heat resistance that is 10–15°C higher than that of PSF-modified compositions.

The pattern of establishment of the adhesive strength during curing can be determined from the data in Figs. 2-4–2-7.

It is evident from the dependences shown in Figs. 2-4 and 2-6 that, for all systems—modified and unmodified—that were cured under conditions providing the achievement of a reactive group conversion of 70–80%, adhesive strength  $\tau$  generally decreases with an increase in the polymer–fiber contact area; the particularly abrupt decrease in  $\tau$  is observed at low  $S$  values (low  $l/d$  values;  $S \leq 0.5 \text{ mm}^2$ ;  $l/d \leq 6$ ).

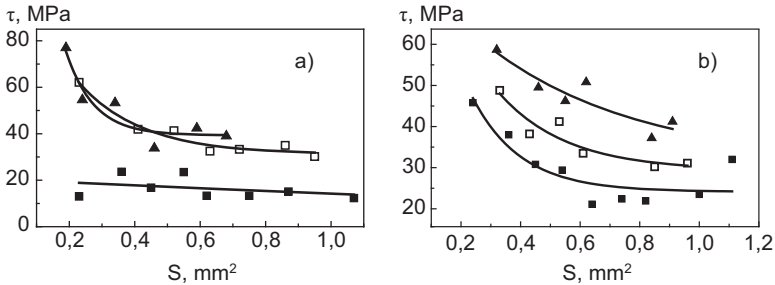


Fig. 2-4. Dependence of the adhesive strength on contact area in the ED-20+DADPS–steel wire system ( $d = 150 \mu\text{m}$ ) at a curing temperature of (a) 160 and (b) 180°C and a curing time of (a) (■) 45, (▲) 105, and (□) 600 min; (b) (■) 30, (▲) 60, and (□) 360 min.

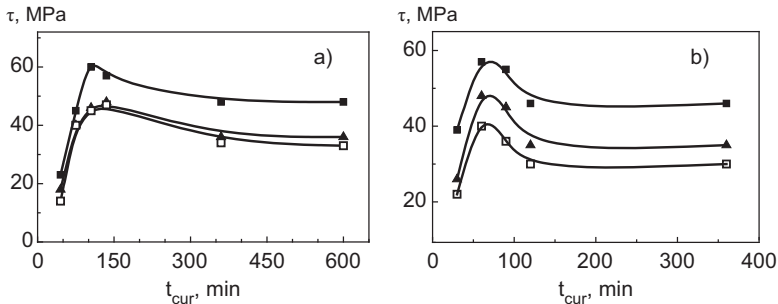


Fig. 2-5. Dependence of the adhesive strength on curing time in the ED-20+DADPS–steel wire system ( $d = 150 \mu\text{m}$ ) at a curing temperature of (a) 160 and (b) 180°C;  $S =$  (■) 0.35, (▲) 0.55, and (□) 0.85  $\text{mm}^2$ .

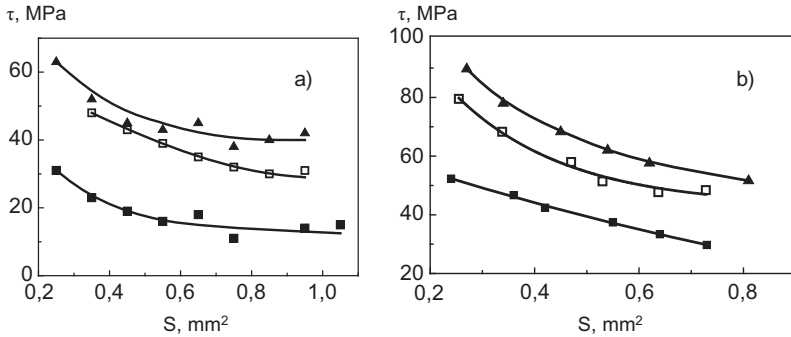


Fig. 2-6. Dependence of the adhesive strength on contact area in modified epoxy binder–steel wire joints ( $d = 150 \mu\text{m}$ ) at a curing temperature of  $180^\circ\text{C}$ :

(a) ED-20+DADPS+15%PSK-1 and (b) ED-20+DADPS+10%PAEK and a curing time of (■) 30, (▲) 90, and (□) 360 min.

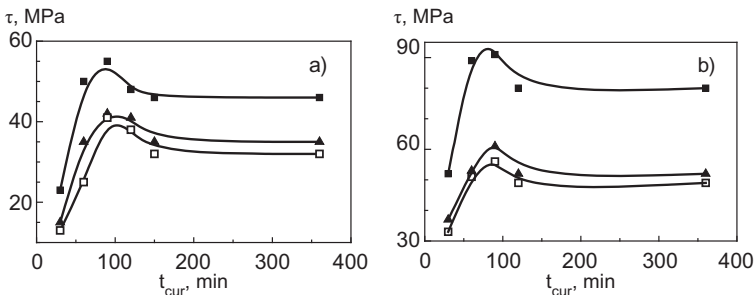


Fig. 2-7. Dependence of the adhesive strength on curing time in modified epoxy binder–steel wire joints ( $d = 150 \mu\text{m}$ ) at a curing temperature of  $180^\circ\text{C}$ :

- (a) ED-20+DADPS+15%PSK-1 and (b) ED-20+DADPS+10%PAEK.  
 (b) Area of adhesive joints: (a) (■)  $0.35$ , (▲)  $0.55$ , and (□)  $0.85 \text{ mm}^2$ ;  
 (c) (b) (■)  $0.25$ , (▲)  $0.55$ , and (□)  $0.65 \text{ mm}^2$ .

It was shown [30, 31] that the main cause of the decrease in  $\tau$  with an increase in the  $S$  value is thermally induced residual stresses  $\tau_{\text{res}}$ . As noted in Chapter 1, they arise at the interface owing to different mechanical and thermal characteristics of the pair (adhesive–fiber). Their values are maximal at the ends of the adhesive joint, pass through zero in the middle of the joint, and depend on joint length  $l$ : they increase with an increase in  $l$ . Upon loading of a joint, maximum stresses arise in the field of application of an external force. Here, the stresses generated by the applied force are added to the existing residual stresses. If we assume that the concepts developed in [30, 31] are true and that failure occurs when the sum of all the stresses acting at the place of their maximum concentration

exceeds the local adhesive strength  $\tau_{loc}$ , then the failure condition can be written as follows:

$$\tau_{exp} + \tau_{res} = \tau_{loc}.$$

The  $\tau_{loc}$  value is determined only by physicochemical interactions at the interface; it does not depend on the shape and size of the specimens, the conditions of their fixation, etc. For this interacting pair,  $\tau_{loc}$  is a constant value. Accordingly, the higher the residual stresses, the lower the external loads at which the interfacial failure occurs. As noted above (all other conditions being equal), the  $\tau_{res}$  values increase with an increase in  $S$ . Therefore, the adhesive strength values measured in experiments  $\tau_{exp}$  decrease with an increase in  $S$ .

The data shown in Figs. 2-4 and 2-6 suggest that, during curing, adhesive strength changes nonmonotonically both for the unmodified epoxy adhesive and for the epoxy resin-PSF and epoxy resin-PAEK blends (Figs. 2-4b, 2-6a, 2-6b): the  $\tau$ - $S$  curves corresponding to curing times of 60 (or 90) min lie higher than the  $\tau$ - $S$  curves recorded after the curing of the joints for 6 h. The nonmonotonic change in  $\tau$  is particularly pronounced in Figs. 2-5 and 2-7. The shown curves are typical: for all the studied adhesives, the  $\tau$ - $t_{cur}$  dependences in joints with fibers are described by curves with a maximum. The higher the curing temperature, the faster (all other conditions being equal) the adhesive strength achieves a maximum value. If the curing time is longer than the time at which the maximum appears in the curve, then the adhesive strength slightly decreases and then remains almost constant, even in the case of a long-term heating. The adhesive strength values of the compositions cured to the maximum possible depth at 160 and 180°C are almost identical (Fig. 2-5).

With an increase in the percentage of the thermoplastic, the shape of the interfacial strength-curing time curves does not change. However, the adhesive strength values for systems containing 10–15% PSK-1 or 10% PAEK are significantly higher than those for the “pure” composition (Fig. 2-8).

The introduction of the PAEK modifier also leads to a certain increase in the time at which a maximum is observed in the  $\tau$ - $t_{cur}$  curve: thus, for the unmodified adhesive and the PAEK-modified specimen, the maximum is observed 75 and ~100 min after the onset of curing, respectively. The dynamics of variation in the position of the maximum in the  $\tau$ - $t_{cur}$  curve can also be attributed to the fact that the introduction of the modifier leads to a significant increase in the viscosity of the composition; as a

consequence, the rate of the curing reaction slightly decreases and the formation of a contact between the polymer and the fiber is complicated.

The  $\tau$ - $t_{\text{cur}}$  curves similar to those shown in Figs. 2-5, 2-7, and 2-8 were previously observed for various epoxy resins, namely, epoxy-diane, epoxy-resorcinol, and epoxy-aniline resins [30, 31]. For joints in which the adhesive is a blend of thermosetting and thermoplastic polymers, similar curves were recorded in [134,135,139]. The preservation of the shape of the curves for this class of materials indicates that the kinetics of variation in the adhesive strength of polymer-fiber joints during curing is largely controlled by physical factors (network density, residual stresses, relaxation processes, etc.) in the absence of a chemical reaction between the thermoplastic modifier and the epoxy oligomer. The chemical nature of the adhesive components, the degree of purity of the polymer products, the types of the occurring reactions, and other factors determine only the interfacial strength, rather than the shape of the  $\tau$ - $t_{\text{cur}}$  curves.

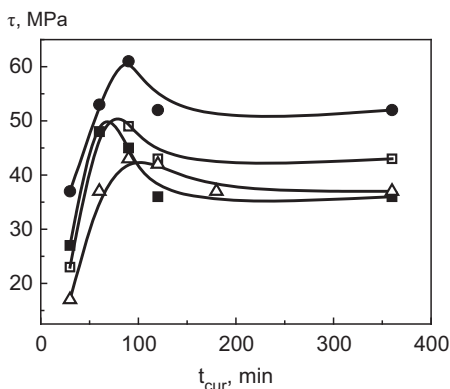


Fig. 2-8. Dependence of adhesive strength on curing time for joints between epoxy binders of different compositions and a steel wire ( $d = 150 \mu\text{m}$ ): (■) ED-20+DADPS, (□) ED-20+DADPS+10%PSK-1, (Δ) ED-20+DADPS+15%PSK-1, and (●) ED-20+DADPS+10%PAEK at a curing temperature of  $T_{\text{cur}} = 180^\circ\text{C}$ . Area of adhesive joints is  $S = 0.55 \text{ mm}^2$ .

The kinetics of variation in the interfacial strength during the formation of joints between fibers and epoxy resin-thermoplastic bipolymer blends is described for systems in which the substrate was steel fibers. However, as noted above, in studying the  $\tau$ - $t_{\text{cur}}$  dependences for a whole set of epoxy binders [30, 31], it was shown that the pattern of the relationships is preserved if any other fibers with a high surface energy are used. Therefore, it can be assumed that the relationships revealed in this book

will also hold true for the interaction of epoxy resin–thermoplastic blends with boron, glass, and other fibers.

After the brief discussion of the kinetics of formation of a network structure and the mechanical properties of unmodified and modified epoxy compositions, we can consider factors that are responsible for changes in adhesive strength during curing and the occurrence of a maximum in the  $\tau$ – $t_{\text{cur}}$  curve.

The shape of the dependences in Figs. 2-5 and 2-7 shows that the adhesive strength of the polymer–fiber system is not established instantaneously: it is a process that develops over time. It is evident that the kinetics of variation in adhesive strength is determined by at least two processes; one of them is responsible for the increase in  $\tau$  values; the other, for their decrease; it is a superposition of these processes that leads to the existence of curves with a maximum.

As noted above, in the initial portion of the  $\tau$ – $t_{\text{cur}}$  curve, the  $\tau$  values are negligible; that is, the establishment of adhesive strength begins with an induction period. A detailed study of the change in adhesive strength during curing was conducted in [30, 31] for joints of an EDT-10 binder (based on the same ED-20 epoxy–diane resin modified with diethylene glycol). It was shown that the existence of an induction period is an objective fact. It is associated with the difference between the kinetics of bond formation at the interface and the kinetics of bond formation in the polymer bulk, rather than with the measurement method used. The extremely low adhesive strength values measured during the induction period represent the fact that the number of bonds at the interface is still small. After the induction period, a rapid increase in the adhesive (interfacial) strength values is observed; it is most natural to attribute this fact to an increase in the number of bonds acting at the fiber–binder interface. It is observed at the same time at which the curing depth, glass transition temperature, and mechanical characteristics of the polymer significantly increase (Figs. 2-1–2-3).

If the cause of an increase in adhesive strength is an increase in the number of bonds formed at the interface, then the most probable cause of a decrease in adhesive strength is an increase in the residual stresses arising at this interface.

It was shown that, during the curing of the composition, a three-dimensional binder structure is formed; with an increase in the density of the formed network, the polymer strength and rigidity increase and the  $T_g$  value of the polymer changes. Accordingly, there should be an increase in the thermoelastic stresses arising at the interface during the cooling of the system from the curing temperature (160–180°C) to the temperature at



which the adhesive strength is measured (in this particular case, to room temperature).

Currently, these residual stresses cannot be measured directly because of the lack of measurement methods. The general picture of their change under the action of a factor can be represented by measuring them on flat joints, for example, using the cantilever beam deflection method (see A8).

The pattern of increase in these stresses during network formation in modified epoxy compositions can be determined using the results shown in Fig. 2-9. It is evident that, for all the studied systems, residual stresses monotonically increase. The time at which the stresses become constant is close to the time when the adhesive strength values cease to change. The steady-state values of residual stresses depend on the blend composition. They are maximal for the unmodified binder and decrease by 27–33% for matrices containing 10–15 wt % PSF. In the case of the modifying of the epoxy–diane oligomer with PAEK, the stress values decrease even more significantly—by 62%. Upon the introduction of the different thermoplastics (PAEK and PSK-1) into the epoxy oligomer, the general shape of the  $\sigma_{\text{res}}-t_{\text{cur}}$  curves does not change. A decrease in the residual stresses leads to an increase in the measured adhesive strength values [30, 31]. Therefore, it is only natural that the maximum  $\tau$  values in the  $\tau-t_{\text{cur}}$  curve are observed for the epoxy oligomer modified with PAEK (Fig. 2-8).

The data shown in Fig. 2-9 were obtained by the cantilever beam deflection method (see A8). Accordingly, they show only the general pattern of variation in residual stresses during curing, because the data were obtained for specimens whose shape and sizes differ from those of the polymer–fiber joints studied in this book.

The laws governing the variation in the interfacial strength of polymer–fiber joints during the curing of epoxy resin–PAEK and epoxy resin–PSF blends are similar: in both cases the  $\tau-t_{\text{cur}}$  (adhesive strength–curing time) dependences are described by curves with a maximum; in addition, the  $\tau$  values at the maximum are higher than those of the unmodified epoxy resin; during curing, residual stresses increase along the curve with saturation; the steady-state values of residual stresses for the blends are lower than those for the unmodified epoxy resin; for all the systems, the scale dependences of adhesive strength are described by smooth monotonically decreasing curves.

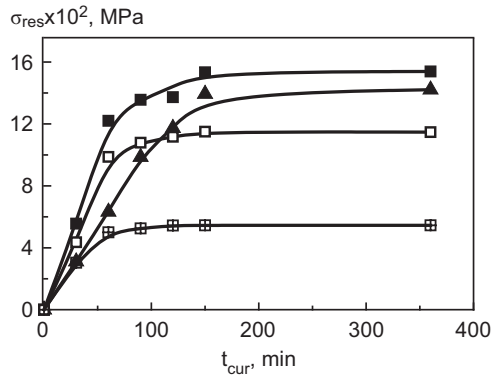


Fig-2.9. Dependence of residual stresses measured by the cantilever beam deflection method on curing time for different compositions and curing temperatures:

- (■) ED-20+DADPS,  $T_{cur} = 180^{\circ}\text{C}$ ; (▲) ED-20+DADPS,  $T_{cur} = 160^{\circ}\text{C}$ ;
- (□) ED-20+DADPS+10% PSK-1; and (⊞) ED-20+DADPS+10%PAEK.

Thus, we can state that there exist general laws that govern the variation in adhesive strength during the curing of epoxy resin–heat-resistant thermoplastic blends. The mechanisms providing the observed laws are most probably identical. The increase in adhesive strength at the initial stage of curing is associated with the fact that bonds responsible for interfacial interactions are formed at the interface. The decrease in adhesive strength (after achieving of a maximum) is determined by the generation (appearance and increase) of residual stresses.

It was shown above that the laws governing the variation in adhesive strength during curing are identical for unmodified and modified epoxy resins. Accordingly, the results obtained in studying the variation in the interfacial strength of epoxy resins modified with heat-resistant thermoplastics confirm the previous conclusions [30, 31] that the kinetics of variation in the interfacial strength in polymer–fiber joints during curing is largely controlled by physical, rather than chemical factors.

# CHAPTER THREE

## ADHESIVE STRENGTH OF FIBER–MODIFIED EPOXY MATRIX JOINTS UNDER OPERATING CONDITIONS

The first chapter was focused on a detailed analysis of the behavior of the interface in fiber–polymer joints for cases where the adhesive is epoxy oligomers modified with various amounts of an active diluent, a heat-resistant thermoplastic, or a fine filler. All the given adhesive strength values were determined at room temperature and a constant loading rate of  $\dot{F} = 1 \text{ N/s}$ .

However, fiber composites based on epoxy matrices are commonly used at various temperatures under not only quasi-static, but also dynamic loading. In addition, composite materials can be stored and used in various liquid and gaseous media. Accordingly, to effectively design these composite materials, it is necessary to know the behavior of the adhesive strength of the components in a fiber–matrix system under these conditions, i.e., in a model of the unit cell of a fiber-reinforced plastic.

Some data on the adhesive strength of fiber–modified epoxy resin joints under these conditions will be given in this chapter.

### *3.1. Effect of Test Temperature*

The behavior of the interface of polymer–fiber joints with a change in test temperature  $T$  was described in considerable detail and discussed in monographs [30, 31]. Analysis of the temperature dependences of adhesive strength that were recorded for a number of thermosetting (epoxy, epoxyphenol, phenol formaldehyde, Butvar phenolic, polyester, polysiloxane) and thermoplastic matrices (mostly polyolefin) interacting with glass, carbon, steel, boron, and polyheteroarylene fibers makes it possible to formulate general physical laws governing changes in the interfacial strength of these joints:

(i) In a wide temperature range covering both the glassy and rubberlike states of the adhesive, not only the values of adhesive strength  $\tau$ , but also the shape of the  $\tau$ - $T$  curves depends on the size of the joints (area  $S$ , their length  $l$ , and  $l/d$  ratio).

(ii) The value of local adhesive strength  $\tau_{loc}$ , which characterizes a given interacting fiber-matrix pair and is determined only by physicochemical interactions across the interface, monotonically decreases with an increase in temperature. The  $\tau_{loc}$ - $T$  curve is clearly divided into three regions: in the region of the glassy state of the adhesive, the  $\tau_{loc}$  values decrease quite slowly with an increase in temperature; the rate of decrease in  $\tau_{loc}$  is maximal in the softening region of the adhesive and negligible (close to zero) above this region. The same pattern of decrease in adhesive strength  $\tau$  with an increase in temperature is observed in joints with a small area, at  $l/d \approx 2-5$ . For large-sized joints ( $l/d \geq 7-20$ ), the variation in the interfacial strength with an increase in temperature is described by curves with a maximum. In this case, the larger the specimen size ( $l/d$  ratio), the more pronounced the maximum.

(iii) The main cause of the complex pattern of the temperature dependence of the measured adhesive strength values in joints with  $l/d \geq 7-20$  is the effect of thermally induced residual stresses  $\tau_T$  acting at the interface.

(iv) The shape of the temperature dependence of local adhesive strength is similar to that for the cohesive strength of a polymer adhesive. At  $T < T_g$  of the adhesive, changes in the  $\tau_{loc}$  value of the polymer-fiber system, in common with changes in the cohesive strength of the polymer, are determined by the thermofluctuation mechanism. The similarity of the laws apparently suggests that the adhesive and cohesive strengths are of the same nature.

(v) A high adhesive strength of a fiber filler-matrix pair can be preserved at temperatures at which the polymer is in the glassy state. Accordingly, the design of more heat-resistant adhesives requires the design of more heat-resistant matrices.

The above generalizations were made in analyzing many diverse adhesive pairs. However, it is still of interest to study each new pair, because the study shows whether the revealed laws are valid for other systems and, thereby, confirms their generality or indicates their limitations.

Below, results of studying the temperature dependence of the adhesive strength of a heat-resistant multicomponent epoxy composition, which consists of epoxy-novolak resin UP-643 and epoxy-amine resin UP-610 modified with the DEG-1 reactive diluent, in joints with fibers are

described. The curing agent was DADPS. The measurement procedure is described in A9.

Fig. 3-1 shows typical dependences of the adhesive strength of the studied joints on their sizes: at 20°C, when the adhesive is in the glassy state; at 200°C in the transition region; and at 250°C on the upper boundary of the softening region of the adhesive, when it passes into the rubberlike state. (The glass transition temperature of the adhesive determined by the DMA method is 215°C.)

It is evident that, at room temperature, the original (unmodified) composition provides a fairly high—at the level of the best epoxy resins—interfacial strength  $\tau$ .

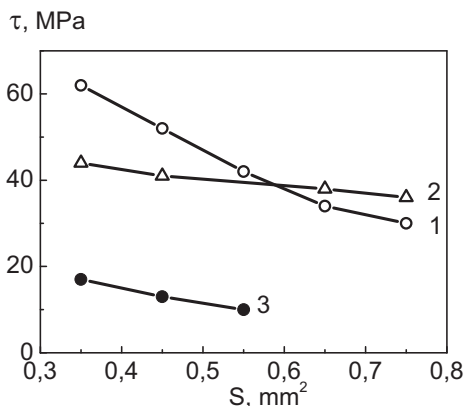


Fig. 3-1. Dependence of the adhesive strength of the epoxy–amine composition–steel wire system ( $d = 150 \mu\text{m}$ ) on the area of joints at the different test temperatures: (1) 20, (2) 200, and (3) 250°C.

With an increase in the area of joints, the  $\tau$  values decrease, as commonly observed for fiber–matrix joints. The lower the measurement temperature, the more abrupt the decrease in the  $\tau$  values with an increase in  $S$ . Thus, an increase in the area of joints from 0.3 to 0.6 mm<sup>2</sup> ( $l/d$  changes from 4 to 8) at room temperature leads to a decrease in the interfacial strength by ~30 MPa; at 200 and 250°C, it is as low as 9–11 MPa (Fig. 3-1). As noted above, a decrease in adhesive strength with an increase in the adhesive–fiber contact area represents the existence of a nonuniform field of residual stresses, primarily, thermally induced stresses, at the interface. With an increase in the test temperature (while approaching the softening region of the adhesive), the residual stresses decrease. Therefore, an increase in temperature leads not only to a change

in the adhesive strength values, but also to the weakening of the  $\tau$ - $S$  dependence, which becomes less pronounced (Fig. 3-1).

The existence of thermally induced residual stresses at the interface is particularly evident from the dependence of the shape of the  $\tau$ - $T$  curves on the size of the joints (see Fig. 3-2). Above the glass transition region, the adhesive strength  $\tau$  values measured in the test are extremely low for specimens of any size. An increase in  $\tau$  values is observed upon the cooling of the specimens, upon the transition of the matrix (adhesive) to the glassy state. In this case, for joints with a small area (in our case, at  $S = 0.35 \text{ mm}^2$ ,  $l/d \approx 4-5$ ), the  $\tau$  values monotonically increase with a decrease in temperature; for joints with  $l/d \approx 6-7$  ( $S = 0.45 \text{ mm}^2$ ), the  $\tau$  values do not depend on temperature, and for joints with  $l/d \geq 7$  ( $S \geq 0.55 \text{ mm}^2$ ), the  $\tau$  values are described by curves with a maximum. Thus, for the same adhesive pair, diverse shapes of  $\tau$ - $T$  curves can be observed; in addition, the shapes of the curves regularly change with a change in the size of the joints.

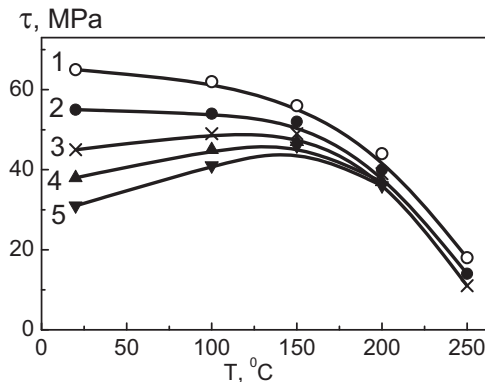


Fig. 3-2. Effect of the test temperature on the adhesive strength of epoxy-amine composition-steel wire joints ( $d = 150 \mu\text{m}$ ):  $S = (1) 0.35, (2) 0.45, (3) 0.55, (4) 0.65, \text{ and } (5) 0.75 \text{ mm}^2$ .

The appearance of various types of  $\tau$ - $T$  curves is schematically shown in Fig. 3-3.

Here, the concept of local adhesive strength ( $\tau_{loc}$ ) introduced in [30, 31] and a criterion for the failure of polymer-fiber adhesive joints proposed in the cited manuscripts are used. It is assumed that an adhesion joint undergoes failure when the sum of all tangential stresses acting at the interface—applied external stresses (measured in the experiment) and

stresses existing at the interface before applying the load (residual)—becomes equal to the local adhesive strength:

$$\tau_{\text{exp}} + \tau_{\text{res}} \approx \tau_{\text{loc}}.$$

The schemes shown in Fig. 3-3 were constructed taking into account the fact that local adhesive strength  $\tau_{\text{loc}}$  monotonically increases with a decrease in temperature (this fact was revealed in experiments in [30, 31]) and, for adhesives in the glassy (solid) state, the  $\tau_{\text{T}}$  values increase approximately linearly with cooling. The last statement follows from the theoretical consideration of thermally induced residual stresses in [30, 31]; an experimental confirmation of this statement is given in the cited manuscripts.

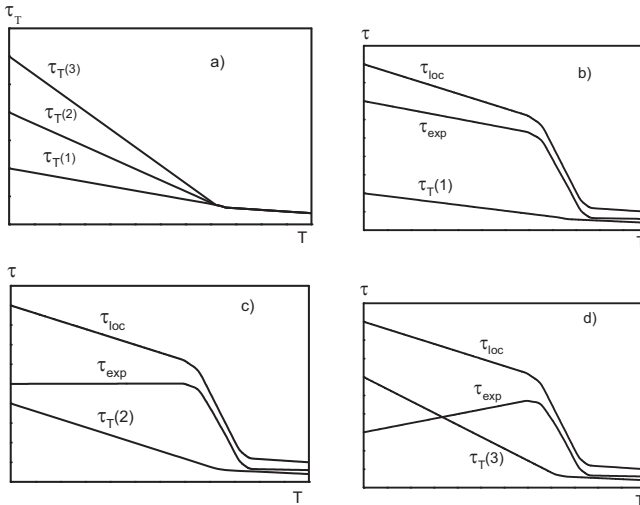


Fig. 3-3. Schematic appearance of various types of temperature dependences of the adhesive strength of polymer–fiber joints: (a) thermally induced residual stresses  $\tau_{\text{T}}$  ( $\tau_{\text{T}(1)}$ ,  $\tau_{\text{T}(2)}$ , and  $\tau_{\text{T}(3)}$  values correspond to joints with contact areas  $S_1 < S_2 < S_3$ ) and (b–d) temperature dependences of  $\tau_{\text{loc}}$ ,  $\tau_{\text{T}}$ , and  $\tau_{\text{exp}} = \tau_{\text{loc}} - \tau_{\text{T}}$ .

The schemes in Fig. 3-3 show that the  $\tau_{\text{exp}}-T$  curves measured in the experiment can have diverse shapes. In the glassy state, with an increase in temperature, the  $\tau_{\text{exp}}$  values can monotonically decrease (Fig. 3-3b), remain constant (Fig. 3-3c), and pass through a maximum (Fig. 3-3d). As shown above (Fig. 3-2), all three types of curves were observed in the experiments. In accordance with the schemes shown in Fig. 3-3, in the region of transition from the glassy to rubberlike state, the measured  $\tau_{\text{exp}}$  values should significantly decrease. The experiments confirm this assumption (Fig. 3-2).

Thus, the obtained new experimental data are consistent with the earlier proposed pattern of failure of polymer-fiber adhesive joints. They show the role of thermally induced residual stresses in pull-out tests and provide still more evidence of the efficiency of using the local adhesive strength concept.

The pattern of change in the strength of the interface between the studied epoxy binder and steel fibers in a wide temperature range is in good agreement with the pattern observed earlier for a number of systems. As a case in point, Fig. 3-4 shows the effect of temperature on the adhesive strength of the EDT-10 epoxy binder.

It is evident that the  $\tau$ - $T$  curves in Figs. 3-2 and 3-4 are really similar. The lower heat resistance of the EDT-10 resin ( $T_g = 80^\circ\text{C}$ ) is evident from the fact that the maxima in Fig. 3-4 are observed at  $\sim 30^\circ\text{C}$ , whereas for a more heat-resistant unmodified test binder, they are observed at  $150^\circ\text{C}$ . The introduction of up to 20 wt % of the DEG-1 reactive glycidyl-containing active diluent into the original composition leads to the plasticization of the composition and a decrease in the glass transition temperature. The  $T_g$  values decrease linearly with an increase in the DEG-1 concentration, namely, by  $\sim 25^\circ\text{C}$  after the addition of every 10 wt % of the modifier. With an increase in the amount of the introduced modifier, the  $\tau$  values monotonically decrease (Fig. 3-5).

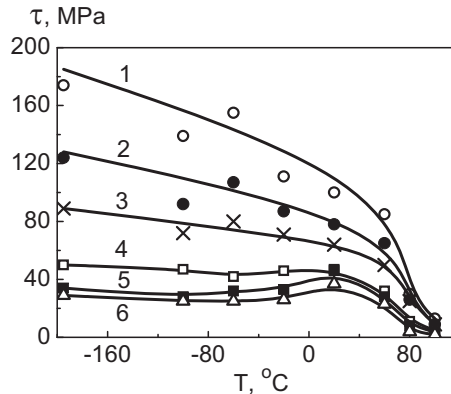


Fig. 3-4. Temperature dependence of the adhesive strength of the EDT-10 binder-steel wire system ( $d = 150 \mu\text{m}$ ):  $S = (1) 0$  ( $\tau = \tau_{\text{loc}}$ ), (2) 0.15, (3) 0.25, (4) 0.55, (5) 0.95, and (6) 1.15  $\text{mm}^2$  [30, 31]. The  $\tau_{\text{loc}}$  value is determined from the experimental data via extrapolating the  $\tau(S)$  curve to zero:

$$\tau_{\text{loc}} = \lim_{S \rightarrow 0} \tau_{\text{exp}} = \lim_{S \rightarrow 0} (F/S).$$



This effect is observed both at 20°C, when all the compositions are in the glassy state, and at a temperature of 200°C, at which two of them (unmodified composition and the sample containing 5 wt % DEG-1) are in the transition region and the other two (containing 10 and 20 wt % DEG-1) are at the upper boundary of this region. Accordingly, at room temperature, the decrease in the  $\tau$  values is slight, namely, 10–15% relative to the  $\tau$  values of the unmodified resin; at 200°C, the decrease achieves 35–42%.

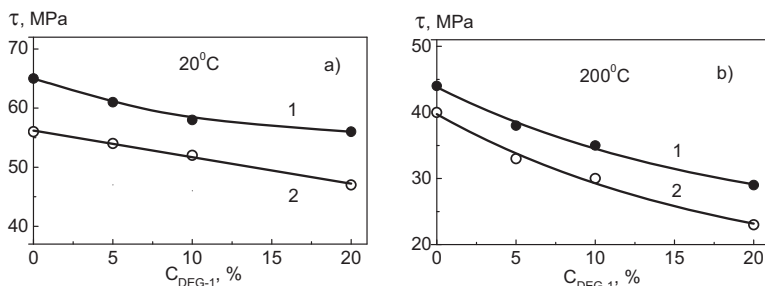


Fig. 3-5. Dependence of the adhesive strength of steel wire–modified epoxy–amine binder joints ( $d = 150 \mu\text{m}$ ) on concentration  $C$  of the DEG-1 modifier in the adhesive at varying temperature;  $S = (1) 0.35$  and  $(2) 0.45 \text{ mm}^2$ . (a) 20 and (b) 200°C.

This effect is observed both at 20°C, when all the compositions are in the glassy state, and at a temperature of 200°C, at which two of them (unmodified composition and the sample containing 5 wt % DEG-1) are in the transition region and the other two (containing 10 and 20 wt % DEG-1) are at the upper boundary of this region. Accordingly, at room temperature, the decrease in the  $\tau$  values is slight, namely, 10–15% relative to the  $\tau$  values of the unmodified resin; at 200°C, the decrease achieves 35–42%.

The causes of the decrease in the  $\tau$  values upon modifying epoxy resins with the DEG-1 active diluent were discussed in detail in Section 1.1. It was shown there that an increase in the amount of the plasticizer is equivalent to an increase in the measurement temperature at which, according to [30, 31], the adhesive strength decreases (for small joints with  $l/d \leq 6-7$ ).

The general pattern of the temperature curves of the adhesive strength of steel wire–modified epoxy resin joints over a wide temperature range remains the same as that of joints with the unmodified resin.

However, since both the glass transition temperature and the region of transition of the adhesive from the glassy to rubberlike state decrease with the addition of DEG-1, the region of an abrupt decrease in adhesive strength with an increase in the concentration of DEG-1 introduced into the composition takes place at lower temperatures (Fig. 3-6); the position of the maximum in the temperature curves of adhesive strength also depends on the plasticizer concentration: for the unmodified composition, the maximum  $\tau$  value is observed at 150°C, i.e., 65°C lower than the glass transition temperature of this composition; for the compositions modified with 20 wt % DEG-1, the maximum is observed at 100°C (compare Figs. 3-2 and 3-6), i.e., also approximately 65°C below  $T_g$ , which for these compositions is  $T_g \approx 167^\circ\text{C}$ .

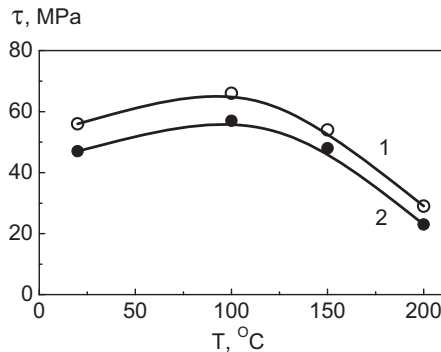


Fig. 3-6. Temperature dependences of the adhesive strength of joints between an epoxy-amine binder modified with 20 wt % DEG-1 and a steel wire ( $d = 150 \mu\text{m}$ ). Area of joints: (1) 0.35 and (2) 0.45 mm<sup>2</sup>.

Thus, the data obtained in studying the effect of test temperature on the adhesive strength of systems composed of fibers and a plasticized epoxy-amine binder, which consists of a large number of components and exhibits a higher heat resistance than that of the epoxy matrices studied in [30, 31], are in good agreement with the previously found laws and, therefore, confirm the generality of these laws. The data provide still more evidence of the fact that, since the measured values of adhesive strength  $\tau$  depend on the chemical nature of the components constituting the pair, the pattern of the change in the interfacial strength is determined primarily by the laws of the physicochemical processes that occur in the system with a change in temperature. These processes are associated with a nonuniform distribution of stresses at the interface, the existence of residual stresses at this interface, stress relaxation, etc.

### 3.2. Effect of Loading Rate on the Interfacial Strength of Fiber–Modified Epoxy Matrix Joints

In studying the interaction of various adhesives (epoxy, phenolic, polyester, etc.) with fibers [30, 31], it was found that, at low loading rates of  $\dot{F} \leq 1$  N/s, the adhesive strength in fiber–thermosetting matrix joints depends on the external load application rate, namely, it increases with an increase in the rate. To the best of our knowledge, there are not published data on the effect of loading rate on the interfacial strength with a change in the concentration of one of the components of the adhesive.

Below, this effect will be discussed for epoxy oligomers modified with an active diluent or a heat-resistant thermoplastic taken in various amounts.

#### 3.2.1. Interfacial strength in fiber–active diluent-modified epoxy resin systems under quasi-static loading

Fig. 3-7 shows typical scale dependences of the adhesive strength of the ED-20+TEAT+DEG-1–steel wire system at extremely low loading rates. It is evident that a decrease in the rate leads to a decrease in the measured  $\tau$  values; however, it does not change the shape of the  $\tau$ – $S$  curves: the adhesive strength monotonously and nonlinearly decreases with an increase in the size of the joints.

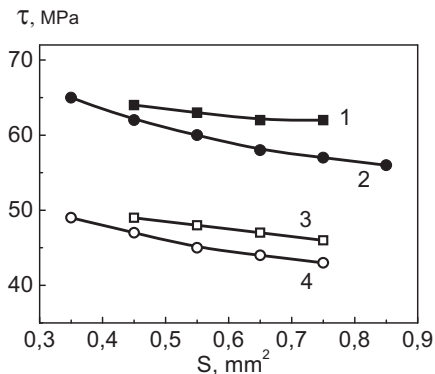


Fig. 3-7. Dependence of adhesive strength  $\tau$  on the area of joints  $S$  for steel wire–modified ED-20 epoxy resin systems ( $d = 150 \mu\text{m}$ ) at the different DEG-1 concentrations in the matrix ( $C = (1, 3) 50$  and  $(2, 4) 30\%$ ) and the different loading rates ( $\dot{F} = (1, 2) 1$  and  $(3, 4) 0.01$  N/s).

The  $\tau$ - $S$  curves characterizing the different loading rates are approximately parallel. The question of how a change in the external load application rate affects the shape of the  $\tau$ - $S$  curves was discussed in [30, 31]. It was shown that the measured adhesive strength value for joints with contact area  $S$  can be written as follows:

$$\tau(S) = \tau_{loc} - \tau_T(S). \quad (3.1)$$

As noted in Section 3.1, the value of local adhesive strength  $\tau_{loc}$  is determined only by the physicochemical interaction at the interface; it does not depend on the geometry of the specimens, the conditions for their fixation, and some other details of the experiment. It is this value that is a characteristic of this interacting pair.

The value of residual stresses  $\tau_T(S)$  in (3.1) depends on the physicommechanical characteristics of the adhesive and the substrate and on the size of the joints, namely, it increases with an increase in  $S$ . These stresses are formed during the preparation of joints, their heat treatment, and subsequent cooling to room temperature. They exist in the specimens before applying an external load to them; accordingly, they do not depend on loading rate. Therefore, Eq. (3.1) for two different loading rates can be written as follows:

$\tau_1 = \tau_{loc1} - \tau_T$ ;  $\tau_2 = \tau_{loc2} - \tau_T$ . Hence,  $\tau_1 - \tau_2 = \tau_{loc1} - \tau_{loc2}$  or, denoting  $\tau_1 - \tau_2 = \Delta\tau$ , we have

$$\Delta\tau = \tau_{loc1} - \tau_{loc2} = \text{const}. \quad (3.2)$$

Relationship (3.2) is valid for joints of any size. Thus, if the developed concepts are correct, then, for any  $S$ , at two different loading rates, the adhesive strength should differ by the same  $\Delta\tau$  value; accordingly, the  $\tau$ - $S$  curves corresponding to these rates should be parallel. However, Fig. 3-7 shows that the  $\tau$ - $S$  curves are parallel only approximately. The absence of strict parallelism is attributed to the fact that the heterogeneity of the tangential stress field at the interface is associated not only with a nonuniform distribution of the above “internal” stresses, but also with the heterogeneity of the external (applied) stress field. Since an external load is applied at different rates, relationship (3.2) is valid only approximately.

It should be noted that nearly parallel  $\tau$ - $S$  curves were previously observed for joints of epoxy, phenol formaldehyde, and polyester matrices with the same steel wire with a diameter of 150  $\mu\text{m}$  [30, 31].

The concentration dependences of the interfacial strength of ED-20+TEAT+DEG-1-steel wire joints under quasi-static loading are shown in Fig. 3-8. It is evident that, at the two rates differing by a factor of 100, the synergism of the adhesive strength is observed.

The  $\tau$  values monotonically increase with an increase in the active diluent concentration to 50%. With the addition of diethylene glycol, the increase in  $\tau$  decreases with a decrease in  $\dot{F}$ . Thus, at  $\dot{F} = 1$  N/s, the  $\tau$  values in joints with a modified matrix can be 25% higher than the  $\tau$  values in joints with the unmodified matrix; at  $\dot{F} = 0.01$  N/s, the increase in  $\tau$  does not exceed  $\sim 15\%$ .

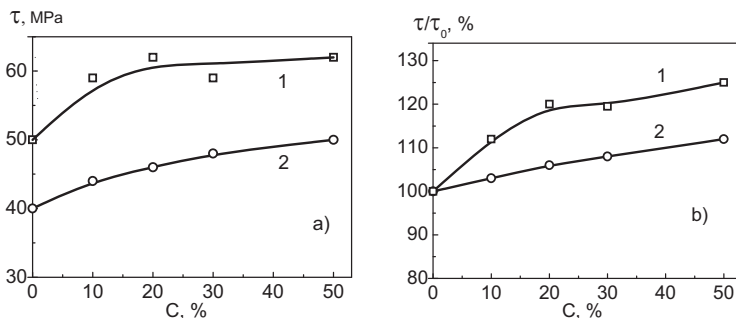


Fig. 3-8. Dependence of adhesive strength  $\tau$  of steel wire–modified ED-20 epoxy resin joints ( $d = 150 \mu\text{m}$ ) on concentration  $C$  of DEG-1 introduced into the resin:  $\dot{F} = (1)$  1 and  $(2)$  0.01 N/s; in (a) absolute and (b) relative units ( $\tau_0 = \tau$  at  $\lg \dot{t} = 2$ ;  $S = 0.65 \text{ mm}^2$ ).

The causes of increase in adhesive strength in the case of modifying the ED-20 resin with diethylene glycol are discussed in detail in Section 1.1.

Adhesive strength measurements at different loading rates make it possible to determine the sensitivity of the interface to the external load application rate. Quantitatively, it can be characterized in terms of an absolute or relative change in  $\tau$  with a change in the rate of increase in the stress by an order of magnitude, i.e., quantities  $k = d\tau/d\lg \dot{t}$  or  $K = k/\tau^0$ . It is convenient to use the  $K$  quantity to compare different systems. It was found that coefficient  $k$  remains almost constant in the studied area range (Fig. 3-9).

However, it changes nonmonotonically with an increase in the DEG-1 concentration in the binder composition (Fig. 3-10a). The highest sensitivity is observed for matrices containing 10–20% of diethylene glycol. At these concentrations, the sensitivity is 1.7–1.9 times higher than that of the unmodified matrix.

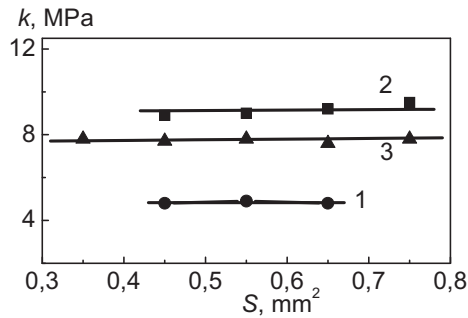


Fig. 3-9. Dependence of coefficient  $k$  on area  $S$  of the adhesive joint. Diethylene glycol concentration in ED-20: (1) 0, (2) 20, and (3) 30%.

The dependence of coefficient  $K$  on the modifier concentration (Fig. 3-10b) shows that the relative sensitivity to the loading rate is also maximal for binders containing 10–20% DEG-1: for them,  $K = 12$ –12.5%. Thus, studies of the adhesive strength in fiber-matrix joints shows that the introduction of an active diluent into an epoxy binder can change the sensitivity of the interface to the external load application rate by about 1.3 times.

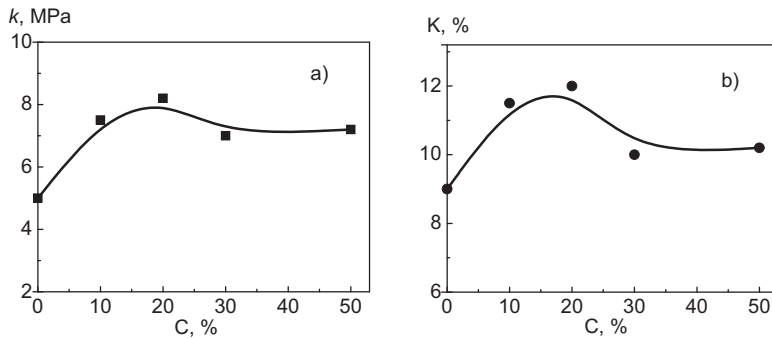


Fig. 3-10. Sensitivity of the interface to the external load application rate for joints containing different amounts of the DEG-1 active diluent in the matrix: in (a) absolute and (b) relative units.

Previously [140], for a matrix containing 10% DEG-1, adhesive strength was measured in joints with glass and carbon fibers directly used for the production of glass fiber- and carbon fiber-reinforced plastics. The tests were conducted at different loading rates covering 3 decimal orders. It was found that, although the absolute values of interfacial strength in the

joints significantly differ (see Table 3-1), the sensitivity to changes in the rate in the studied systems is almost identical:  $K = 10\text{--}12\%$ . For comparison, the authors of [141] give the coefficient  $K$  value obtained in [140] in studying the adhesive strength of a system composed of this matrix and a steel wire. The equality of the  $K$  coefficients for adhesion in the case of fibers of different chemical nature and different diameters suggests that the sensitivity to the external load application rate in the unit cell of a fiber-reinforced plastic is largely determined by the nature of the matrix.

**Table 3-1. Adhesive strength of fiber–modified epoxy matrix joints and their sensitivity to loading rate**

Fibers	$d, \mu\text{m}$	$l, \mu\text{m}$	$S \times 10^3, \text{mm}^2$	$k, \text{MPa}$	$K, \%$	$\tau^{**}, \text{MPa}$
Carbon*	7.1	56.5	1.2	10.5	12	68
Glass*	13.5	165	7.0	4.5	10	38
Steel	150	1300	650	8.5	12.5	56

\*According to [140]. \*\*At  $\lg \dot{\tau} = 0$ .

For matrices containing a different amount of DEG-1, direct measurements of adhesive strength in joints with glass and carbon fibers have not been conducted. However, there is no reason to believe that the laws revealed in these experiments will differ from those observed for compositions containing 10% DEG-1. Therefore, it can be assumed that, in the case of adhesion to industrial glass and carbon fibers, the adhesive strength increases with an increase in the amount of the introduced modifier, and the sensitivity to the external load application rate is described by a curve with a maximum.

### ***3.2.2. Interfacial strength in fiber–heat-resistant thermoplastic-modified epoxy resin systems under quasi-static loading and a low-speed impact***

It was shown in Section 1.2 that the clearest picture of change in adhesive strength caused by modifying epoxy oligomers with rigid-chain thermoplastics is observed in fiber–epoxy resin+PSF blend joints. Using the example of these joints, let us discuss how a change in the external load application rate under quasi-static and dynamic loading (under a low-speed impact) affects the interfacial strength.

It was found that a change in the loading rate leads to a change in the  $\tau$  values; however, it does not change the pattern of the scale dependences of

adhesive strength, as in the case of quasi-static loading of joints of epoxy resins modified with an active diluent.

The concentration dependences of the adhesive strength under quasi-static loading are shown in Fig. 3-11. They show that a decrease in the rate leads to a decrease in the  $\tau$  values. However, at a two orders of magnitude lower rate, the shape of the  $\tau$ - $C$  dependence does not change either: after the addition of a thermoplastic, the  $\tau$ - $C$  curve passes through a maximum, which is observed at 10 wt % PSK-1; the synergism of the interfacial strength takes place. The sensitivity of the interface to the loading rate (at extremely low rates) weakly depends on the size of the joints: the coefficient  $K$  values are 10–16%.

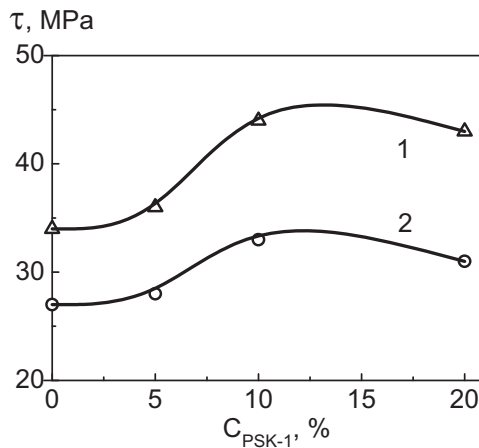


Fig. 3-11. Concentration dependences of adhesive strength  $\tau$  of the ED-20+ PSK-1+ TEAT-steel wire system ( $d = 150 \mu\text{m}$ ) under quasi-static conditions. Loading rate: (1) 1 and (2) 0.01 N/s;  $S = 0.95 \text{ mm}^2$ .

To determine the strength of polymer-fiber joints under impact loading, a setup was constructed; the setup makes it possible to record shock pulse oscillograms, while pulling out fibers from the matrix, and transfer the data to a computer.

The setup is described in A10.

Typical oscillograms for two loading rates differing by an order of magnitude are shown in Fig. 3-12. They provide still more information on the effect of the amount of PSK-1 introduced into ED-20 on the impact load resistance of the joints and the interface failure process. The ascending branches of the  $F$ - $t$  curves are linear almost to failure; that is, the systems undergo elastic deformation; the failure occurs



"instantaneously"; the force immediately decreases to zero. With an increase in the PSK-1 content in the matrix, the shape of the  $F-t$  curves changes; before failure, a nonlinear portion appears in them; that is, before failure, the system undergoes inelastic deformations (most probably, plastic). According to expectations, this effect is particularly pronounced in steel fiber-PSF joints (Fig. 3-12a).

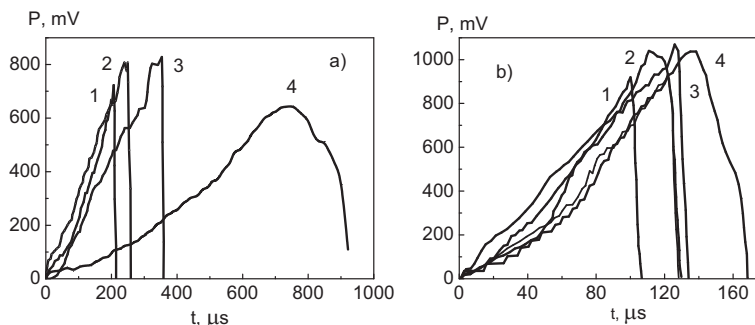


Fig. 3-12. Typical loading diagrams of the ED-20+PSK-1+TEAT-steel wire system ( $d = 150 \mu\text{m}$ ).  $S = 0.55 \text{ mm}^2$ . Loading rate: (a)  $\sim 10^3$  and (b)  $\sim 10^4$  N/s. The content of PSK-1: (1) 0, (2) 10, (3) 15, and (4) 20%.

The failure of these joints is accompanied by significant energy dissipation. The failure time is 10–15% of the total test time. The higher the external load application rate, the lower the energy dissipation, the shorter the failure time, and the lower the fraction of inelastic deformations (Figs. 3-12a, 3-12b).

Under dynamic loading, an increase in the modifier concentration leads, as in the case of quasi-static loading, to a strengthening of the interface; the synergism of the adhesive strength is observed (Fig. 3-13). A change in the rate does not change the shape of the concentration dependence: the  $\tau-S$  curves are also curves with a maximum at  $C \cong 10$  wt %. The pattern of the scale dependence of adhesive strength is preserved under a low-speed impact (Fig. 3-14).

An increase in the interfacial strength with an increase in the loading rate on the specimen is in qualitative agreement with the thermofluctuation (kinetic) theory of strength [143]. This theory was developed to describe the behavior of homogeneous isotropic materials under tensile loading. It was shown [30, 31, 141] that this theory can describe the laws governing the change in the strength of complex systems, such as polymer-fiber adhesive joints (systems characterized by the presence of an interface and a heterogeneous stress field, whose failure largely depends on tangential

stresses), if the residual stresses acting at the interface are taken into account correctly. According to the kinetic theory, in the entire range of loading rates, the strength should be described by a single straight line in semilogarithmic coordinates  $\tau$ - $\lg \dot{\epsilon}$ .

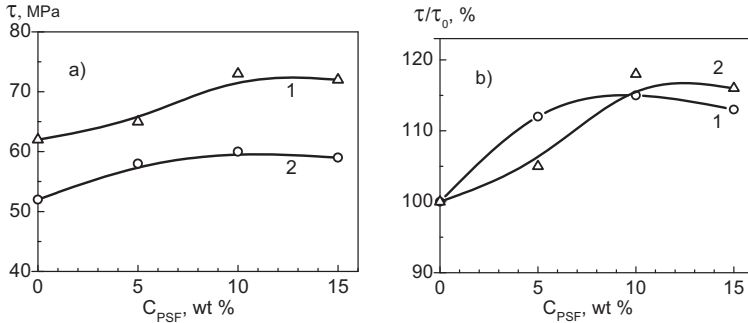


Fig. 3-13. Adhesive strength at the blend matrix-fiber interface for different amounts of PSF in (a) absolute and (b) relative units. The curing agent is TEAT. Loading rate: (1)  $10^4$  and (2)  $10^3$  N/s;  $S = 0.55$  mm<sup>2</sup>.

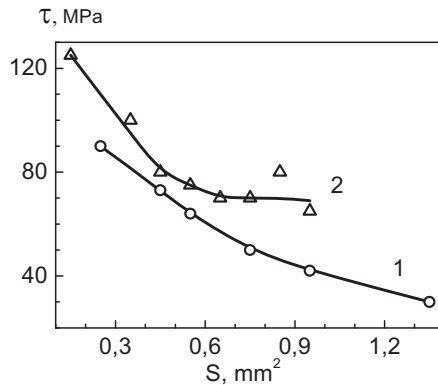


Fig. 3-14. Dependence of adhesive strength  $\tau$  of the ED-20+10% PSK-1+TEAT-steel wire system ( $d = 150$   $\mu$ m) on joint area  $S$  under impact loading. Loading rate: (1)  $10^3$  and (2)  $10^4$  N/s.

Fig. 3-15 shows results obtained under “fast” and “slow” loading for ED-20+TEAT+PSK-1-steel wire joints in the above coordinates. It is evident that, with a wide variation in the rate, the dependence is described by portions of two straight lines with different slopes. The sensitivity of interfacial strength under dynamic loading is higher than that under quasi-

static loading. For the moment, this conclusion is only qualitative. The derived data do not provide a quantitative value of coefficient  $K$ , because the loading rates under a low-speed impact differed as slightly as by an order of magnitude. Studying of the interfacial strength of polymer–fiber joints at high loading rates (under impact loading) is a matter for the future.

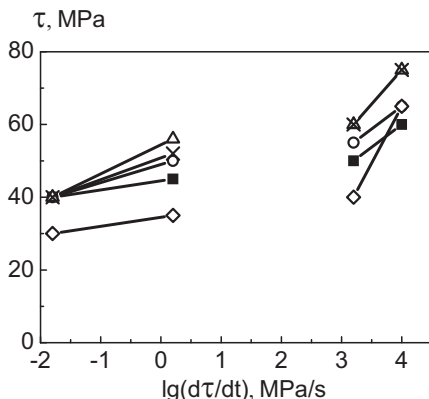


Fig. 3-15. Dependence of adhesive strength  $\tau$  of the ED-20+PSK-1+TEAT–steel wire system ( $d = 150 \mu\text{m}$ ) on loading rate  $\lg \frac{d\tau}{dt}$  ( $\lg(d\tau/dt)$ ). The area of the adhesive joint is  $S = 0.55 \text{ mm}^2$ . Polysulfone content: (■) 0, (○) 5, (Δ) 10, (x) 15, and (◇) 100%.

### 3.3. Effect of Liquid Medium on the Interfacial Strength of Polymer–Fiber Joints

It was found [30, 31] that the interfacial strength of fiber–crosslinked polymer systems stored under normal conditions remains almost unchanged for a long time, if the adhesive is cured to a maximum possible degree. The constancy of the  $\tau$  values was shown for a wide variety of resins—epoxy, phenolic, polyester, etc.—interacting with glass, steel, and high-strength organic fibers. To the best of our knowledge, there are no published data on systematic studies of the interfacial strength of these systems during storage and, particularly, during their loading in liquid media (primarily, in water).

However, these issues are of interest for both theorists and practitioners. In terms of theory, this knowledge is important, because the mechanisms of action of moisture in composites and their model joints are

still not fully understood. The practical importance is determined by the fact that composite materials are frequently used in various liquid media.

Below, it will be shown how storage in water affects the strength of joints composed of a modified epoxy resin and fibers of different chemical nature and how the adhesive strength of a modified epoxy resin and the resin components in joints with various fibers changes during testing the specimens directly in liquids.

### ***3.3.1. Changes in adhesive strength during storage of fiber-epoxy binder joints in water***








The effect of the residence time in water on the adhesive strength of fiber-modified epoxy resin systems was studied for joints in which the adhesive was the ED-20+TEAT+DEG-1 composition, which has one of the strongest interfaces (in the case of adhesion to high surface energy fibers) [144]. The curing conditions (160°C, 8 h) provided the maximum possible degree of cure. The residence time of the specimens in water was varied from 1 day to 9 months.

The substrate in the joints was steel fibers with a diameter of  $d = 150$   $\mu\text{m}$ , boron fibers with a diameter of  $d = 140$   $\mu\text{m}$ , and alkali-free glass fibers (counterpart of E-glass) with a diameter of  $d = 10\text{--}30$   $\mu\text{m}$ . The main measurements were conducted with boron fibers, because the strength of glass fibers in water significantly decreases over time, while steel fibers quite rapidly lose the entire strength (owing to corrosion).

To elucidate the mechanisms of penetration of a liquid into an adhesive joint, it is desirable to study specimens into which liquids can penetrate via various routes. These conditions can be provided by studying the strength of polymer-fiber joints with a fiber diameter of  $d \geq 80$   $\mu\text{m}$  and using specimens prepared in aluminum cups (see Fig. A1). A possible contact of these specimens with a liquid and possible routes of penetration of the liquid to the interface are shown in Table 3-2. Specimens in cups can float on the surface of the liquid (nos. 2, 3) or be immersed into it (no. 4); to obtain specimens in which the resin surface is completely accessible to the penetration of a liquid (nos. 6, 7), before the test, aluminum cups are treated with a releasing agent (silicon); after curing, the joints can be easily removed (nos. 5-7).

The data in Figs. 3-16-3-19 represent the kinetics of variation in adhesive strength during the aging of joints in water. It is evident that, after a short exposure (1 day), the adhesive strength of all the systems remains almost unchanged (Figs. 3-16a, 3-16b).

**Table 3-2. Methods of exposure of specimens to water (boron fiber–modified ED-20 epoxy resin joints)**

No.	Position of specimens	Designations in Figs. 3-16 and 3-18	Possible water penetration routes	
			Along the interface	Through the resin layer
1*		•	–	–
2		o	from below	–
3		▲	from above	from above
4		x	from below and from above	from above
5*		□	–	–
6		Δ	from below	from below
7		■	from below and from above	from below and from above

\*Reference specimens stored in air.

After a 10-day storage, the  $\tau$  values also vary only slightly (Figs. 3-17a, 3-17b). After that, the interfacial strength begins to decrease. In joints with boron fibers, significant changes occur after 3 months (Figs. 3-17, 3-18). Figure 3-18 shows that the kinetics of strength loss depends on the route of water diffusion into the specimen. For system no. 2, in which water (liquid) can penetrate to the interface only along the fiber, strength losses are observed as late as 1.5 months after the beginning of storage. In systems nos. 3 and 4, in which water penetrates to the interface both along the fiber and across the resin layer, a faster strength loss is observed in the first weeks. The routes of liquid penetration into these systems (nos. 3 and 4) are nearly identical. The kinetics of variation in the strength of these specimens in the first 1.5–2 months is also similar. (Note that the scatter of results in the tests is 8–10%. The difference between the systems goes beyond this range only slightly; therefore, it is reasonably safe to state only tendencies of changes).

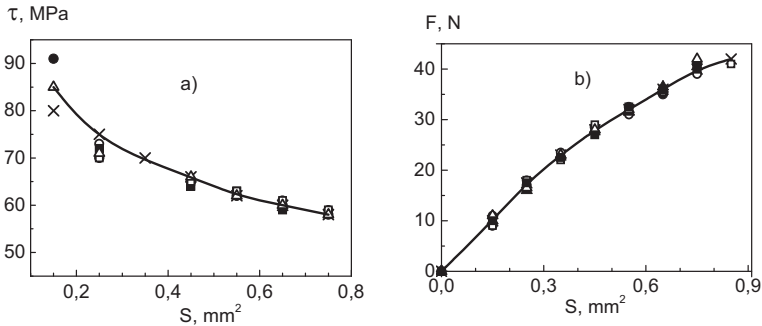


Fig. 3-16. Dependence of (a) adhesive strength  $\tau$  and (b) force  $F$  required for the failure of boron fiber-modified ED-20 resin joints on the area of the joints. The time of exposure of the joints to water is 1 day. Designations are given in Table 3-2.

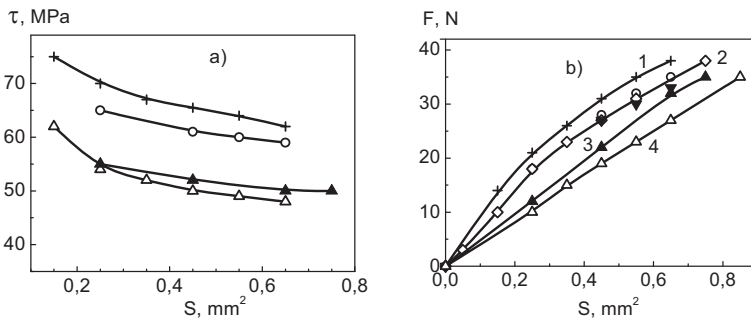


Fig. 3-17. Effect of the storage time of ED-20+DEG-1+TEAT-boron fiber joints in water on (a) adhesive strength  $\tau$  and (b) force  $F$  required for the failure of the joint. Storage time: (+) reference specimens, (◇) 10 days, (○) 3 weeks, (▼) 7 weeks, (▲) 3 months, and (Δ) 6 months. System no. 4.

Figures 3-17 and 3-18 show that the maximum loss of adhesive strength during exposure of boron fiber-modified epoxy binder joints to water does not exceed 15–20% (relative to the strength of reference specimens stored in air under normal conditions). Maximum losses are observed for systems nos. 4 and 7.

In the case of exposure of joints of the same binder with a steel wire to water, the interfacial adhesive strength (in common with the strength in joints with boron fibers) remains almost unchanged in the first 10 days (Fig. 3-19). After a 2-week exposure to water, the  $\tau$  value cannot be determined, because most of the joints undergo cohesive failure (across the fiber) owing to the corrosion of the wire under loading.

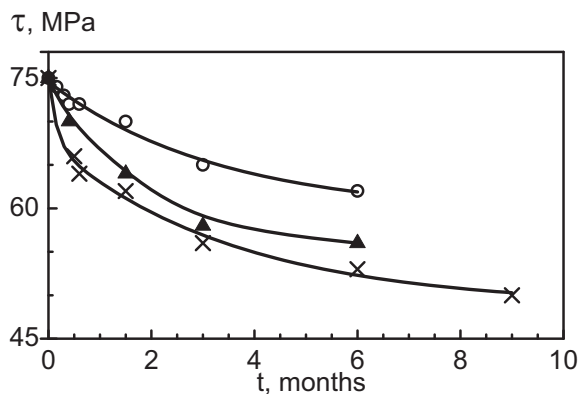


Fig. 3-18. Adhesive strength of boron fiber-modified ED-20 epoxy resin joints after exposure to water. The area of the joints is  $S = 0.25 \text{ mm}^2$ . Designations are given in Table 3-2.

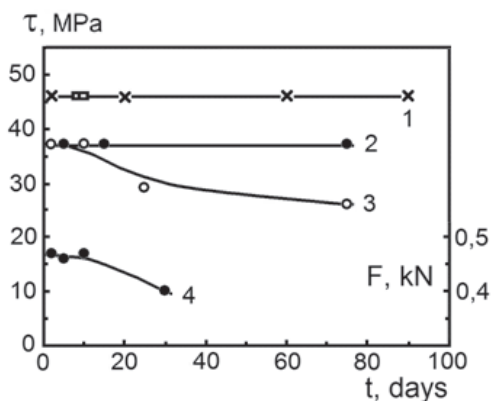


Fig. 3-19. (1-3) Adhesive strength of fiber-modified ED-20 epoxy resin joints and (4) strength of microplastics based on the same binder and alkali-free glass fibers after aging in air and water: (1) joints with a steel wire,  $d = 150 \text{ }\mu\text{m}$ ,  $S = 0.95 \text{ mm}^2$ , aging (x) in air and ( $\square$ ) in water; (2, 3) joints with glass fibers,  $d = 10\text{-}13 \text{ }\mu\text{m}$ ;  $S = 8 \times 10^{-3} \text{ mm}^2$ , aging (2) in air and (3) in water; (4) aging in water.

In the case of aging the joints with glass fibers in water, a monotonic decrease in strength begins after a 10-day exposure. By the end of 2.5 months, the loss of  $\tau$  is 43% (Table 3-3). It should be noted that, during

storage, the ratio of the number of specimens undergoing adhesive ( $n_\tau$ ) and cohesive failure ( $n_\sigma$ ) changes; the  $n_\tau/n_\sigma$  value significantly increases (Table 3-3). This increase is only natural, because, under the action of water, the strength of the fiber decreases to a lesser extent than the interfacial strength does.

It should be emphasized that the studied specimens are under the most unfavorable conditions: the length of the joints is extremely small, namely, 200–240  $\mu\text{m}$  in joints with glass fibers and 1–2 mm in joints with boron and steel fibers. Therefore, a liquid can penetrate to the interface along the fiber and through the resin layer.

**Table 3-3. Adhesive strength of alkaline-free glass fiber-modified epoxy resin joints ( $d = 10\text{--}13 \mu\text{m}$ ) after storage in water**

Exposure time, days	$\alpha$ , %*	$n_\tau$	$n_\sigma$	$\tau_0$ , MPa**	$n_\tau/n_\sigma$
0 (reference)	92	56	47	35.5	1.12
10	92	39	48	36.6	0.81
30	91	43	23	23.8	1.90
75	93	45	16	20.3	2.80

\* $\alpha$  is the degree of cure of the resin; the  $\alpha$  values are determined by argentometric titration. \*\* $S = 8 \times 10^{-3} \text{ mm}^2$ .

In real fiber-based compositions, the loss of strength during aging should be less than that in the unit cells under discussion. Analysis of a number of studies focused on the water resistance of reinforced plastics shows that this assumption is true.

Fig. 3-20 shows how resin castings and fiber bundles impregnated with the same resin adsorb moisture. It is evident that saturation of the resin with moisture is achieved within 2.5–3 months. Comparison of adhesive strength losses ( $\Delta\tau/\tau_0 = (\tau_0 - \tau_t)/\tau_0$ , where  $\tau_0$  and  $\tau_t$  are the adhesive strengths in the original joints and the joints aged in water for time  $t$ , respectively) with the amount of moisture sorbed within this time ( $W$ ) shows the correlation of these values (Fig. 3-21). Microplastics almost stop absorbing water 1.5–2 months after the beginning of storage (Fig. 3-20).

Within this time, both the mechanical characteristics and the glass transition temperature of the resin cease to change (Fig. 3-22). The rigidity and strength of moisture-saturated microplastic specimens is 20–25% lower than the respective parameters of the dry (air-stored) specimens; their glass transition temperature is 32–35°C lower than the  $T_g$  value of the original specimens.



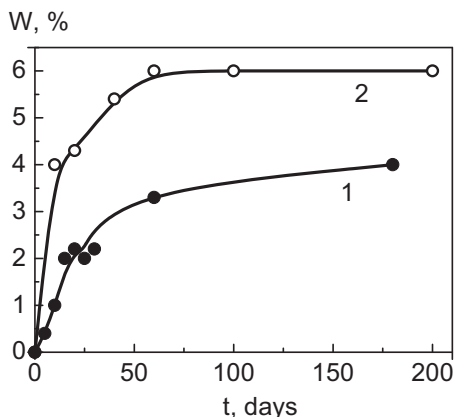


Fig. 3-20. Amount of water absorbed by (1) an epoxy resin and (2) microplastics based on the same resin upon exposure of the specimens to water at 20°C. Curve (2) is constructed, while relating the amount of sorbed water to the weight of the resin.

In addition, Figs. 3-19 and 3-22 shows that the curves describing the loss of rigidity (and strength) in fiber-glass-reinforced plastics and the adhesive strength in their unit cells have identical shapes.

Using these data, we can try to answer the question of what is responsible for the loss of the interfacial strength during the storage of joints in a liquid.

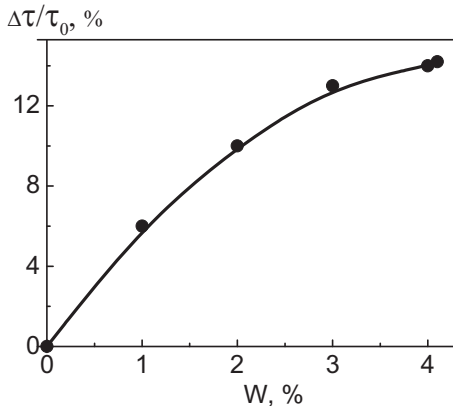


Fig. 3-21. Decrease in the adhesive strength of boron fiber-modified ED-20 resin joints with an increase in the amount of water sorbed by the resin. System no. 7 (see Table 3-2).

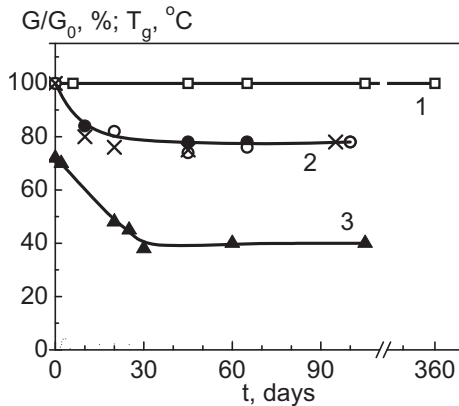


Fig. 3-22. Effect of storage time in (1) air and (2, 3) water on (1, 2) the rigidity of epoxy microplastics and (3) the glass transition temperature of the resin. The different symbols in curve (2) denote specimens with different initial rigidities.

Let us discuss possible causes of the losses.

(i) Below the glass transition temperature of the polymer at the fiber-polymer interface, there exists a heterogeneous (nonuniform) field of residual stresses. These stresses act throughout the entire aging process. It is known [143] that a long-term action of stresses leads to a loss of strength. If adhesive strength losses mostly depend on the effect of residual stresses, then, in the case of aging the joints in water, the decrease in  $\tau$  should not exceed the loss of the interfacial strength in the case of aging the joints in air, because water adsorption causes a decrease in residual stresses (see below). Data in Fig. 3-19 suggest that the strength of adhesive joints does not change during aging in air; that is, residual stresses cannot be regarded as the main factor of decrease in interfacial strength.

(ii) During storage, the polymer structure can change owing to the further formation and scission of bonds. The formation and scission of bonds in the polymer bulk can actually be accompanied by their formation and scission at the interface. Structural changes can lead to a change in physicomechanical properties (bulk and surface), residual stresses, and, as a consequence, the adhesive strength in the fiber-polymer system. In the case under discussion, the specimens were cured to the maximum possible degree. Changes in the degree of cure of the polymer were not observed during storage either in air or in water (see Table 3-2). Accordingly, the decrease in adhesive strength during storage of the joints in water cannot considerably depend on changes in the chemical structure of the polymer.

(iii) If fiber–polymer joints are immersed into a liquid, the liquid molecules diffuse through the polymer layer and along the fiber. Being at the interface, they can be adsorbed on it and/or displace the resin molecules from the interface (preferential adsorption). This factor can lead to a decrease in  $\tau$ . Moreover, the liquid can exert a disjoining pressure, while penetrating to the interface. This factor can also cause bond scission, an increase in the interfacial imperfection, and a decrease in the strength of the joints. However, the assumption that the main factor determining the loss of adhesive strength is the presence of liquid molecules at the interface is not consistent with the data on the dependence of the kinetics of decrease in  $\tau$  on the moisture penetration route (Fig. 3-18). In fact, as noted above, liquid molecules penetrate to the interface both through the resin layer and along the fiber. In this case, to interpret the data in Fig. 3-18, it should be assumed that the interface cannot serve a “facilitated” liquid penetration route (channel along which water molecules freely move) and that diffusion from the bulk of the resin to the interface occurs at a rate that, in any case, is not lower than the rate of diffusion along the fiber.

If water molecules can penetrate to the interface not only along the fiber, but also through the resin, then the loss of adhesive strength in systems nos. 3, 4, 6, and 7 will be observed much earlier than that in system no. 2, in which only surface diffusion can take place.

The assumption of a low diffusion rate of water molecules along the interface is in conflict with the published data: the authors of [145] reported that the diffusion rate of water molecules along fiber fillers (along the glass fiber–polymer interface) is  $10^3$ – $10^4$  times higher than that into a polymer matrix.

The following should be added to the above.

The lower end of the studied joints, i.e., the end to which an external force is applied during loading, is the site of the maximum stress concentration. It was shown [146] that, in the vicinity of this point (under applying an external load), there is a “singularity”; that is, this end can be regarded as the site of a dangerous defect. It can be shown that this singularity arises due to the action of thermally induced residual stresses.

If we assume, as usually, that the failure begins at the site of the maximum stress concentration, then the conditions that exist at this site (site of a dangerous defect) become particularly important.

From this viewpoint, in the case under discussion, the adhesive strength and the kinetics of variation in it will be determined by the presence of water molecules at the site where the fiber emerges from the joint. At this site, in all the systems, except for system no. 3, liquid

molecules are present from the very beginning of storage (exposure). Therefore, in all the systems, except for system no. 3, the kinetics of variation in  $\tau$  should be identical. If the diffusion rate of water molecules along the interface is high, then the kinetics of loss of adhesive strength in system no. 3 will not differ from that in all the other systems. However, if this rate is low, then, in system no. 3, the  $\tau$  values should remain unchanged for a long time. It is evident (Fig. 3-18) that the experiment shows a different picture.

Thus, the derived results cannot be attributed only to the presence of liquid molecules at the interface.

(iv) A liquid penetrating a polymer can plasticize the polymer. The plasticization of epoxy matrices with water was studied in considerable detail [147–151]. It is known that plasticization leads to a decrease in the glass transition temperature of the polymer. In this case, the adhesive strength and physicochemical characteristics of the polymer measured at room temperature can decrease, because the measurement temperature is closer to the transition temperature and the physicochemical characteristics (in particular, adhesive strength in joints with any substrates) decrease, while approaching the region of transition from the glassy to rubberlike state [30, 31]. On the other hand, plasticization leads to a decrease in the rigidity and elastic modulus of the polymer and, as a consequence, in the residual stresses acting at the interface [43]. Their decrease leads to an increase in the adhesive strength of polymer–fiber joints. It is not improbable that bonds can be formed directly between the plasticizer and substrate molecules; the bonds can contribute to an increase in the interfacial strength.

Thus, three competing mechanisms act during plasticization. One of the mechanisms causes a decrease in the  $\tau$  values; the other two cause an increase in  $\tau$ . As a consequence,  $\tau$  values can vary in a complicated way, for example, along a curve with a maximum, as observed in the case of modifying epoxy oligomers with active diluents (see Chapter 1). The plasticization effect is evidenced by the data in Fig. 3.18 and a direct relationship between the loss of adhesive strength and the amount of sorbed water (Fig. 3-21). The amount of water in the adhesive more significantly depends on diffusion through the resin layer than on the capillary penetration of moisture along the interface. This fact was clearly shown by the authors of [152], who studied water penetration into Al–epoxy resin–Al joints using labeled atoms. They found that water penetrates the joints mostly owing to diffusion through the resin layer, and diffusion along the interface does not significantly contribute to the amount of absorbed water.

To prove that the losses of  $\tau$  can be attributed only to a change in the physicochemical characteristics of the adhesive (owing to plasticization) and can occur without an active interaction of water molecules with the interface, an independent experiment should be conducted, in which equivalent changes in the physicochemical characteristics of the polymer will be observed, while the nature of the forces acting at the interface will remain unchanged.

Let us consider a change in the physicochemical properties and adhesive strength of the studied adhesive with a change in the test temperature as an example of a fairly close model of the above experiment. The data are shown in Fig. 3-23. They suggest that, in a temperature range of 5–150°C, the pattern of change in the adhesive strength of joints of a modified epoxy polymer with glass and boron fibers is identical to the pattern of change in the rigidity of microplastics based on this polymer and glass fibers. Identical patterns of change in the adhesive strength and mechanical properties of polymers were also observed in [30, 31].

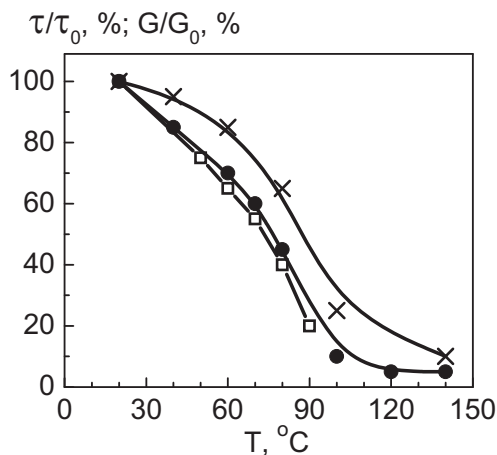


Fig. 3-23. Temperature dependence of ( $\tau$ , x) the adhesive strength of fiber-modified ED-20 resin joints and ( $\bullet$ ) the rigidity of microplastics based on the same binder and alkali-free glass fibers. Joints: ( $\square$ ) with boron fibers and (x) with alkali-free glass fibers. The  $\tau$  and  $G$  values at 20°C are assumed to be 100%.

It was shown (Fig. 3-22) that the plasticization of the polymer during exposure to water leads to a decrease in the glass transition temperature from 73 to 38°C. This decrease is equivalent to an increase in the

measurement temperature by 35°C. Figure 3-23 suggests that, with this increase in temperature, the loss of adhesive strength in joints with boron fibers is 25–28%. The rigidity of the polymer decreases by nearly the same value. The maximum losses of  $\tau$  during a long-term aging in water (for the studied system) do not exceed 20% (Figs. 3-17, 3-18). Thus, the effect of moisture can be attributed to a change only in the mechanical properties of the polymer (without any additional change in the interfacial interactions).

It is obvious that the change in the mechanical characteristics of the polymer with an increase in temperature is not identical to their change during plasticization with water. However, according to our reckoning, the described results provide fairly convincing evidence in favor of the decisive role of plasticization. These conclusions are true for aging of boron fiber-modified epoxy binder joints in water. The properties of these fibers depend on the action of moisture only weakly. After aging in water for 160 days, the strength of boron fibers remains almost unchanged.

After a long-term aging of joints of the same binder with alkali-free glass fibers in water, the loss of adhesive strength achieved 43% (Table 3-2). However, according to Fig. 3-23, the decrease in adhesive strength corresponding to an increase in the glass transition temperature (and hence in the measurement temperature) by the same 35°C is as low as 17%. Apparently, in this case, the effect of water on the properties of the fibers plays a significant role. (It is known that a long-term action of moisture causes a chemical “damage” to the glass surface and leaching of the glass).

Thus, the study of the effect of the storage time of joints of various fibers (glass, steel, boron) with a modified ED-20 epoxy resin and the study of the physicochemical characteristics of epoxy microplastics based on alkali-free glass fibers have shown the following:

- (i) The kinetics of variation in adhesive strength in polymer-fiber systems depends on the route of moisture penetration into the joint.
- (ii) Losses of adhesive strength increase with an increase in the amount of absorbed water.
- (iii) The kinetics of variation in the strength of microplastics and adhesive strength are similar.
- (iv) The main factor that determines the loss of adhesive strength during storage of joints in water is the plasticization of the epoxy resin with water.

### ***3.3.2. Strength of polymer–fiber joints in tests in liquid media***

The use of polymer–fiber joints has revealed the effect exerted on interfacial strength by various factors that act during the formation, storage, and testing of joints, which primarily include the nature of the fibers, their surface treatment, the structure and composition of the polymer adhesive, the joint preparation conditions, and the shape and size of the specimens.

The behavior of joints under loading in liquid media has hardly been studied until recently. However, it is of interest to study this behavior from both the theoretical and practical points of view, because the presence of a liquid can lead to a change in the kinetics of the nucleation and development of defects responsible for the failure of the interface and, accordingly, a change in both the failure mechanism and the adhesive strength.

It is well known that the presence of a surrounding liquid can lead to a significant decrease in the strength of solids. This effect was thoroughly studied by P.A. Rehbinder, his colleagues, and students [153, 154]. It is currently known as the Rehbinder effect. According to Rehbinder and his school, the problem essentially consists in the following: molecules of the surrounding liquid can be adsorbed on the surface of a solid and thereby decrease the surface energy of the solid. In addition, these molecules can penetrate surface defects and contribute to the development of cracks. As a consequence, the strength of solids under loading in liquid media can be lower than the strength under loading in dry air or a vacuum. The decrease is most pronounced under static and quasi-static (slow) loading.

The Rehbinder effect has been thoroughly studied for solids. The effect of the surrounding liquid on the properties of adhesive joints has not been studied until recently, although the behavior of the interface under various combinations of loading conditions in a liquid is of interest to both scientists and technologists, primarily, those who are involved in the design and use of various dispersion-filled and fiber-reinforced composite materials.

It is well known that the failure and physicomechanical properties of composites significantly depend on the adhesive strength of their components. If the interfacial adhesive strength is low, then the interface can become a “weak link” of the composite material and a factor that controls the strength of the material [28].

Therefore, to design composite materials that can be effectively used under certain conditions, it is necessary to know the effect of these conditions not only on the behavior of the fibers and matrices, but also on the behavior of the interface between them. The surrounding liquid can be

one of those conditions. The following questions now arise, “Does the Rehbinder effect exist for adhesive joints, and what are the factors that control it?”

The effect of the surrounding liquid on interfacial strength is also a fundamental problem for “pure” science. The presence of a liquid medium can lead to a change in the kinetics of the formation and propagation of cracks responsible for the failure of joints, as it takes place in solids. However, the behavior of adhesive joints has some specific features: in joints, crack formation and propagation occurs between materials of different nature. This is the first specific feature of joints. The second feature of joints is the penetration of the liquid to the interface. If a solid is placed into a liquid medium, then this medium is in contact with the entire surface of the solid and, accordingly, with all defects present on the surface. In the case of an adhesive joint, the liquid is in direct contact only with the edges of the joint. The liquid can penetrate to the entire interfacial surface only via diffusion. These features complicate studies of the Rehbinder effect for adhesive joints.

Studies of the behavior of polymer-fiber joints under loading in liquid media were started at Semenov Institute of Chemical Physics of the Russian Academy of Sciences [155–157]. Results of experiments in which the adhesives were not only multicomponent (modified) epoxy matrices, but also individual components of these matrices will be described below.

### ***3.3.2.1. Loading of fiber-epoxy resin and fiber-heat-resistant thermoplastic joints in a liquid***

Figure 3-24 shows the change in the adhesive strength of joints of a typical representative of epoxy resins—epoxy binder EDT-10—with a steel wire under loading in polar liquids (water and ethanol).

The specimens were subjected to a heat treatment in drying ovens under isothermal conditions without applying a pressure at 160°C for 8 or 12 h. It was previously shown [30, 31] that, under these conditions, the binder is completely cured and the conversion of reactive epoxy groups achieves a maximum (96%). Accordingly, the interfacial strength of the test joints under loading in air is extremely high (Fig. 3-24).



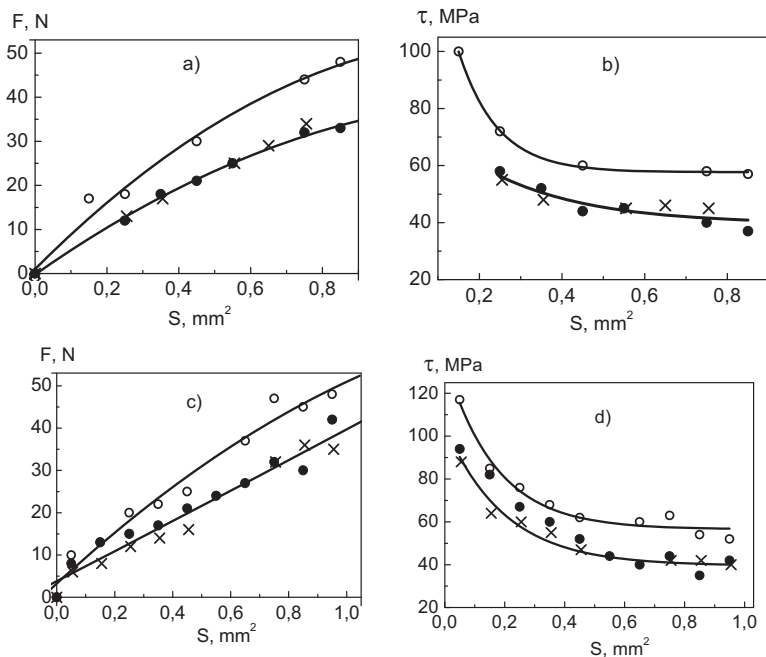


Fig. 3-24. (a, c) Forces required for the failure of steel wire–EDT-10 epoxy binder joints and (b, d) their adhesive strength under loading in (o) air, (●) water, and (x) ethanol. The joints were cured at 160°C for (a, b) 8 and (c, d) 12 h.

The resulting joints were tested in air and a liquid using an improved model of an adhesion tester (tensile microtester) developed at Semenov Institute of Chemical Physics of the Russian Academy of Sciences.

It is evident that, in the case of loading the joints in water and alcohol (Fig. 3-24), the forces required for their failure and the interfacial strength of the joints are lower than the respective characteristics of the reference joints (tested in air). A decrease in strength is observed for joints of any size. The level of decrease can achieve 25–30%. In addition, the loss of adhesive strength varies only slightly with a change in the interfacial strength (Fig. 3-25).

It was found that the  $\tau$ – $S$  curves for joints tested in water and alcohol were close (Fig. 3-24). However, the surface tension of these two liquids differs quite significantly: 72 and 23.5 mN/m, respectively. Thus, at room temperature, the failure of the fiber–epoxy polymer interface depends on the surface tension of the liquid only slightly.

In addition, it was found that a change in the curing conditions (increase in the heat treatment time from 8 to 12 h) does not change the qualitative picture of the behavior of the joints in liquids, if the conversion of reactive groups is fairly high (cf. Figs. 3-24a, 3-24b, 3-24c, 3-24d). The  $\tau$  values for joints cured for 8 and 12 h are identical; the strength losses under loading in polar liquids are also similar: the  $\Delta\tau/\tau_r$  value is  $\approx 20\text{--}30\%$  and depends on the area of the joints only slightly ( $\Delta\tau = \tau_r - \tau$ , where  $\tau_r$  and  $\tau$  are the adhesive strength of the reference specimens (tested in air) and the specimens tested in a liquid, respectively).

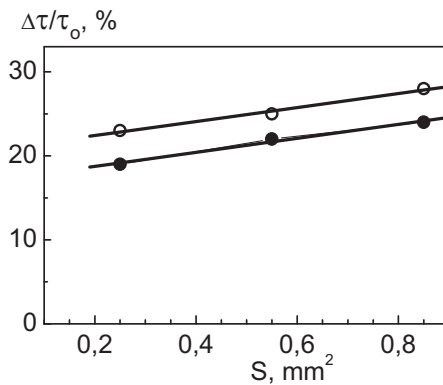


Fig. 3-25. Relative decrease in adhesive strength in the case of loading steel wire-EDT-10 epoxy binder joints in water. Curing time: (o) 8 and (●) 12 h.

The fact that the adhesive strength of epoxy binder-steel wire joints subjected to loading in polar liquids does not depend on the surface tension of these liquids is also evidenced by the data shown in Fig. 3-26. Here, the strength of the joints under loading in water-alcohol mixtures of various concentrations is shown. It is evident that, with an increase in the ethanol concentration, the surface tension of the mixtures monotonically decreases (see also Table 3-4), while the  $\tau$  value remains almost unchanged. This is true of joints of any size.

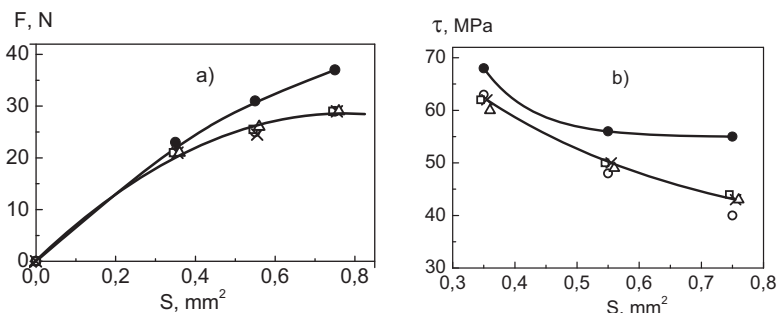


Fig. 3-26. (a) Forces required for the failure of steel wire–EDT-10 epoxy binder joints and (b) their adhesive strength under loading in (●) air, (○) water, (x) ethanol, and water–ethanol mixtures of various concentrations.

Mixture concentration: (□) 4.4 and (Δ) 15.5%.

**Table 3-4. Surface tension of water–ethanol mixtures of various concentrations and the properties of the interface of EDT-10 epoxy binder–steel wire joints loaded in these mixtures**

Ethanol concentration, wt %	0	4.4	8.4	15.5	100
Surface tension, mN/m	72.5	55.5	47.0	33.5	23.5
Breaking load, N*	27.5	27.0	27.0	26.0	27.0
Adhesive strength, MPa*	50	50	49	48	50

\* $S = 0.55 \text{ mm}^2$ .

Tests of the same joints in nonpolar liquids and glycerol show a different picture (Fig. 3-27): in the presence of a surrounding liquid (hexane, silicone oil, glycerol), the interfacial strength does not change.

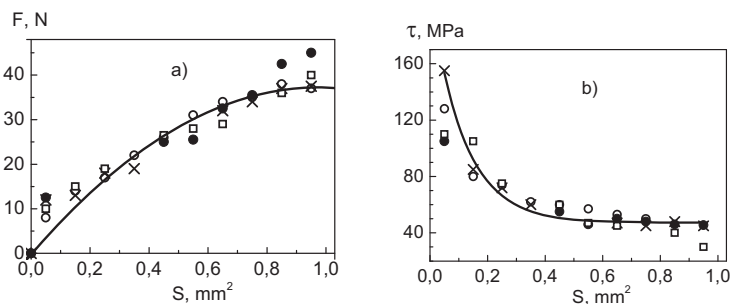


Fig. 3-27. Results of testing of the same compounds as in Fig. 3-26 in (○) air, (●) glycerol, (□) hexane, and (x) silicone oil (polydimethylsiloxane).

In tests of joints of a typical heat-resistant thermoplastic (PSK-1) with a steel wire in a liquid, the adhesive strength of the joints remains the same as that in the tests in air, regardless of the polarity of the liquid used. Figure 3-28 shows the adhesion characteristics of specimens formed at 300°C for 30 min. It is known [31, 158] that, in the case of formation of specimens in an air medium, the strength of joints of representatives of this class of polymers with fibers significantly depends on formation time  $t_f$  and formation temperature  $T_f$ ; in this case, the  $\tau$ - $t_f$  and  $\tau$ - $T_f$  dependences are described by curves with a maximum. Specimens whose adhesive strength is shown in Fig. 3-28 are formed under conditions providing a maximum interfacial strength.

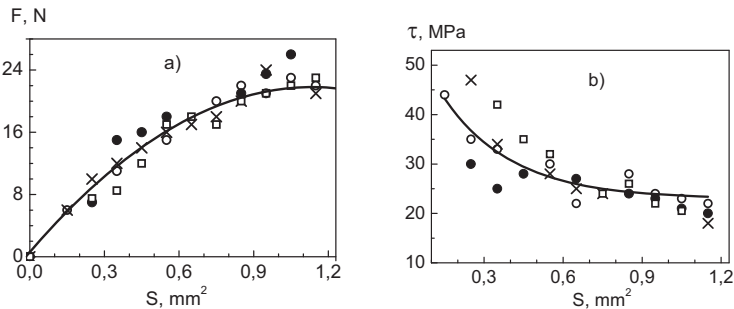


Fig. 3-28. (a) Forces required for the failure of PSK-1 poly(arylene sulfone)-steel wire joints and (b) their adhesive strength under loading in (o) air, (x) water, (●) ethanol, and (□) silicone oil (polydimethylsiloxane).

It is evident from Fig. 3-28 that the  $F$ - $S$  and  $\tau$ - $S$  curves recorded for specimens loaded in air, water, ethanol, and silicone oil (dimethylsiloxane), i.e., in both polar and nonpolar liquids, almost coincide. Thus, the behavior of polymer-fiber joints in liquids significantly depends on the nature of the adhesive.

The effect of the liquid medium on the strength of polymer-fiber joints can change not only with a change in the nature of the adhesive, but also with a change in the nature of the substrate. Figure 3-29 shows the effect of the presence of a liquid on adhesive strength in the case where the substrate is a carbon fiber of the UKN-5000 brand (Russia)—instead of a steel wire—and the adhesives are the same EDT-10 epoxy binder and the PSK-1 heat-resistant thermoplastic. The procedures for preparing the specimens and processing the results are described in detail in [159]. It is evident that the use of a substrate of a different nature changes the picture observed during the failure of these joints in a liquid. Under loading in any

of the studied liquids, their presence does not affect the interfacial strength.

Since in testing the polymer–carbon fibers joints, the specimens underwent not only adhesive failure (along the interface), but also cohesive failure (across the fiber) and the number of specimens that underwent cohesive failure was fairly large (see Tables 3-5, 3-6), Fig. 3-29 shows not only the  $\tau$  values calculated directly from the test results as the arithmetic mean of the strength of all specimens that underwent adhesive failure, but also the  $\tau_0 = \tau + \Delta\tau$  value, where  $\Delta\tau$  is the correction associated with the presence of specimens that underwent cohesive failure. (The necessity of introducing the  $\Delta\tau$  correction was discussed in [30, 31], where an algorithm for calculating this quantity is given).

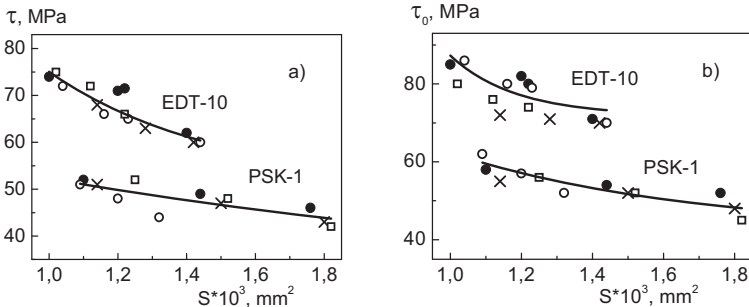


Fig. 3-29. Dependence of adhesive strength on the area of specimens for UKN-5000 carbon fiber–EDT-10 epoxy binder and UKN-5000–PSK-1 poly(arylene sulfone) joints tested in (●) air, (○) water, (x) ethanol, and (□) hexane. The meaning of the  $\tau$  and  $\tau_0$  quantities is given in the text.

Figure 3-29 suggests that the presence of a liquid in the test systems does not change either the  $\tau_0$  value or the  $\Delta\tau$  value. It should be noted that these results confirm the conclusion made earlier [30, 31] that the introduction of the correction leads to an increase in the measured value of this strength; however, it does not change the pattern of the dependence of adhesive strength on the studied factor.

Data on the effect of the surrounding liquid medium on the strength of the adhesive joints tested in it are summarized in Table 3-7. It is evident that the presence of a liquid leads to a change in the adhesive strength of the components only in 5 out of 17 systems.

**Table 3-5. Adhesive strength of UKN-5000 carbon fiber-EDT-10 epoxy binder joints under loading in liquids**

Liquid medium	$d$ , $\mu\text{m}$	$S \times 10^3$ , $\text{mm}^2$	$n_\tau^a$	$n_\sigma^a$	$\tau_0^b$ , MPa
Air	7.1	1.19	67	33	80
Water	7.2	1.24	67	33	78
Ethanol	7.5	1.29	63	37	71
Hexane	6.8	1.11	35	15	75

<sup>a</sup> $n_\tau$  and  $n_\sigma$  are the number of joints that underwent adhesive and cohesive failure, respectively. <sup>b</sup> $S = 1.2 \times 10^{-3} \text{ mm}^2$ .

**Table 3-6. Adhesive strength of UKN-5000 carbon fiber-PSK-1 poly(arylene sulfone) joints under loading in liquids**

Liquid medium	$d$ , $\mu\text{m}$	$S \times 10^3$ , $\text{mm}^2$	$n_\tau^a$	$n_\sigma^a$	$\tau_0^b$ , MPa
Air	7.1	1.76	175	91	57
Water	7.2	1.20	32	18	57
Ethanol	7.2	1.50	32	18	55
Hexane	6.8	1.52	34	16	59

<sup>a</sup> $n_\tau$  and  $n_\sigma$  are the number of joints that underwent adhesive and cohesive failure, respectively. <sup>b</sup> $S = 1.2 \times 10^{-3} \text{ mm}^2$ .

The data in Figs. 3-24 and 3-26–3-29 show that adhesive strength significantly depends on the interracial area of joints not only under loading in air, but also under loading in a liquid. The presence of a liquid does not change the scale effect of adhesive strength either in the case of crosslinked polymers (EDT-10) or in the case of heat-resistant linear polymers (PSK-1): during testing in air and in a liquid, the  $\tau$ - $S$  curves are almost parallel to each other. This fact provides still more evidence that the large-scale effect in the polymer-fiber joints is primarily associated with thermally induced residual stresses. As noted above, these stresses exist at the interface before applying external forces; accordingly, they do not depend on loading conditions. Therefore, in the case of loading the joints in air and in various liquids, the pattern of the scale dependence of adhesive strength should be identical, as observed in the tests.

**Table 3-7. Variation in adhesive strength of polymer–fiber joints under loading in a liquid**

Liquid medium for loading	EDT-10		PSK-1	
	Steel fiber	Carbon fiber	Steel fiber	Carbon fiber
Water	Decreases	Does not change	Does not change	Does not change
Ethanol	Decreases	Does not change	Does not change	Does not change
Water–ethanol mixtures of three concentrations	Decreases	–	–	–
Hexane	Does not change	Does not change	–	Does not change
Glycerol	Does not change	–	–	–
Silicone oil (dimethylsiloxane)	Does not change	–	Does not change	–

The surrounding liquid can lead to a change in the state of the interface before loading and in the nucleation and growth of a dangerous defect during loading. The latter process appears to be the most probable cause of the effect of the liquid. In fact, it was shown above (Fig. 3-19) that, during the storage of steel wire–EDT-10 epoxy binder joints in water at 20°C, their adhesive strength remains unchanged for 10 days. Special tests showed that, during the storage of these joints in ethanol, their strength, similarly, does not change for 10 days. These facts show that even this long-term contact of the joints with the studied liquids before testing does not affect the behavior of a dangerous defect during subsequent loading.

In these tests, the loading time of a specimen to failure did not exceed 50 s, and the total contact time between a specimen and a liquid was less than 2 min. Hence, water and alcohol, into which the specimens are immersed before applying an external force, do not have a significant effect on the nucleation of a dangerous defect. The above is true of any other liquid characterized by a similar rate of diffusion into a polymer.

The presence of a liquid does not give rise to defects of a new type at the interface. This fact is evidenced by analysis of adhesive strength distribution curves. Figure 3-30 shows these curves for joints with a fairly narrow area distribution. It is evident that, in the case of failure of the specimens in both air and a liquid medium, the shape of the distribution curve does not change, and the curve remains unimodal.

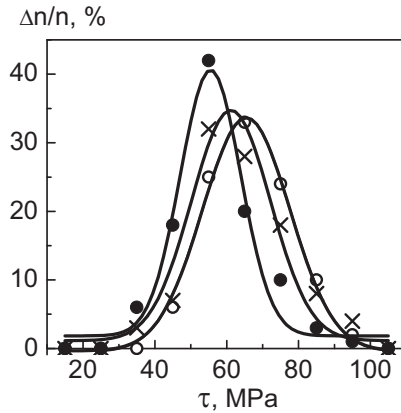


Fig. 3-30. Adhesive strength distribution curves for steel wire-EDT-10 epoxy binder joints under loading in (o) air, (•) water, and (x) ethanol.

The relatively small decrease in  $\tau$  (no more than 30%) suggests that the formation and propagation of a crack occurs at stresses close to limiting stresses and quite rapidly. This assumption was confirmed by direct tests, in which the effect of the preloading of specimens on the interfacial strength was studied. In those tests, a large number of cured specimens were divided into four sets. Specimens from the first and second sets were tested in air and water by a conventional method, i.e., until failure. According to the test results, the  $F-S$  and  $\tau-S$  dependences were constructed; using these dependences, forces  $F$  were determined to be 0.8 of breaking forces  $F_{br}$ :  $F = 0.8F_{br}$ . Specimens from the third and fourth sets were loaded to these values (in air and water, respectively) using the same adhesion tester, unloaded at the same force application rate of  $\dot{F} = 1$  N/s, and loaded again: in this case, until failure. It was found that a single preloading of the joints to  $F = 0.8F_{br}$  does not affect the adhesive strength value (Table. 3-8).

Thus, the loading of the specimens to a stress of 80% of the breaking stress does not lead to a significant increase in the interfacial imperfection and does not cause an irreversible intergrowth of defects. The entire failure process develops at the last stage of loading. It is this stage when the liquid surrounding the specimen can affect the failure of the specimen. Apparently, it is this factor that is responsible for relatively small change in adhesive strength observed during the loading of the joints in water and ethanol.



**Table 3-8. Effect of a single loading on the adhesive strength of EDT-10 epoxy binder–steel wire joints (wire diameter of  $d = 150 \mu\text{m}$ )**

Specimens	Breaking load, N		Adhesive strength, MPa	
	$S = 0.25 \text{ mm}^2$	$S = 0.55 \text{ mm}^2$	$S = 0.25 \text{ mm}^2$	$S = 0.55 \text{ mm}^2$
Reference	15.5	23.0	62.0	42.0
After loading to 80% of the breaking stress	15.0	22.0	60.0	40.0

To date, a reliable physicommechanical interpretation of the effect of liquid medium on adhesive strength has not yet been provided. Two interrelated mechanisms can be proposed.

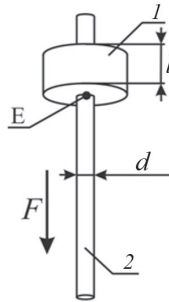


Fig. 3-31. Specimen to determine the shear adhesive strength in fiber–polymer joints: (1) a polymer layer with thickness  $l$  and (2) a fiber with diameter  $d$ .

The lower end of the test joints, i.e., the end to which an external force is applied (e.g., point E in Fig. 3-31), is the site of maximum stress concentration. This end can be regarded as the site of a dangerous defect [146]. The liquid is present at this end from the beginning of the test until the failure of the joint. (The occurrence of a dangerous defect at other sites of the interface is scarcely probable.) Being in contact with a dangerous defect, the liquid can penetrate the crack tip and exert a disjoining pressure. This pressure is added to the stresses acting at the interface. In this case, the failure occurs at lower loads  $F$  than the loads in the tests in air. The ability of a liquid to penetrate the crack mouth is determined by the ability of the liquid to wet the joint components and by the surface tension of the liquid.

Poly(arylene sulfone) is a hydrophobic polymer almost nonwetttable with water. In this case, the strength of the joints does not change. Epoxy

binders are less hydrophobic and partially wettable. Accordingly, in the case of loading epoxy binder-steel fiber joints in a liquid, the  $F$  and  $\tau$  values decrease.

It would seem that the proposed interpretation, which is based on the idea that the liquid in which the polymer-fiber joint is tested changes the interfacial strength by exerting a disjoining pressure in the zone of a dangerous defect, qualitatively describes all the observed results.

However, the liquid that has penetrated the crack can be compared to a liquid in a capillary. If so, then the disjoining pressure value should be approximately proportional to the surface tension of the liquid. However, it was observed (Fig. 3-27, Table 3-4) that a change in the surface tension from 23.5 to 72 mN/m (with a change in the composition of water-ethanol mixtures) does not have any considerable effect on the decrease in the force required for the failure of the joints and a decrease in the interfacial strength. Therefore, disjoining pressure should not be apparently regarded as the main factor controlling the decrease in the interfacial strength.

Another possible mechanism providing an interpretation of the effect of the surrounding liquid on the interfacial strength value in the polymer-fiber system is molecular absorption on the crack walls. This sorption can lead to a decrease in surface energy of substances constituting the crack walls and, therefore, can provide a decrease in the work required for the formation of a new surface. If so, then the measured strength value can be lower than the value in the case of loading in air. It is not improbable that this second mechanism (which is quite similar to the mechanism of the Rehbinder effect in solids) is the main mechanism that controls the loss of interfacial strength during loading of polymer-fiber joints in a liquid medium. However, further research is required to argue for something more specific. Thus, it is necessary to study the wetting of fibers and cured polymers with liquids, the kinetics of the failure process (loading at various  $F$  values), the effect of a surface treatment of the fiber on the change in the interfacial strength under loading in a liquid, etc.

### ***3.3.2.2. Loading of fiber-epoxy resin+PSF matrix joints in a liquid***

As noted above, thermosetting plastic-thermoplastic blends are being increasingly used in actual practice. Their use as matrices of composites (primarily unidirectional) provides the formation of materials that exhibit, along with a high strength and rigidity, a high fracture toughness, crack resistance, and post-impact characteristics. Therefore, it is only natural that the behavior of these systems under operating conditions, in particular, under the action of liquid media, is of particular interest.

It was shown above that the interfacial strength of joints of PSF with fibers of different nature remains constant during loading in polar and nonpolar liquids. This fact suggests that the addition of PSF to an epoxy resin will contribute not only to an improvement of the adhesive properties of the resin (see Figs. 1-6-1-9), but also to the preservation of these properties during the loading of joints of a modified epoxy resin in polar liquids, in which the adhesive strength of unmodified joints decreases.

Figure 3-32 shows the change in the interfacial strength of joints of a typical representative of epoxy resins—the ED-22 oligomer—with a steel wire during tests in polar and nonpolar liquids upon the introduction of 5–20 wt % PSF PSK-1 into the composition.

It is evident that, in the case of loading of joints of an unmodified epoxy resin in water, their interfacial strength is lower than that of the reference joints (tested in air). A decrease in strength is observed for joints of any size. The level of decrease can achieve 20–25%. In this case, the decrease in adhesive strength varies only slightly with a change in the interfacial area. All these relationships were also observed in the case of loading of joints of the EDT-10 epoxy binder in water (see Fig. 3-24).

The addition of poly(arylene sulfone) to ED-22 leads to a regular reduction in the decrease in the adhesive strength (Figs. 3-32b–3.32e); the distance between the  $\tau$ - $S$  curves describing the behavior of the joints under loading in air and water decreases with an increase in the PSK-1 concentration. For the unmodified resin in water, as low as 65% of the adhesive strength is preserved; upon the introduction of 10 wt % PSK-1 and 20% PSF, this value increases to 80 and 90%, respectively. The  $\tau$ - $S$  curves, as in the case of the unmodified resin, are approximately parallel to each other. This fact provides still more evidence to confirm the assumption that the main cause of the occurrence of the  $\tau$ - $S$  dependence is thermally induced residual stresses (see Section 3.3.2.1). A decrease in strength is observed for joints of any size.

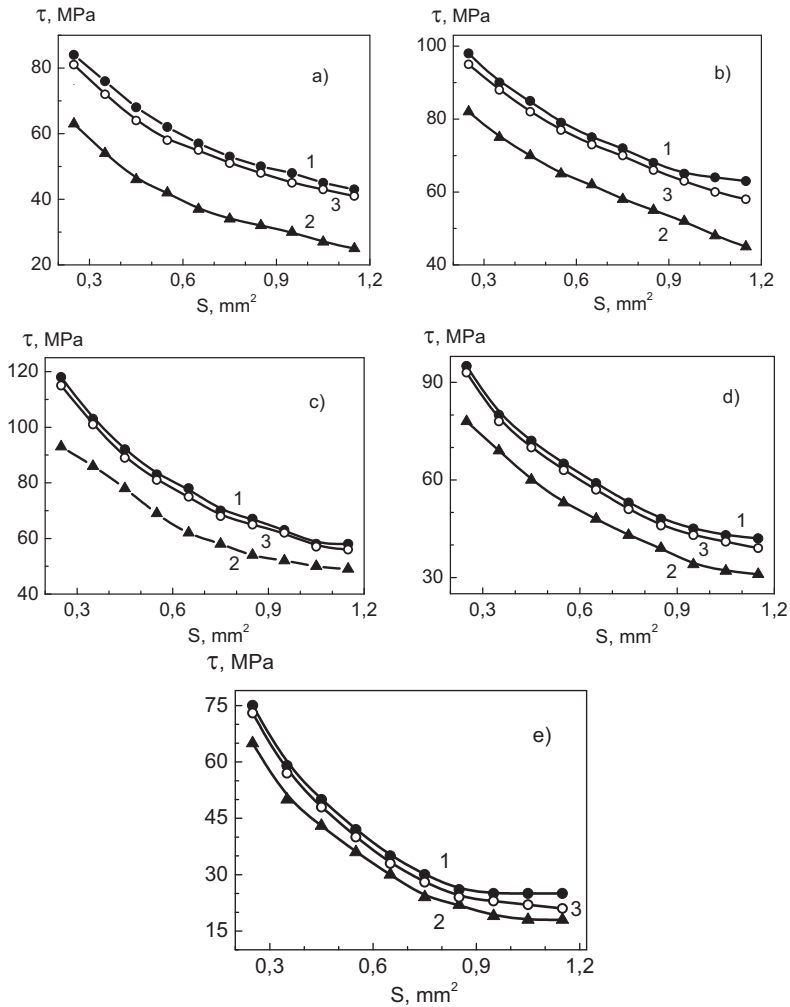


Fig. 3-32. Interfacial strength of ED-22+TEAT+PSK-1-steel wire joints under loading in (1) air, (2) water, and (3) silicone oil. Thermoplastic content: (a) 0, (b) 5, (c) 10, (d) 15, and (e) 20 wt %.

The dependences shown in Fig. 3-32 suggest that the addition of a linear thermoplastic (poly(arylene sulfone)) to the ED-22 thermosetting resin leads to a nonmonotonic change in the interfacial strength in both air and water. This change is clearly seen in Fig. 3-33, which shows the concentration dependences of the adhesive strength of steel fiber-epoxy

resin+PSF blend joints. Under loading in air, the patterns of change in the interfacial strength for the studied joints do not differ from those observed in the case of loading of joints of ED-20+TEAT+PSK-1 blends with various fibers in air (see Section 1.2).

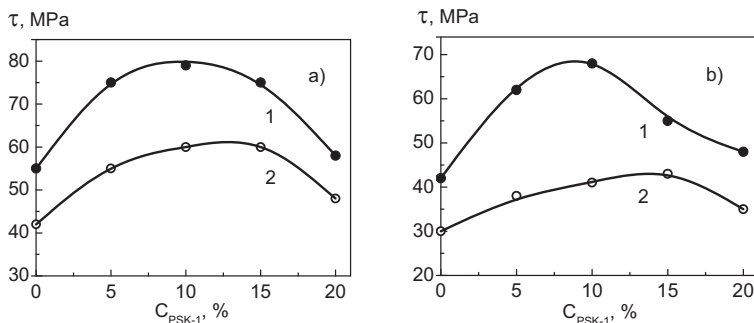


Fig. 3-33. Dependence of the strength of ED-22+TEAT+PSK-1-steel wire joints ( $d = 150 \mu\text{m}$ ) on the modifier concentration at different areas of the joints in (a) air and (b) water. Area of joint:  $S = (1) 0.55$  and (2)  $0.95 \text{ mm}^2$ .

The introduction of small amounts of PSK-1 (up to 20 wt %) contributes to an increase in the adhesive strength: the concentration dependence of adhesive strength exhibits a maximum. The increase in adhesive strength at the maximum (in air and water) achieves 40% of the adhesive strength of systems with an unmodified (original) epoxy matrix. The position of the maximum depends on the test specimen size only slightly. Thus, for joints with an area of  $S = 0.35$  and  $0.55 \text{ mm}^2$ , a maximum is observed at 10% PSK-1 (in air and water), whereas for joints with an area of  $S = 0.95 \text{ mm}^2$ , it takes place at 15% of the modifier in the same media.

Thus, while using joints in an aggressive medium (in our case, in water), it is reasonable to use blends containing 10–20 wt % PSK-1; however, since an increase in the thermoplastic polymer content leads to a significant decrease in the processing properties of the binder (increases the viscosity of the binder), matrices containing 10% PSK-1, which provide a 25–40% increase in the interfacial strength, should be considered optimal.

In all adhesive joints whose behavior in air and a liquid was discussed in this section, the epoxy resin-PSF blends were cured with TEAT. It was found that the replacement of one amine curing agent with another (DADPS), which provides the formation of polymers with a higher heat resistance, does not change the behavior of the fiber-PSF matrix joints not

only during testing in air, but also during loading in a liquid medium. A change in the adhesive strength of fiber-ED-22+PSK-1+DADPS joints under loading in both air and a polar medium (water) with the addition of a thermoplastic is described by a curve with a maximum; as in the case of matrices cured with TEAT, a maximum is observed at a small amount of the modifier (approximately 10 wt %). The introduction of PSK-1 leads to a significant increase in the percentage of strength preserved during loading in water; the higher the PSK-1 concentration, the higher the increase. Upon the introduction of 20 wt % PSK-1, the loss of strength under loading in water is less than 10%.

Thus, in the case of loading in polar liquids, the nature of the amine curing agent does not affect the pattern of the  $\tau$ - $C$  dependence and, apparently, does not change the interface failure mechanism.

In the case of loading of epoxy resin+PSF binder-fiber joints in nonpolar liquids (polydimethylsiloxane), the adhesive strength remains the same as that under loading in air. This is true of curing of adhesives with both TEAT and DADPS; that is, in the case of using both heat-resistant linear polymers (PSF) and blend matrices (EDT-10, epoxy resin-PSF blends with different PSF concentrations) as the adhesives, loading of the joints in nonpolar liquids does not lead to a loss of interfacial strength.

# CHAPTER FOUR

## FURTHER DEVELOPMENT OF THE PULL-OUT METHOD

Most of the data on adhesive strength in polymer–fiber systems have been obtained by the pull-out method, while pulling a fiber out of a polymer layer. A fairly large number of studies have been focused on the development of this method (see, e.g., [30–32, 35–40, 43–46, 92, 144, 159–178]. The fragmentation (“single fiber composite”) [168, 169, 172, 174, 179–209] and pushing out (“indentation”) methods [165, 169, 210] have been used less commonly. From the above list of studies, which is fairly extensive, although far from being complete, it is clear that the main studies focused on the development of an experimental and methodological base for determining the interfacial strength of polymer–fiber joints had been conducted until the 1990s. However, even today, the measurement technique cannot be considered definitely worked out. Many issues associated with the interpretation of the obtained data involving an experimental substantiation of the prerequisites underlying the calculation of the results and the description of the failure of polymer–fiber joints are far from a final solution.

This chapter describes studies conducted at the Laboratory of Reinforced Plastics of Semenov Institute of Chemical Physics of the Russian Academy of Sciences that contribute to solving of the above problems by using the pull-out method and enable a further development of this method.

### ***4.1. On the Interpretation of Results Obtained in Studying the Adhesion of Polymers to Fibers of Different Diameters by the Pull-Out Method***

The pull-out method is used to measure the adhesive strength in joints of polymers with fibers of any diameter ranging from the thinnest fibers with  $d = 7\text{--}9\ \mu\text{m}$  (e.g., carbon, glass, basalt) to the thickest fibers with  $d = 300\text{--}400\ \mu\text{m}$  (e.g., nylon, metal). Diagrams of the main experimental

versions of the method providing the formation of joints in the entire range of fiber diameters are shown in Figs. 4-1, 4-2, 4-3.

For all the versions, it is characteristic that a portion of a fiber with an extremely small length  $l$ , which typically does not exceed 10–20 fiber diameters  $d$  ( $l/d \leq 10-20$ ), is immersed into the polymer layer. Only joints with this short length and, accordingly, a small contact area  $S$  between the polymer and the fiber can undergo adhesive failure; that is, upon the application of a load to these joints, a fiber can be pulled out of the matrix layer. Joints with a higher  $l/d$  ratio undergo cohesive failure: loading of these joints leads to the rupture of the fibers or a failure within the matrix layer.

The resulting joints can be tested (at least under normal conditions) on the same tensile machines that were used to test the fibers or on specially designed adhesion testers (microtensile machines) [30, 31]. Accordingly, for joints of polymers with fibers of any diameter, it is possible to determine the breaking load values and calculate the adhesive strength values. However, there is still no answer to the question of how the adhesive strength values determined in studying joints in which the substrates are fibers of different diameters should be compared; that is, the problem of interpreting the results remains unsolved.

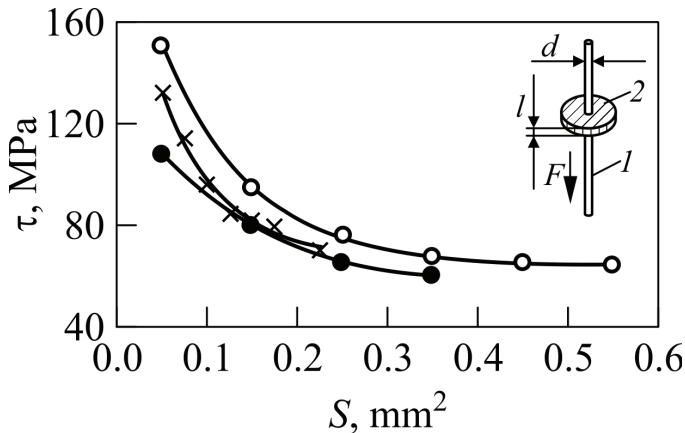


Fig.4-1. Adhesion of the EDT-10 binder to boric fibers with a diameter of (●) 95 and (○) 135  $\mu\text{m}$  and (x) silicon carbide fibers with a diameter of 100  $\mu\text{m}$ . The classical pull-out method; (1) a fiber with diameter  $d$  and (2) a polymer layer with thickness  $l$ .



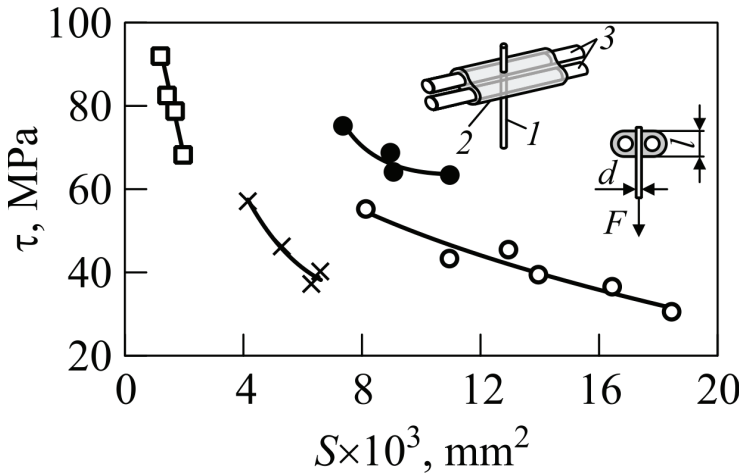


Fig. 4-2. Adhesion of the EDT-10 binder to ( $\square$ ) UKN-5000P carbon fibers with a diameter of 7.5  $\mu\text{m}$ , ( $\bullet$ ) Terlon fibers with a diameter of 17.7  $\mu\text{m}$ , and alkali-free glass fibers with a diameter of ( $\times$ ) 9.6 and ( $\circ$ ) 22.5  $\mu\text{m}$ . The pull-out method in the three-fiber version: (1) a "thin" fiber with diameter  $d$ , (2) a polymer layer with length  $l$ , two thick fibers as "carriers" of the resin.

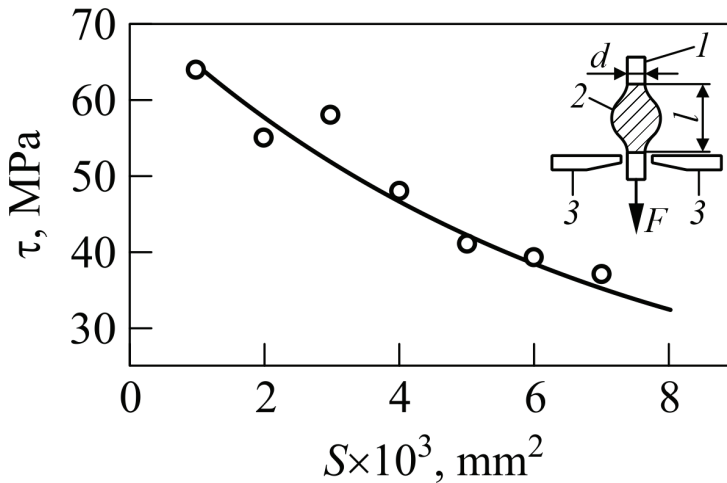


Fig.4-3. Adhesion of the Epon-828 epoxy resin to Kevlar-49 fibers with a diameter of 11.4  $\mu\text{m}$  (according to [39]). The droplet method: (1) a fiber with diameter  $d$ , (2) a polymer droplet with length  $l$ , and (3) razor blades.

In all the versions of the pull-out (microbond) method, the value of tangential adhesive strength  $\tau_i$  of each tested ( $i$ th) joint is calculated by the formula

$$\tau_i = \frac{F_i}{S_i}, \quad (4.1)$$

where  $F_i$  is the load required to pull the fiber out of the polymer layer (breaking load) and  $S_i$  is the area of this joint, the contact area between the polymer and the fiber:

$$S_i = \pi d_i l_i; \quad (4.2)$$

$d_i$  and  $l_i$  are the fiber diameter and the length of the adhesive joint, i.e., the length of the fiber portion immersed into the polymer.

The use of this formula assumes a uniform distribution of stresses at the interface. However, if adhesive strength is measured at temperatures below the glass transition temperature  $T_g$  of the matrix (polymer), then the above assumption is obviously not fulfilled. As shown in the previous chapters, the nonuniform distribution of tangential stresses along the interface is evident from the dependence of the measured adhesive strength values on the size of the joints. If adhesive strength is determined using fibers with a constant diameter, then the size of the joint is determined by the length  $l$  of the fiber portion immersed into the polymer (matrix) layer. In this case, at temperatures below the glass transition temperature of the polymer, adhesive strength  $\tau$  monotonically and nonlinearly decreases with an increase in length  $l$  or, accordingly, area  $S$ :  $\tau = \tau(S)$ ;  $\tau = \tau(l)$  (Figs. 4-1, 4-2, 4-3).

This shape of the  $\tau$ - $S$  dependence is typical. It is observed for fibers of any diameter, any chemical nature, and any strength in the case of their interaction with both network and linear polymer matrices. In addition, it is not of fundamental importance which of the versions of the pull-out method is used. By way of example, Figs. 4-1, 4-2, 4-3 shows the  $\tau$ - $S$  curves recorded with the use of the pull-out method in all versions in testing the joints of typical representatives of epoxy binders with various fibers. A recent study of the adhesion of new classes of polymers to fibers confirmed the existence of the described  $\tau$ - $S$  dependence for all the systems without any exception.

It is clear from the above that the interfacial strength in polymer-fiber joints should be compared using specimens with an identical geometry. This condition can be quite easily fulfilled, if the study is focused on the adhesion of various binders to fibers with an identical diameter. In this case, each polymer-fiber adhesive pair corresponds to one  $\tau$ - $S$  curve:  $\tau =$

$\tau(S) = \tau(l)$  at  $d = \text{const}$ . Joints with an identical geometry are joints with an identical length.

The relative position of the  $\tau$ - $S$  curves makes it possible to compare the binders with each other, while the  $\tau$  values at  $S = \text{const}$  (or  $l = \text{const}$ ) make it possible to quantitatively assess (compare) the strength of the joints of different pairs.

In most cases in all the previous chapters, comparisons were conducted in exactly the same way.

If interfacial strength is measured using fibers with different diameters, then the measured values of adhesive strength  $\tau$  are not only a function of  $l$ , but also a function of  $d$ :  $\tau = \tau(S) = \tau(l, d)$ , while the  $\tau$ - $S$  curves recoded in studying the adhesion of the same polymer to fibers having an identical chemical composition and different diameters  $d$  do not coincide.

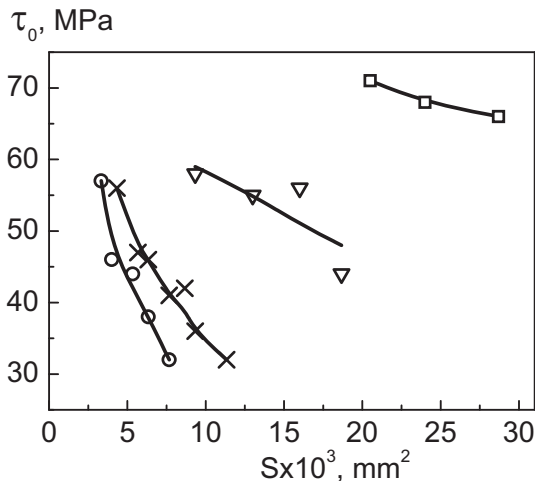


Fig. 4-4. Dependence of the interfacial strength in the glass fiber-epoxy resin matrix joints on the area of the joints; the fiber diameter is (o) 9, (x) 13, (V) 22, and ( $\square$ ) 40  $\mu\text{m}$ .

By way of example, Fig. 4-4 shows the results of measurements of the adhesive strength in the joints of the EDT-10 epoxy binder with glass fibers with a diameter of 9, 13, 22, and 40  $\mu\text{m}$ . The measurements were conducted by the pull-out method in the three-fiber version (Fig. 4-2). It is evident from Fig. 4-4 that adhesive strength is a decreasing function of the area of the joint; in addition, the function is not single-valued: for different

$d$  values, the  $\tau_0$ - $S$  dependence is represented by portions of four different curves.

In the experiments, the results of which are shown in Fig. 4-4, the joints underwent not only adhesive failure (along the interface), but also cohesive failure (across the fiber). Therefore, the ordinate axis shows the average  $\tau_0$  values calculated (for each narrow interval  $\Delta S$ ) by the following formula:  $\tau_0 = \tau + \Delta\tau$ . The meaning of the  $\tau_0$ ,  $\tau$ , and  $\Delta\tau$  quantities was discussed above.

Figure 4-4 shows that the same adhesive pair is characterized by several  $\tau$ - $S$  curves. The following questions now arise: which specimens can be considered specimens with an identical geometry and how the interfacial strengths of polymer-fiber joints should be compared, if the study is focused on the adhesion to fibers of different diameters.

It was repeatedly noted above that the existence of a scale effect of adhesive strength (dependence of  $\tau$  on the geometric parameters of the joints) is associated with the nonuniform distribution of stresses arising from the application of an external load (in testing the joints) and with the nonuniform distribution of residual stresses acting at the interface, primarily, thermally induced residual stresses.

The distribution of residual stresses in polymer-fiber joints was analytically studied in [30, 31], where a simplified—providing only a qualitative description of the phenomenon—simple shear analysis was performed. The analysis showed that the main source of the nonuniformity of tangential stresses acting at the interface is thermally induced residual stresses.

At temperatures higher than the glass transition temperature of the adhesive  $T_g$ , residual stresses can undergo relaxation; below  $T_g$ , they increase almost linearly with a decrease in temperature. The residual stresses are maximal at the ends of the joint, pass through zero in the middle of the joint, depend on the sizes of the specimen, and represent the function of  $l/d$ :  $\tau_T = f(l/d)$ .

The dependence of stresses  $\tau_T$  on dimensionless parameter  $l/d$  suggests that data on the adhesive strength should be represented as a function of dimensionless ratio  $l/d$ , rather than as a function of the area of the joint  $S$  (or joint length  $l$ ).

Figure 4-5 represents data shown in Fig. 4-4 in the  $\tau$ - $l/d$  coordinates. To plot the graph in Fig. 4-5, the entire range of  $l/d$  values was partitioned into subintervals as described above for the area of joints  $S$ . It is evident that, in the proposed coordinates, the experimental results in fact are satisfactorily described by a single curve. Comparison of these curves

makes it possible to compare the adhesive strength of different pairs (to a first approximation).

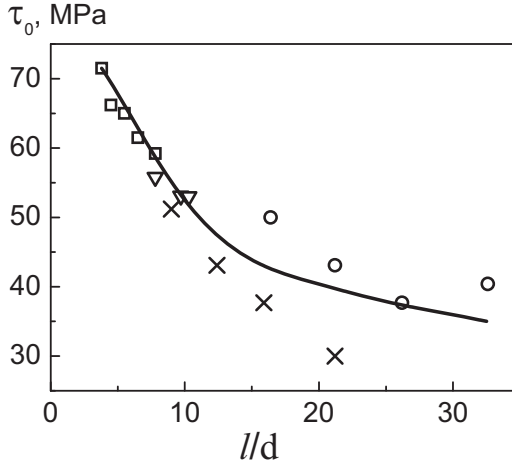


Fig. 4-5. Data of Fig. 4-2 in the  $\tau$ - $l/d$  coordinates.

In addition, the existence of a single  $\tau = \tau(l/d)$  curve clearly indicates that the main factor responsible for the scale effect of adhesive strength really is residual stresses.

Thus, it has been shown that the results obtained in studying the adhesion of polymers to fibers of various diameters should be compared in the  $\tau$ - $l/d$  coordinates. This condition opens up possibilities for a more complete discussion of experimental data. (Note that, in the previous chapters, where appropriate, comparison of the results was conducted in exactly the same way (see, e.g., Section 1.2, Table 1-1; Section 3.2.1, Table 3-1)).

#### ***4.2. Use of Scale Dependences and Variance of Adhesive Strength in Studying the Failure of Polymer–Fiber Joints***

It was shown in the previous chapters that it is currently known how the adhesive strength of polymer–fiber joints changes under the action of a variety of factors, such as test temperature, loading rate, specimen geometry, the nature of the surrounding liquid, and temperature–time conditions of formation.

Almost all experimental data were obtained by the pull-out method. The observed relationships are frequently interpreted using (explicitly or implicitly) the concepts developed in [30, 31, 210] that the failure of the polymer–fiber system begins when the sum of all stresses acting at the site of their maximum concentration (at the locus of failure) exceeds a certain limit, which is referred to as the local adhesive strength and designated as  $\tau_{loc}$ . The  $\tau_{loc}$  value is determined only by the physicochemical interaction at the interface, i.e., the nature of the joint components and the temperature–time conditions for the formation of the joint. Accordingly,  $\tau_{loc}$  values do not depend on the geometry of the joint, the method of fixation of the specimen, and some other details of the experiment. It is  $\tau_{loc}$  that characterizes a given interacting pair, whereas the experimentally measured value of adhesive strength  $\tau_i$  (Eq. (4.1)) characterizes a certain specific joint of this pair.

It was shown [30, 31] that the  $\tau_{loc}$  value can be determined from experimental data, if the  $\tau$ – $S$  dependence and the law of extrapolation of this dependence to  $S = 0$  (to extremely small areas of the joint) are known. The question of localization of the maximum stress concentration at the interface was theoretically studied in detail in analyzing the scale effect of adhesive strength.

The scale effect and possible causes of it were discussed in many studies (see, e.g., [30–32, 35–46, 92]). The calculations were based on different models with different degrees of rigor.

Calculation of stresses by a simple approximate method (simple shear analysis), which was proposed by Cox [211] and modified by Kelly [212], showed that tangential stresses caused by an applied external force  $F$  are maximal at the lower end of the joint, i.e., at the end where the force is applied. In addition, it was shown that thermally induced residual stresses are maximal at both ends of the joint. The conclusion that the maximum stress concentration is achieved near the loaded end of the joint was also made in studying the stress field at the interface by the "intermediate layer" method [213, 214].

The idea that the lower end of the joint is really the region from which the failure begins was used to interpret the relationships determined in studying the effect of various factors on the adhesive strength value measured by the pull-out method. Therefore, any experimental, albeit indirect, evidence of the correctness of this hypothesis was highly desirable.

This kind of evidence was particularly urgent until the direct observations of the formation and development of defects (cracks) at the loaded end of polymer–fiber joints.

These observations in the chamber of an electron microscope were performed in [215- 217]. They will be discussed in the next section.

Indirect experimental evidence of the correctness of the described picture of the failure of polymer–fiber joints was provided in [218, 219], where a new approach to the problem of the failure of these joints was proposed; the approach was based on analysis of the scale dependences of the measured adhesive strength values and adhesive strength variance.

The approach was used in studying the adhesion of the EDT-10 epoxy binder to a steel wire and boron fibers. The joint formation method was described earlier [30, 31] (see A1). Data on the sizes of the joints and the number of tested specimens are given in Table 4-1.

**Table 4-1. Adhesion of the EDT-10 epoxy binder to fibers. Number of tested specimens and sizes of the joints**

Fibers	Fiber diameter $d, \mu\text{m}$	Average breaking load, N	Number of tested specimens	Joint length $l$ , mm	Area of the joint $S, \text{mm}^2$
Steel	150	500	1269	0.08–2.5	0.03–1.2
Boron	135	370	334	0.1–1.4	0.04–0.6

The steel wire and boron fibers used in the experiments as substrates have an almost constant diameter. Therefore, the area of the joints  $S$  changed at the expense of length  $l$  of the adhesive joint (owing to the different amounts of the liquid binder poured into the cups during the formation of the specimens). The joints were cured at  $160^\circ\text{C}$  for 8 h. This mode provides the maximum possible curing depth, which (all other things being equal) contributes to the formation of joints with high and highly reproducible interfacial strength values.

To plot the scale dependences of breaking force  $F = F(S)$ , strength  $\tau = \tau(S)$ , and variance  $D = D(S)$ , the entire range of areas was partitioned into subintervals, each with an area of  $0.1 \text{ mm}^2$ . Note that it is the interval of  $0.1 \text{ mm}^2$  that is usually used by us to process the results obtained in studying the adhesion of polymers to fibers with a diameter of 100–200  $\mu\text{m}$  (see, e.g., [30, 31, 33]).

In accordance with the partition of the entire range of areas into narrow intervals, two indices were used for numbering the test specimens: one of them— $m$ —denoted the number of the interval, the other— $i$ —denoted the number of the specimen whose area fell into the  $m$ th interval.

For each interval  $\Delta S_m$ , the average value of breaking load  $\bar{F}_m$ , adhesive strength  $\bar{\tau}_m$ , and absolute variance  $D_m$  was calculated:

$$\bar{F}_m = \frac{1}{N_m} \sum_{i=1}^{N_m} F_i$$

$$\bar{\tau}_m = \frac{1}{N_m} \sum_{i=1}^{N_m} \tau_i \quad (4.3)$$

$$D_m = \frac{1}{N_m - 1} \sum_{i=1}^{N_m} (\bar{\tau}_m - \tau_{mi})^2. \quad (4.4)$$

The accuracy of determination of variance  $\Delta D_m$  was calculated by the following formula:

$$\Delta D_m = \left[ \frac{1}{N_m - 4} (M_{4m} - D_m^2) \right]^{1/2}, \quad (4.5)$$

where  $M_{4m} = \frac{1}{N_m} \sum_{i=1}^{N_m} (\bar{\tau}_m - \tau_{mi})^4$  (see, e.g., [220-222]). The source

of the error in  $\Delta D$  is the finiteness of the number of test specimens.

In plotting the  $\bar{F}_m$ - $S$ ,  $\bar{\tau}_m$ - $S$ , and  $D_m$ - $S$  curves, the  $\bar{F}_m$ ,  $\bar{\tau}_m$ , and  $D_m$  values fell into the middle of the  $\Delta S_m$  interval.

To analyze the scale dependence of adhesive strength and adhesive strength variance, it is apparently necessary to vary the area of the joint over a wider range. To this end, a large number of specimens should be prepared and tested, because at least a few tens of specimens should fall into each  $\Delta S_m$  interval to provide the calculation of the  $D_m$  value with a sufficient accuracy.

Therefore, it is highly desirable to conduct measurements using a system in which all specimens undergo failure along the interface (adhesive failure) and there are no specimens that undergo failure across the fiber and/or within the adhesive (cohesive failure). It is also desirable to use joints with a well-shaped interface to obtain highly reproducible results from test to test. As noted above, the fulfillment of the last-mentioned condition was provided by the mode used to cure the joints.

That is why a high-strength steel wire was used as the main substrate. The load required to break this wire is higher than the average breaking load of other fibers with the same diameter, such as boron, silicon carbide, and glass fibers (see Table 4-1). Therefore, joints with a steel wire, which undergo failure along the interface under load, can have the widest possible range of areas (compared with joints of the same adhesive with other substrates). In addition, the low variance of the strength of the used wire and the high stability of the wire diameter values along the length contribute to a high reproducibility of results.

In these experiments, all tested EDT-10 binder-steel wire joints underwent adhesive failure. Cohesive failure of the specimens (across the wire) was not observed.



### ***Choice of partition interval $\Delta S_m$***

Since adhesive strength depends on the area of the joint ( $\tau = \tau(S)$ ), both the variance  $D$  values and the variance determination accuracy can depend on the value of the  $\Delta S$  interval in which the averaging was conducted. Accordingly, this interval should be chosen so that a change in the interval would not lead to a significant decrease in the variance determination accuracy. In the case of an infinite number of specimens, a decrease in the partition interval should lead to an increase in the variance determination accuracy, because, in this case, the spread of  $\tau_i$  values relative to the average  $\bar{\tau}_m$  value in the interval decreases. However, in real experiments, a decrease in the  $\Delta S$  interval can lead to both an increase and a decrease in the accuracy of determination of variance  $D_m$ . An increase in accuracy, however, is associated with a decrease in the spread of  $\tau_i$  values relative to  $\bar{\tau}_m$ . However, in the case of a finite number of specimens, a decrease in  $\Delta S_m$  leads to a decrease in the number of specimens used to calculate the average  $D_m$  value in the interval, which can lead to a decrease in the accuracy of determination of  $D_m$ .

To verify the correctness of choice of the partition interval in the described experiment and determine the effect of a decrease in this interval on the variance value and the variance determination accuracy, the change in the  $D_\tau$  and  $\Delta D_\tau$  values upon partitioning the selected  $\Delta S$  interval into two parts was studied.

Let  $\tau_1, \tau_2, \dots, \tau_{N-1}, \tau_N, \tau_{N+1}, \dots, \tau_{2N}$  are the adhesive strength values in a certain interval  $\Delta S$  (symbol  $m$  is omitted for simplicity); the average adhesive strength value in this interval is as follows:

$$\tau = \frac{1}{2N} \sum_{i=1}^{2N} \tau_i \quad (4.6)$$

Let us partition this interval into two parts— $\Delta S_1$  and  $\Delta S_2$ —so that an identical number of specimens  $N$  falls into each of the parts. The average adhesive strength values in each of the new intervals are as follows:

$$\bar{\tau}_1 = \frac{1}{N} \sum_{i=1}^N \tau_i, \quad \bar{\tau}_2 = \frac{1}{N} \sum_{i=N+1}^{2N} \tau_i.$$

The variance values of quantities  $\bar{\tau}_1$  and  $\bar{\tau}_2$  are, respectively, as follows:

$$D_1 = \frac{1}{N} \sum_{i=1}^N (\bar{\tau}_1 - \tau_i)^2, \quad D_2 = \frac{1}{N} \sum_{i=N+1}^{2N} (\bar{\tau}_2 - \tau_i)^2.$$

(For simplicity of calculation, a biased estimate of the variance value was used. In the case of a fairly large number of specimens, it almost coincides with the unbiased estimate value [220-222]).

Putting

$$\bar{\tau}_1 - \bar{\tau}_2 = 2\Delta\tau$$

and taking into account that

$$\bar{\tau}_1 + \bar{\tau}_2 = 2\bar{\tau} \text{ (see Eq. (4.6)),}$$

we have

$$\bar{\tau}_1 = \bar{\tau} + \Delta\tau, \quad (4.7)$$

$$\bar{\tau}_2 = \bar{\tau} - \Delta\tau. \quad (4.8)$$

Substituting the  $\bar{\tau}_1$  and  $\bar{\tau}_2$  values defined by Eqs. (4.7) and (4.8) into the expressions for variances  $D_1$  and  $D_2$  and conducting simple calculations, we obtain

$$D_1 = \frac{1}{N} \sum_{i=1}^N (\bar{\tau}_1 - \tau_i)^2 + (\Delta\tau)^2, \quad (4.9)$$

$$D_2 = \frac{1}{N} \sum_{i=N+1}^{2N} (\bar{\tau}_2 - \tau_i)^2 + (\Delta\tau)^2. \quad (4.10)$$

Let us express the variance  $D$  value in the initial interval  $\Delta S$  (before partitioning) in terms of variances  $D_1$  and  $D_2$  in intervals  $\Delta S_1$  and  $\Delta S_2$  (after partitioning):

$$D = \frac{1}{2N} \sum_{i=1}^{2N} (\bar{\tau} - \tau_i)^2.$$

Using (4.9), (4.10) and (4.7), (4.8), we have

$$D = \frac{1}{2N} \sum_{i=1}^N (\bar{\tau}_1 - \tau_i)^2 + \frac{1}{2N} \sum_{i=N+1}^{2N} (\bar{\tau}_2 - \tau_i)^2 = \frac{D_1 + D_2}{2} + (\Delta\tau)^2. \quad (4.11)$$

The  $(\tau\Delta)^2$  quantity characterizes that part of the variance that is associated with the  $\tau$ - $S$  dependence. The partition of the  $\Delta S$  interval into narrower intervals can be considered reasonable, if the variance of  $\tau$  values in each of the newly formed intervals does not exceed the variance in the initial  $\Delta S$  interval (in the interval that is being partitioned).

Expression (4.11) suggests the following: if the  $(\tau\Delta)^2$  value is low compared with  $D$

then

$$(\Delta\tau)^2 \ll D, \quad (4.12)$$

$$D \approx \frac{D_1 + D_2}{2}.$$

This means that partitioning into smaller intervals does not lead to a change in the variance; accordingly, further partitioning is not reasonable, because it does not provide a more accurate definition of  $D$ . In other words, the use of the initially selected partition interval  $\Delta S$  does not introduce any significant error in the variance  $D$  value. Therefore, condition (4.12) can be used to assess the correctness of the choice of the partition interval. This condition is a mathematical expression of the partition criterion. Examples of choice of the partition interval are given in Table 4-2.

Figure 4-6 shows the scale dependences recorded in studying the adhesion of the EDT-10 binder to steel (strongest) fibers. Figures near the points in the  $\bar{F}_m-S$  curve indicate the number of specimens whose strengths were averaged to obtain a given adhesive strength value. It is evident that the  $\bar{F}_m-S$  and  $\bar{\tau}_m-S$  curves are quite typical. With a variation in  $S$  over a wide range, the force required for the failure of the specimen and the shear adhesive strength are nonlinear functions of the area of the joints. The larger the range of areas in which adhesive strength is measured, the more pronounced the nonlinearity. For large and small joints, the  $\tau$  and  $F$  values differ by a factor of 3–4. It should be noted that, if the range of variation in areas is small, then the nonlinearity of  $\tau$  and  $F$  is expressed only weakly. In this case, the  $F-S$  dependence can be approximated by portions of a straight line; accordingly, the  $\tau$  values can be considered constant. Frequently, this is the case in determining the adhesion of polymer binders to thin fibers (with a diameter of 7–20  $\mu\text{m}$ ), such as carbon, glass, and polymer fibers (see Fig. 4-6b). Apparently, for this reason, the authors sometimes write about adhesive strength values that are constant and independent of the area of the joint.

**Table 4-2. To the choice of partition interval  $\Delta S$** 

$S, \text{mm}^2$	$N$	$\bar{\tau}, \text{MPa}$	$\Delta\tau, \text{MPa}$	$D, \text{MPa}^2$	$D - \frac{D_1 + D_2}{2}, \text{MPa}^2$	$\Delta D, \text{MPa}^2$	$(\Delta\tau)^2, \text{MPa}^2$	$(\Delta\tau)^2/D \times 10^3$
<u>0.3–0.4</u>								
0.3–	150	63.7		72				
0.35								
0.35–	73	64.3	0.75	79	3	9	0.56	8
0.4	77	62.8		58				
<u>0.4–0.5</u>								
0.4–	173	60.2		72				
0.45								
0.45–	85	61.5	0.85	86	–8	9	0.72	12
0.5	88	59.8		73				
<u>0.7–0.8</u>								
0.7–	87	47.8		99				
0.75								
0.75–	43	51.9	4.0	68	16	14	16	166
0.8	44	43.8		99				
<u>0.9–1.0</u>								
0.9–	65	41.1		64				
0.95								
0.95–	33	44.3	3.2	38	10	10	10.6	166
1.0	32	37.8		70				

Figure 4-6 shows the change in adhesive strength variance with a change in the area of the joint. In each  $S_m$  interval,  $D$  values were calculated by Eq. (4.4). It is evident that the  $D_m$  values hardly change with a change in area  $S$  (length  $l$ ), except for variances corresponding to joints of extremely small sizes ( $l/d \leq 2-3$ ).

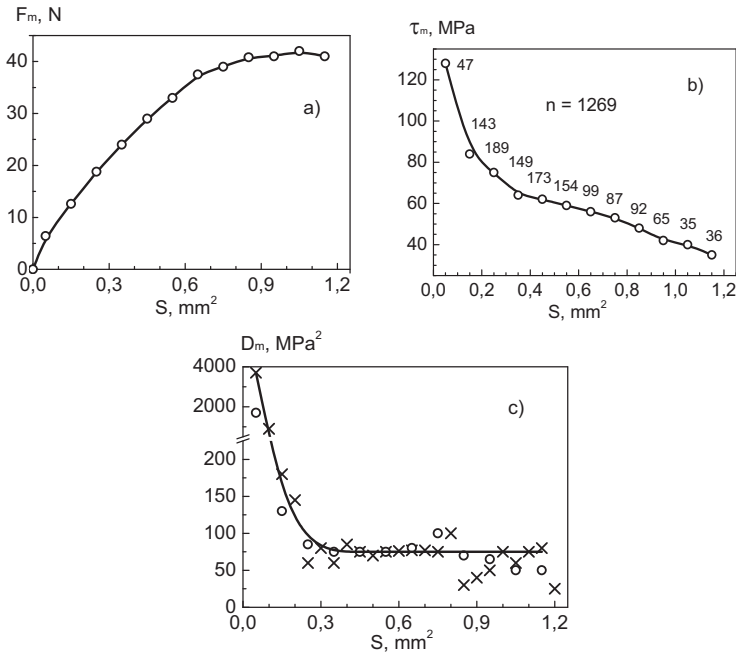


Fig. 4-6. Dependence of (a) breaking force  $F$ , (b) shear adhesive strength  $\tau$ , and (c) adhesive strength variance  $D$  on the area of the joint  $S$  for the EDT-10 binder–steel wire system ( $d = 150 \mu\text{m}$ ):  $\Delta S =$  (o) 0.1 and (x) 0.05  $\text{mm}^2$ . Explanations in the text.

The crosses in Fig. 4-6 show the variance values obtained for the case where the  $\Delta S_m$  partition interval is 0.05  $\text{mm}^2$ , rather than 0.1  $\text{mm}^2$ . The points fit well into the  $D_m$ – $S$  curves constructed during the initial partition. The larger the number of specimens tested in a given interval (the larger the sampling frame), the better the coincidence. Verification in accordance with criterion (4.12) confirms the result.

Some of the quantities used for the calculation are listed in Table 4-2. It is evident that the  $(\tau\Delta)^2$  value is significantly lower than the values of variance  $D_m$ . However, in the case of a large number of specimens in area intervals of  $\Delta S = 0.3$ – $0.4$  and  $0.4$ – $0.5$   $\text{mm}^2$ , the  $(\tau\Delta)^2/D_m$  ratio is a few thousandths; in the case of a relatively small number of specimens in an interval of  $S = 0.9$ – $1.0$   $\text{mm}^2$ , it increases by a factor of 15–20.

Formula (4.11) suggests that the  $D - \frac{D_1 + D_2}{2}$  difference is always positive. However, the data in Table 4-2 show that, in an interval of  $\Delta S = 0.4$ – $0.5$   $\text{mm}^2$ , this difference is negative. Apparently, this fact is attributed

to the spread in the determination of  $D_m$  values. Some  $D_m$  values calculated by Eq. (4.5) are given in the same Table 4-2. It is clear that the  $\Delta D$  and  $D - \frac{D_1 + D_2}{2}$  values are fairly close in all the cases.

Thus, the method of partitioning the areas of adhesive joints into intervals of  $\Delta S_m = 0.1 \text{ mm}^2$ , which was chosen during the processing of the results, does not introduce any significant error in the determination of variance  $D$ ; that is, the method was chosen correctly.

The scale dependences of adhesive strength value and adhesive strength variance for joints of the same EDT-10 binder with boron fibers are shown in Figs. 4-7 and 4-8.

Figure 4-7 shows that the interfacial strength in these joints is fairly high: it is in no way inferior to that in joints with a steel wire.

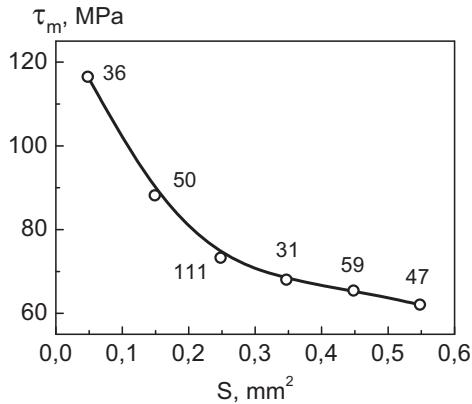


Fig. 4-7. Dependence of adhesive strength  $\bar{\tau}_m$  on contact area  $S$  for EDT-10 binder-boron fiber joints ( $d = 135 \mu\text{m}$ ). Figures near the points show the number of specimens that were tested in a given  $\Delta S_m$  interval.

The average breaking load for boron fibers is less than that for steel fibers. Accordingly, the range of areas of the studied joints is small: the  $S$  values do not exceed  $0.6 \text{ mm}^2$ . It was found that it is this range in which the number of specimens that underwent cohesive failure (across the fiber) does not exceed 5% of the total number of the studied specimens. It was shown earlier [30, 31] that, at this ratio of joints that underwent adhesive and cohesive failure, in processing the experimental results, it is possible to ignore data on the strength of joints that underwent cohesive failure and use Eqs. (4.3) and (4.4) to calculate the adhesive strength value and adhesive strength variance. It is evident from Fig. 4-7 that the  $\bar{\tau}_m$ - $S$  curve

is also quite typical: the shear adhesive strength decreases monotonically and nonlinearly with an increase in the area of the joint.

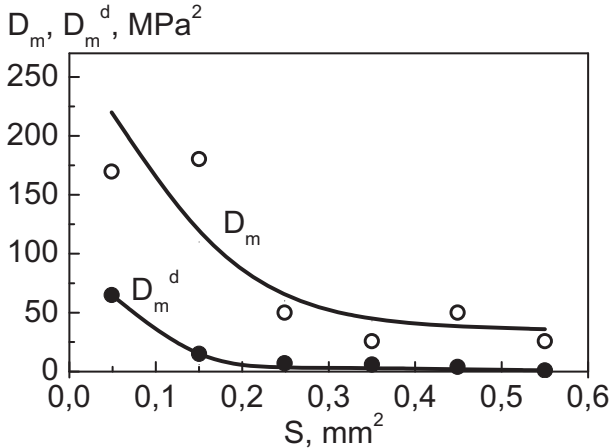


Fig. 4-8. Dependence of variance  $D_m$  of the measured adhesive strength values and variance  $D_m^d$  determined by instrumental errors on the area of adhesive joints for the system shown in Fig. 4.5. The  $D_m^d$  values are calculated by Eqs. (4.13) and (4.14).

The adhesive strength variances of the studied system (Fig. 4-8), except for values corresponding to joints of extremely small sizes ( $S < 0.2$  mm<sup>2</sup>,  $l/d \leq 2-3$ ), hardly depend on  $S$ , as observed in the case of adhesion of EDT-10 to a steel wire. Thus, the shapes of the scale dependences of the adhesive strength variance of EDT-10, which is a typical epoxy resin binder, are identical in the case of adhesion to fibers of different chemical nature, namely, steel and boron fibers. It should be emphasized that we discuss measurements of adhesive strength in joints with high-strength fibers with a large diameter under conditions where cohesive failure across the fiber can be ignored.

It should be noted that the  $D_m$  variances of the measured adhesive strength values are significantly higher than the  $D_m^d$  variances determined by instrumental errors. This is clear from comparison of the data shown in Fig. 4-8. The  $D_m^d$  values were calculated using the formula

$$D_m^d = (\delta \bar{\tau}_m)^2, \quad (4.13)$$

where  $\delta\tau_m$  is the relative error of the measured adhesive strength values; in accordance with Eqs. (4.1) and (4.2), it is as follows:

$$\delta\tau_m = \delta d + \delta l_m + \delta \bar{F}_m, \quad (4.14)$$

where  $\delta d$ ,  $\delta l_m$ , and  $\delta \bar{F}_m$  are the relative errors in measuring the fiber diameter, the adhesive joint length, and the breaking force, respectively. The second and third terms in Eq. (4.14) depend on the size of the joints: all other things being equal, the  $\delta l_m$  and  $\delta \bar{F}_m$  values monotonically increase with a decrease in  $l$  and  $F$ ; a particularly abrupt increase is observed when joint length  $l$  becomes comparable with fiber diameter  $d$  (at  $l/d \approx 2-3$ ). In this region, the instrumental error increases by more than an order of magnitude (see Fig. 4-8). This is one of the reasons for which the region of small areas  $S$  should not be used in studying the scale dependences of the adhesive strength value and adhesive strength variance. Outside this region, i.e., at  $l/d \geq 2-3$  ( $S > 0.2 \text{ mm}^2$ ), the variance of  $\bar{\tau}_m$  values associated with the inaccuracy of the used instruments is 10–25 times lower than the variance of the experimentally measured  $\bar{\tau}_m$  values.

The obtained data make it possible to discuss some issues related to the failure mechanism of polymer–fiber adhesive joints.

As noted above, in measuring the adhesive strength, a variance of adhesive strength values is always observed; in addition, the spread of  $\tau_i$  values always exceeds the instrumental errors. The data shown in Figs. 4-6 and 4-7 suggest that the spread of  $\tau_i$  values can be attributed to the existing spread of the areas of the joints  $S_i$ . However, it is not fundamentally determined by the spread of areas. This assumption is supported by the extremely small  $(\Delta\tau)^2/D_m$  ratio (see Table 4-2), because it is the  $(\Delta\tau)^2$  quantity that characterizes the part of the adhesive strength variance that is determined by the existence of the  $\tau$ – $S$  dependence. The shape of the distribution curves of  $\tau_i$  values in narrow  $\Delta S_m$  intervals also supports the above assumption. A quite clearly pronounced strength distribution is observed even for specimens whose lengths differ only slightly. This is clearly seen in Fig. 4-9, which shows the distribution curves of the measured adhesive strengths of steel fiber–EDT-10 binder joints in area intervals of  $\Delta S_m = 0.1 \text{ mm}^2$ , i.e., joints whose lengths  $\Delta l_m$  differ by no more than 0.2 mm, i.e., by 1.3 the diameter of the fiber the adhesion to which is determined. In this case, the distribution pattern does not differ from a normal (Gaussian) distribution; for different  $\Delta S_m$  intervals, these curves are fairly similar.

The data shown in Fig. 4-9 provide still more evidence of the fact that adhesive strength, as any strength, is a statistical quantity. It is determined by a random distribution of defects responsible for the failure of the studied object. It is only natural to assume that these defects are defects localized in a region where maximum external and internal stresses arise.



It is these defects that most probably become dangerous under loading, and it is the region of localization of these defects where the failure begins.

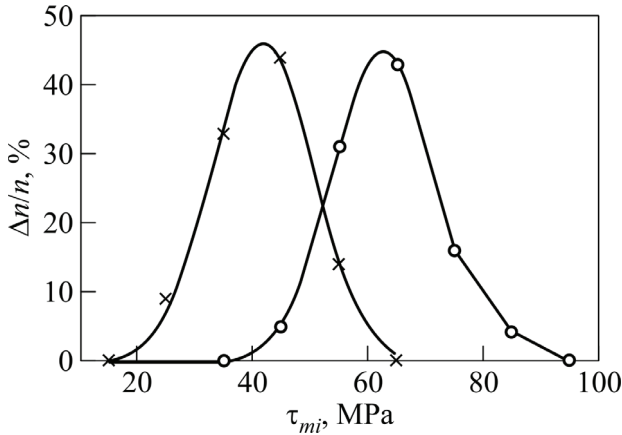


Fig. 4-9. Distribution of adhesive strength values in area intervals of  $S = (x)$  0.9–1.0 and  $(o)$  0.3–0.4 mm<sup>2</sup> for the EDT-10–steel wire system ( $d = 150 \mu\text{m}$ ).

A distinctive feature of polymer–fiber joints is that the localization of the locus of failure in them is predetermined. For all specimens, it is localized near the end of the joint (at the site of maximum stress concentration). This feature makes the studied joints different from specimens with a uniform stress field, in which the probability of encountering a dangerous defect (responsible for the formation of the locus of failure) increases with an increase in the size of the object, and the localization of this defect is, generally speaking, arbitrary.

In terms of the concept developed in [30, 31, 106, 163, 174, 209], the failure of a polymer–fiber system begins when the sum of all stresses acting at the site of their maximum concentration (at the locus of failure) exceeds a certain limit, which is referred to as the local adhesive strength and designated as  $\tau_{loc}$ .

The above can be written as follows:

$$\tau_{mi} + \tau_R = \tau_{loc\ mi} . \quad (4.15)$$

Here,  $\tau_{mi}$  is the experimentally measured adhesive strength value calculated by Eq. (4.1),  $\tau_{loc\ mi}$  is the above-discussed local adhesive strength value of a given specimen, and  $\tau_R$  is all other stresses acting near the end of the joint, primarily, thermally induced residual stresses.

(By implication, the local adhesive strength value does not depend on interval number  $m$ ; the appearance of index  $m$  in Eq. (4.15) is associated with the numbering of specimens adopted here).

Formula (4.15) is a linear equation. Therefore, it suggests that the variance of experimentally measured adhesive strength values is determined by the variance of local adhesive strength  $D_{\tau_{\text{lock}}}$  and the variance of residual stresses.

Stresses  $\tau_R$  depend on the macroscopic—mechanical and thermal—properties of the joint components, such as elastic moduli, linear expansion coefficients, and Poisson's ratios. The variance of these macroscopic quantities is not associated with the distribution of defects at the interface; therefore, it should not be in any way noticeable, at least in specimens prepared from the same set of materials under identical curing conditions. Therefore, to a first approximation, it can be ignored. In this case, Eq. (4.15) suggests that the observed variance of experimentally measured adhesive strength values  $D_m$  is determined by the  $D_{\tau_{\text{lock}}}$  value:

$$D_m = D_{\tau_{\text{lock}}}. \quad (4.16)$$

The variance of  $D_{\tau_{\text{lock}}}$  values is determined by the distribution of defects at the interface in the region of stress concentration near the end of the joint. This distribution arises during the formation of the joint. It cannot depend on the joint size, because the formation of interfacial bonds at the end of the joint does not depend on their formation in other places. Therefore, it is only natural that the absolute variance  $D_m$  of adhesive strength values  $\tau_m$  should not significantly depend on the joint sizes. It is this picture that was observed experimentally (see Figs. 4-6c, 4-8).

In the reasoning on which Eq. (4.16) is based, it was assumed that the region where the locus of failure is formed (interface near the loaded end of the fiber) is small compared with the entire area of the joint  $S$ . The dependence of  $D$  on  $S$  in the region of small lengths (areas) of joints (Figs. 4-6c, 4-8) should apparently be attributed to a violation of this condition. This is yet another argument in favor of the fact that, in studying the scale dependence of adhesive strength value and adhesive strength variance, the region of small  $S$  should be excluded from consideration. The data in Fig. 4-6c and 4-8 show that the length of the region in which the locus of failure is formed is comparable with the fiber diameter.

Equation (4.16) suggests that the distributions of experimental adhesive strength values relative to their average (i.e., the distribution of the  $\Delta\tau_{mi} = \bar{\tau}_m - \tau_{mi}$  quantity) plotted for different measurement intervals  $\Delta S_m$  should coincide.

In fact, writing

$$\bar{\tau}_m = \bar{\tau}_{\text{loc}} - \bar{\tau}_R, \quad \tau_{mi} = \tau_{\text{loc } mi} - \tau_{R } mi$$

and subtracting one equation from the other, we have

$$\Delta\tau_{mi} = \bar{\tau}_m - \tau_{mi} = \bar{\tau}_{loc} - \tau_{loc\ mi}. \quad (4.17)$$

(Here, it is taken into account that  $\bar{\tau}_R = \tau_{R\ mi}$ ).

Some distributions of the  $\Delta\tau_{mi}$  value are shown in Fig. 4-10a. They are plotted for the results shown in Fig. 4-9. It is evident that these distributions are really close.

The distribution curves of  $\Delta\tau_{mi}$  values recorded in studying the adhesion of the same EDT-10 binder to boron fibers are shown in Fig. 4-10b. In is evident that, in this case, the distributions corresponding to different intervals are also hardly distinguishable.

The observed coincidence provides still more evidence that adhesive strength variance is determined by the statistical nature of adhesive strength, rather than by the different sizes of the specimens.

Thus, the fact that  $D$  values do not depend on  $S$  and identical shapes of the  $\Delta\tau_{mi}$  distribution curves for joints of different sizes (see Eq. (4.17)) experimentally confirm the assumption that the region near the end of a polymer–fiber joint to which an external force is applied acts as a stress concentrator, a site of a dangerous defect, and a locus from which the failure of the interface begins. The identical shapes of the  $D$ – $S$  curves for joints of an epoxy polymer with fibers of different chemical nature (Figs. 4-6c, 4-8) indicate an identical mechanism of their failure.

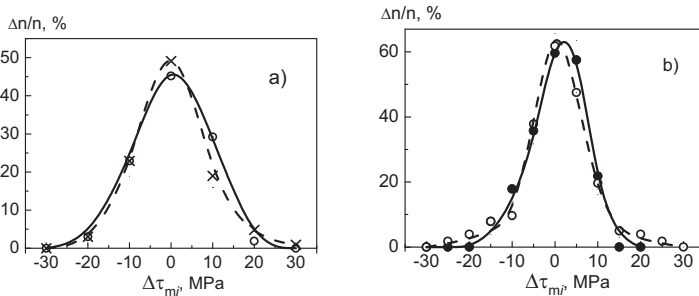


Fig. 4-10. Distribution of  $\Delta\tau_{mi} = \tau_m - \tau_{mi}$  values for (a) the EDT-10–steel wire system,  $\Delta S = (x)$  0.3–0.4 and  $(o)$  0.9–1.0 mm<sup>2</sup> (see Fig. 4-9) and (b) the EDT-10–boron fiber system,  $\Delta S = (o)$  0.2–0.3 and  $(\bullet)$  0.5–0.6 mm<sup>2</sup>.

The EDT-10 epoxy binder is a typical representative of thermosetting matrices. It is reasonable to expect that, in the case of adhesion of other thermosetting resins to high surface energy fibers, the adhesive strength variance will also be independent of the joint sizes; that is, the conclusion about the localization of the locus of failure at the end of the specimen to

which an external force is applied is fairly general and valid for a wide range of pairs.

### 4.3. Electron Microscopic Study of Crack Formation and Propagation at the Binder–Fiber Interface

Until recently, there have been no reports on experiments in which the kinetics of formation and propagation of cracks responsible for the failure of the interface is studied at the electron microscopic level. However, as noted in Section 4.2, a direct experimental study of crack formation and propagation at the interface makes it possible to verify the idea of many authors that the initial crack is formed at the end of the joint loaded with an external force—at the site of maximum stress concentration—and provides a clearer picture of the processes that occur during the failure of the compositions. The lack of those data is attributed to the difficulty of designing the respective experiments. It is clearly visible from Figs. 4-1–4-5 that cracks formed at the interface are poorly accessible for observation: the processes that occur at the interface are hidden by a layer of the binder. Crack propagation at the fiber–polymer interface can be assessed only via recording the shift of the fiber relative to the adhesive layer.

The authors of [215– 217] have made an attempt to observe the failure of the interface in a fiber–matrix joint under loading directly in the chamber of a scanning electron microscope (SEM). The joint contained the SVM organic polyheteroarylene fiber with a diameter of 13–14  $\mu\text{m}$  and the EDT-10 epoxy binder. The specimens were prepared by the three-fiber method (see Fig. 4-2).

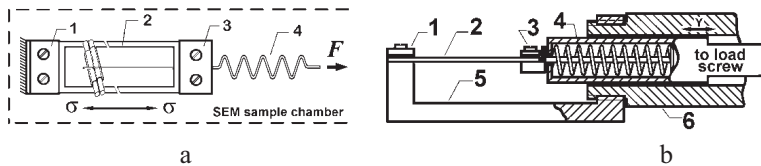


Fig. 4-11. (a) Scheme of specimen loading and (b) scheme of a loading device: (1) fixed clamp of the loading device, (2) test specimen, (3) movable clamp of the loading device, (4) force adjusting spring, and (5, 6) body parts.

Figure 4-11a shows a scheme of specimen loading in an electron microscope chamber; Fig. 4-11b shows a loading device. The proposed design makes it possible to observe the specimen while rotating it by 360° around the loading axis. The applied force is adjusted by compressing the spring. The frame pulse count (25 frames/s) was added to the SEM video

signal to measure the loading time. The observed process was recorded on a videotape recorder for subsequent analysis. The details of the method are described in [215 - 217].

Figure 4-12 shows electron micrographs of the test specimen before testing. The SVM fiber with a diameter of  $13.6\ \mu\text{m}$ , the adhesion to which is determined, is glued between two thick glass fibers whose diameter ( $100\ \mu\text{m}$ ) determines the joint length. Figure 4-13 shows a small meniscus formed by the adhesive at the end of the adhesive joint (at the exit of the thin fiber from the joint) at a higher magnification.

The experiment was conducted in the creep mode; the specimen was placed in the SEM chamber under a load of  $\sim 70\%$  of the breaking load. The average breaking load was known, because the adhesive strength of the pair was predetermined on an adhesion tester (in the = const mode).



Fig. 4-12. Electron micrographs of the test specimen before testing in the SEM chamber.

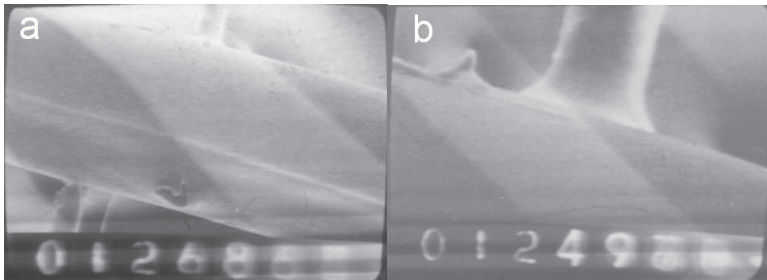


Fig. 4-13. The specimen loaded in the SEM chamber at a moderate magnification (a, b).

It should be noted that the interfacial strength of the test pair is fairly high. This fact is represented in Table 4-3.

**Table 4-3. Adhesive strength the EDT-10 epoxy binder interacting with organic and glass fibers with a diameter of 13–13.5  $\mu\text{m}$  ( $S = 6 \times 10^{-3} \text{ mm}^2$ )**

Fiber type	$n_\tau$	$n_\sigma$	$n$	$\tau_0$ , MPa
SVM	40	52	92	57.0
Glass	129	157	286	43.0
Kevlar	39	60	99	44.0

$n_\tau$  is the number of specimens that underwent adhesive failure;  $n_\sigma$  is the number of specimens that underwent cohesive failure (across the fiber);  $n$  is the total number of specimens tested in the experiment; and  $\tau_0 = \tau + \Delta\tau$ , where  $\Delta\tau$  is the correction associated with the presence of specimens that underwent cohesive failure. The algorithm for data processing and the  $\Delta\tau$  correction calculation is given in [30, 31].

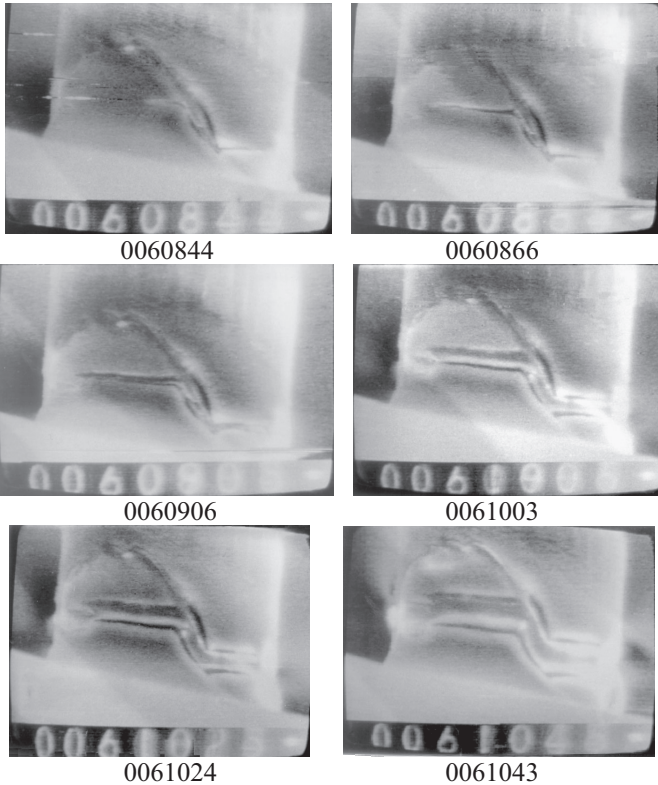


Fig. 4-14. Typical videotaping frames of the sequential development of an annular crack in the meniscus of a thin fiber.

It lists, in addition, the adhesive strengths of two other pairs. One of the joints is formed due to the interaction of the same EDT-10 epoxy binder with the Kevlar polyheteroarylene fiber (DuPont, United States). The other pair is formed by the EDT-10 binder and an alkali-free glass fiber, which is a counterpart of E-glass. It is evident that the adhesive strength in the test system is significantly higher (by ~30%) than that in the other two systems, although the sizes of all the joints are identical. It is this fact that determined the choice of the studied pair.

Figure 4-14 shows typical micrographs recorded during the test. A crack was formed at the end of the joint to which the force was applied—close to the end of the meniscus. About 10 min passed from the beginning of the experiment to the time of crack formation. Apparently, this time can be regarded as the crack initiation time. The crack gradually became annular; after that, the crack "banks" began to diverge. This fact suggests that the crack propagates along the interface (fiber is shifted relative to the resin layer).

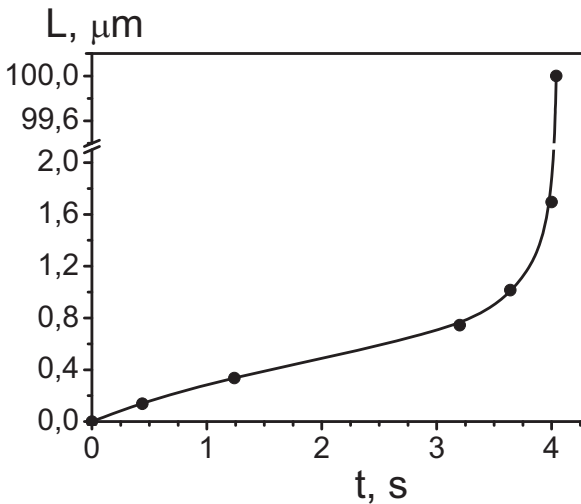


Fig. 4-15. Distance traveled by an annular crack along the binder–fiber interface. The origin of coordinates corresponds to the appearance of the crack in the field of view.

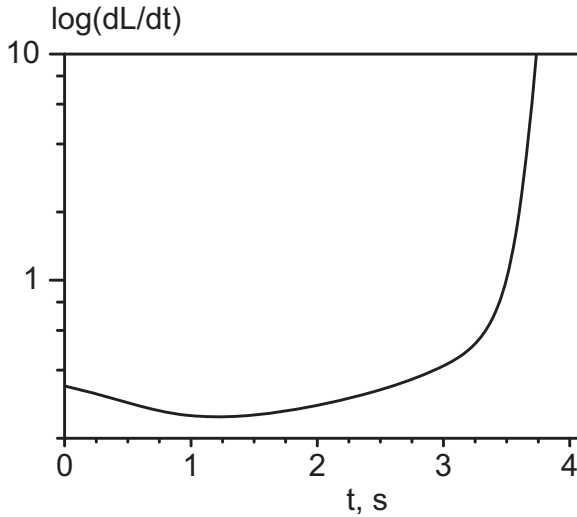


Fig. 4-16. Logarithm of the propagation rate of an annular crack along the binder–fiber interface. The plot is constructed by differentiating the approximating curve shown in Fig. 4-15.

Analysis of the frames shown in Fig. 4.14 and similar frames made it possible to observe the kinetics of the failure process. Figure 4.15 shows the distance traveled by the crack from the time of formation to the complete failure of the adhesive joint. It is evident that, initially, the crack propagates along the fiber at an approximately constant rate. This initial period lasts about 3 s. After that, the crack propagates along the interface at an ever increasing rate, so that the entire failure process of the specimen lasts no more than 4 s. The final "catastrophic" crack propagation and the pulling out of the fiber almost over the entire joint length ( $\sim 120\text{--}150\ \mu\text{m}$ ) occurs within just a few hundredths of a second (0.04 s).

A closer inspection of the initial portion of the  $L$ – $t$  curve (in Fig. 4-15) shows that, before the failure of the specimen, before the almost instantaneous crack propagation, the crack propagation rate decreases.

This tendency is clearly visible in Fig. 4-16, which shows the change in the crack propagation rate during failure.

The minimum rate is observed 1–2 s after the appearance of the crack in the field of view (after crack initiation). Apparently, this time corresponds to the final formation of the annular crack. The further mechanism of the failure process can be represented as follows. Crack propagation along the interface is associated with the failure of adhesive



bonds, which leads to a decrease in the length and area of the unfailed portion of the joint. Since force  $F$  applied to the specimen is maintained almost constant during the entire experiment, a decrease in the area of the adhesive joint leads to an increase in the stress in the joint portion that remained unfailed. This increase, in turn, leads to a continuous increase in the crack propagation rate and an avalanche—almost "instantaneous"—failure of the specimen.

The results show that, under the described conditions, the lifetime is determined by the time of initiation of a dangerous defect (crack). In this experiment, it was  $\sim 10$  min; the entire further process of crack formation and propagation lasted  $\sim 4$  s; that is, it occurred 150 times faster. However, it should be noted that the time of each of the three stages into which the "lifetime" of a crack can be conventionally divided (initiation, formation, propagation) significantly depends on the conditions of the experiment. In the case under study, it depends on the applied force value.

Figure 4-17a shows the end of the SVM fiber after the described test. The annular portion of the meniscus remaining on the fiber is visible. The clean portion torn from the joint indicates the adhesive pattern of failure. Figure 4-17b shows a clean hole in the joint after testing.

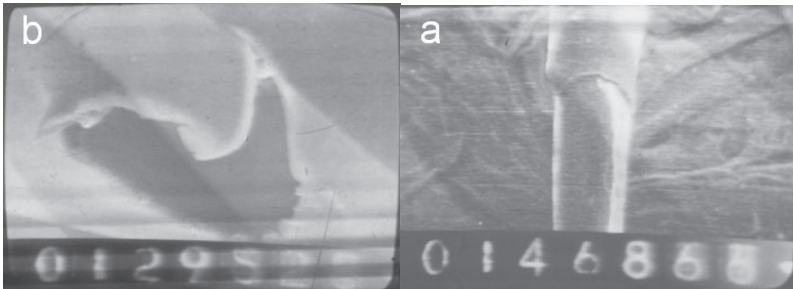


Fig. 4-17. (a) End of the SVM fiber and (b) clean hole in the resin after testing.

It should be noted that, after the adhesive failure of the joints, a round hole with smooth edges is not always formed in the adhesive. It is typical for the failure of joints of polymers with fibers into which the polymer cannot diffuse.

These joints are formed with glass, basalt, metal, carbon, and other similar fibers. The studied high-strength super-high-modulus SVM polymer fiber consists of fibrils weakly bound together in the transverse direction. During the formation of the joint, the binder components can diffuse into this fiber. Therefore, the binder interacts with the fiber not only along the interface, but also in the bulk. As a consequence, after the

failure of the joints, there are specimens in which a round hole with "whiskers" sticking out of it is observed in the adhesive. Apparently, these whiskers are groups of fibrils split off from the fiber. Examples of these cases are shown in Fig. 4-18.

Strictly speaking, in this case, it is necessary to state the occurrence of a mixed failure of joints. However, the area of the interface changes only slightly upon splitting off of the surface fibrils. Hence, the failure of these specimens can be assigned to an adhesive failure; however, this assignment is conventional.

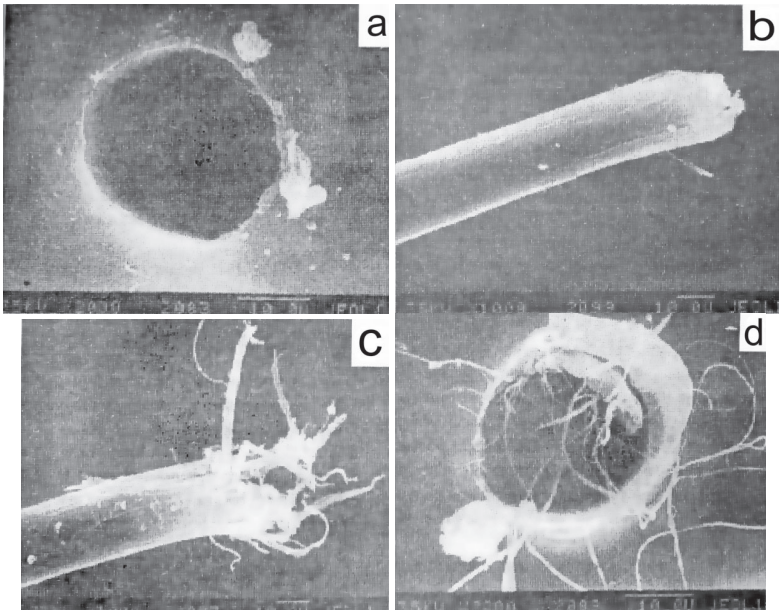


Fig. 4-18. Pattern of failure of adhesive joints: (a, b) pure adhesive failure in the joint and (c, d) a "whisk" of the fiber and whiskers in the hole of a conventional adhesive failure [45].

Thus, the development of a technique for loading fiber–binder adhesive joints directly in a SEM chamber has first made it possible to observe the development of the failure of fiber–matrix joints in the unit cell of a fiber-reinforced plastic and study the kinetics of the process at the electron microscopic level. It has been found that, under the action of a constant force, a dangerous defect (crack) is formed in the resin at the edge of the meniscus at the end of the joint to which an external force is applied. Within a short time, the crack becomes annular. It expands and

propagates inside the joint, most probably, because of an increase in the load. Thus, the assumption that a crack (dangerous defect) responsible for failure is formed at the site of maximum stress concentration has been experimentally confirmed; it has been shown that this site is localized in the resin at a certain distance from the end of the joint, rather than at the end of the joint.

IN LIEU OF AN AFTERWORD

DEVELOPMENT OF STUDIES ON  
ADHESION IN THE LABORATORY OF  
REINFORCED PLASTICS OF SEMENOV  
INSTITUTE OF CHEMICAL PHYSICS OF THE  
RUSSIAN ACADEMY OF SCIENCES

All the main results described in this monograph were obtained in the adhesion research group of the Laboratory of Reinforced Plastics of the Department of Polymers and Composite Materials of Semenov Institute of Chemical Physics of the Russian Academy of Sciences. This group was organized by the head of the laboratory Galya Dmitrievna Andreevskaya in 1959. In the same year, G.D. Andreevskaya and her postgraduate student G.V. Shiryayeva began to study adhesion to fibers; since then—for 60 years—the study of adhesion is one of the priority directions in the research activities of the Laboratory.

Interest in processes that occur at the fiber–polymer interface is attributed to the fact that fibrous composite materials came into operation. It soon became clear that, to design these materials, directionally control their properties, and predict changes in these properties under the action of various operating factors, it is necessary to know not only the properties of fibers and polymer matrices and the laws governing changes in these properties, but also the properties (primarily, strength) of the fiber–polymer matrix interface.

The first report on studying the adhesive strength in polymer–fiber joints appeared in the world literature in 1959. The author of that report—F.I. McGarry—proposed a method to determine the adhesive strength in systems composed of polymers and so-called "thick" fibers, i.e., fibers with a diameter of 100–200  $\mu\text{m}$  [223]. At that time, only glass fibers were used as reinforcing fillers. It was adhesion to glass fibers that was the focus of the McGarry's study.

At that time, the researchers of the Laboratory of Reinforced Plastics also worked on the development of a method to determine the adhesive

strength of glass fiber–polymer systems. However, unlike McGarry, efforts were aimed at measuring the adhesion to the surface of fibers that were directly used in the production of fiber-glass reinforced plastics (FGRPs), i.e., "thin" fibers with a diameter of 10–20  $\mu\text{m}$ . The aim was to "invent" a principle and construct devices that would provide the formation of a joint in which the contact between the resin and the fiber has so short length  $l$  that, in the case of a failure of the joint, the fiber can be pulled out of the joint without being ruptured.

This method has been developed (with the participation of A.D. Bernatskii and E.S. Zelenskii in the design). In 1962–1963, at the Laboratory, the first measurements of the adhesive strength in a polymer–thin fiber system were conducted, and, accordingly, the first reports on the measurements were published [224–226]. Since then, the Laboratory has long taken one of the leading places in studying the adhesion of polymer to fibers. The main results obtained from the 1960s to the 1990s are summarized in monographs [30, 31].

All the 1960s were the years of vigorous research on FGRPs. The researchers of the adhesion research group, as researchers elsewhere in the world, studied the adhesion of crosslinked thermosetting binders (mostly epoxy, phenol-formaldehyde, polyester, and organosilicon)—"pure" and modified—to glass fibers of various chemical compositions. In the 1960s, basalt plastics and metalloplastics, in addition to FGRPs, were produced and studied. Accordingly, the adhesion to basalt fibers and a metal wire was studied. The adhesive strength of a system with a wire with a diameter of  $d \geq 100 \mu\text{m}$  was measured using an upgraded version of the McGarry technique adapted for the preparation of a large number of specimens.

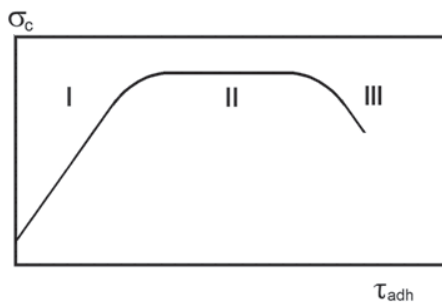
At that time, the main aim was to increase the interfacial strength. It was assumed that, in this case, the physicomechanical characteristics of FGRPs would also increase. Our laboratory worked on designing composite materials for structural purposes, i.e., high-strength unidirectional composites. For these materials, the formation of a strong interface was particularly important. Quite frequently, we were asked to "increase the adhesion by 2 times"!

Adhesive strength can be changed (all other conditions being equal) either by modifying the fiber surface or the polymer matrix or by changing the curing mode. In the 1960s (and in subsequent years), huge efforts were exerted to design all kinds of finishing agents and lubricants, primarily, those based on vinylsilanes and aminosilanes. An extremely large number of reports were focused on studying the adhesive strength of systems composed of thermosetting binders and fibers whose surface was treated with the above compounds.

Gradually, it became clear that an increase in adhesion by a factor of 2–3 (for resins with a high adhesion) is hardly possible, and, probably, inappropriate.

In fact, the relationship between the strength of a fibrous composite  $\sigma_c$  and the adhesive strength of the components that constitute it  $\tau_{adh}$  can be schematically represented as follows (see the scheme).

If there is no adhesion, then the composite does not exist. There exists simply a bundle of fibers, and the strength of the "reinforced plastic" is equal to the strength of that bundle. At low adhesion values (portion I), the interface can be a "weak link" in the composite material; the failure process will begin from the interface. At high adhesive strength values (portion II), the strength of the composite can be independent of the interfacial strength. Here, the weak link will be either the matrix or the fiber. Above the  $\tau_{0max}$  value, the adhesive strength probably should not be increased (portion III has not yet been confirmed experimentally).



Schematic dependence of the strength of composites  $\sigma_c$  on the adhesive strength of fiber–matrix joints  $\tau_{adh}$ .

The shape of the  $\sigma_c$ – $\tau_{adh}$  dependence and the validity of this dependence for composites based on fibers of different chemical nature were experimentally determined significantly later. (The data are summarized in [28]). In the 1960s, it was shown that the strength of FGRPs really increases, if the adhesive strength increases; that is, the  $\sigma_c$ – $\tau_{adh}$  relationship is described by portion I of the curve in the scheme. The increase can be quite significant.

Thus, the main factors whose effect on adhesive strength value was studied in the 1960s were (1) the nature of the binder and (2) the surface treatment of glass fibers.

The 1960s are the years of foundation of a methodological base for studying the interfacial strength in fiber–polymer systems. This is particularly true for the specimen preparation procedures. In those years, various specimen preparation methods were proposed not only by researchers from the Soviet Union, but also by scientists from other countries, such as France, Finland, and the United States. Subsequently, techniques for measuring the strength of polymer–fiber joints were also developed in Germany and Israel.

In that first decade of the vigorous study of the adhesive strength in glass fiber–polymer systems, it became clear that the procedure for the preparation of polymer–fiber joints cannot be regulated, and, accordingly, there can be no standards for determining the  $\tau_{adh}$  value. In fact, composites are produced using fibers of various origins, diameters, and strengths and binders that are liquids of various viscosities, powders, and films.

To effectively determine the adhesive strength of the entire variety of the used pairs (i.e., prepare specimens with a fairly short joint length for each of these pairs), it is frequently necessary to introduce something new—changes that cannot be foreseen in advance—into the joint formation method.

At the same time, the test conditions can be regulated upon availability of standard typical tensile microtesters. At that time, these testers were not available; testers of the Schopper type from Germany were the most common. In the 1960s, a complex of adhesion testers was designed at the Laboratory; it provided the testing of fiber–polymer joints not only at room temperature, but also in a wide temperature range (–200 to +200°C) at different loading rates (3 decimal orders) and in different liquid (and gaseous) media.

The researchers, primarily, V.G. Ivanova-Mumzhieva and Z.A. Pavlova, have invested a lot of efforts and love in the design of the adhesion testers and the development of the testing procedure. These devices have proven to be reliable, convenient, and long-running. Their improved models still serve us today. Their design has made it possible to study the temperature–time and temperature–rate dependences of the adhesive strength of fiber–polymer joints and, accordingly, the nature of adhesive strength. At that time, C.N. Zhurkov and his colleagues were intensively and effectively developing the thermofluctuation (kinetic) theory of the strength of solids, in particular, glassy polymers (and composites). Studying the laws governing the change in the adhesive strength under the action of temperature and loading rate, we showed that the adhesive failure mechanism is also of a kinetic (thermal fluctuation)

nature. In addition, it was shown that the presence of an interface (the fact that the study is focused on the strength and failure of joints composed of two different solids) introduces some features into the relationships: the presence of an interface makes the dependence of strength on temperature and loading time (rate) more complex. The observed loss of simplicity of the relationships is primarily associated with the fact that the stress field in the specimens (polymer–fiber joints) is inhomogeneous. An experimental evidence of this fact is that the value of adhesive strength  $\tau$ , which was calculated as  $\tau = F/S$ , was found to be dependent on the shape and size of the specimen ( $F$  is the force at which the fiber is shifted relative to the adhesive layer and the adhesive joint undergoes failure,  $S$  is the area of the joint, i.e., the contact area between the polymer and the fiber). For specimens in which a fiber of an identical diameter is used, the  $\tau$  values depend on the length of the joint  $l$  (on  $S$ ); with an increase in  $l$ , they monotonically decrease, whereas the breaking load increases monotonically, yet nonlinearly, with an increase in  $S$ .

In the late 1960s and early 1970s, especially when electronic computers became available, the stress field in small polymer–fiber joints was studied quite thoroughly and vigorously. The studies were conducted by different methods (at different levels of rigor): analytically, by the finite element method. In our laboratory, R.A. Turusov proposed that the strength should be calculated by the boundary layer method [213, 214].

Calculations of the stress field continued further on. The nature of the scale dependence of interfacial strength was revealed; this quantity should be used to discuss the nature of adhesive strength and study the relationship between the strength of a fiber-reinforced plastic and the adhesive strength in the unit cell of the plastic. New experimental  $\sigma_c$ – $\tau_{adh}$  curves were recorded.

By the end of the 1960s, another problem—processing of the results of strength measurements in polymer–fiber joints—had also been solved.

In studying the strength of the fiber–binder interface, a fundamental difficulty arises: the higher the adhesion, the more difficult the measurement, because, in the case of a high adhesion, in joints under loading, the fibers are readily being ruptured rather than pulled out of the joint; that is, the joint undergoes cohesive failure, rather than adhesive failure. In addition, the higher the adhesion (all other conditions being equal), the larger the number of cohesively ruptured specimens. These specimens will include those for which the  $\tau$  values are fairly high. Accordingly, the arithmetic mean value of strength  $\tau$  of all joints that underwent adhesive failure



$$\bar{\tau} = \frac{1}{n_{\tau}} \sum_{i=1}^{n_{\tau}} \tau_i$$

does not determine the "true" average value of the test pair  $\tau_0$  (even in the case of a quite large number of specimens that underwent adhesive failure  $n_{\tau}$ ). For resins with a high adhesion, in general,  $\bar{\tau} < \tau_0$ .

This situation cannot be remedied by increasing the number of tested specimens. It is fundamental and determined by the statistical nature of adhesive strength (and the final strength of the fibers). Therefore, even at a fairly short length of the joint, competing (either adhesive or cohesive) failure processes are observed.

We have derived relationships that make it possible to determine the true average value of  $\tau_0$ , which does not depend on the cohesive strength of the components (the fiber and the binder), from the results of tests in which both adhesive and cohesive failure of specimens is observed. The derived relationships were used to develop programs for processing results of tests with competing failure processes. The programs were effectively used in subsequent years.

Unfortunately, the proposed algorithm has not been commonly used. Until now, in a number of studies on the adhesive strength of polymer–fiber joints, the specimens that underwent cohesive failure are simply excluded from consideration without any analysis; accordingly, the interfacial strength of the tested pairs is characterized by underestimated values.

In the 1970s, industrial carbon fibers came into operation. Their diameter is smaller than that of glass fibers, namely, 5–9  $\mu\text{m}$ . The study of adhesion to these thin fragile fibers also began with the foundation of an experimental base. The procedures used for working with glass fibers—mostly the specimen preparation methods—were changed. Note that the entire subsequent experience in studying the adhesion in polymer–fiber systems showed that the efficiency of the study is generally determined by the ability to prepare a sufficient number of specimens with a well-formed interface. This ability is determined by the strength, diameter, and flexibility of the fiber.

The techniques for preparing joints of polymers with fibers with a diameter of 5–10 to 40–50  $\mu\text{m}$  differ from each other only in details, rather than fundamentally. A change in these techniques frequently consists in searching for these details and their working out.

The preparation of high-quality joints with carbon fibers is more labor-intensive and time-consuming than the preparation of joints with glass

fibers and requires higher skill. Therefore, the number of reports on studies of adhesion to carbon fibers is significantly smaller than the number of reports in which the study is focused on adhesion to glass fibers. This is also true for the publications of our Laboratory.

The range of issues that were studied upon the development of each new type of fibers remained approximately the same: the studies were focused on factors affecting the physicochemical characteristics of composite materials, in which these new fibers are used as a reinforcing filler. The nature and composition of the matrix, the surface state of the fiber, curing conditions, and operating conditions (temperature, loading rate, ambient environment, etc.) were considered as the main factors.

Carbon fibers are heat-resistant fibers. Therefore, the effect of the nature of the matrix on adhesive strength was studied using not only epoxy, phenolic, and other resins, but also more heat-resistant matrices, primarily, polyimide ones.

As in the case of glass fibers, the effect of the surface treatment of the fiber on interfacial strength was studied. It was found that the most effective surface treatment for carbon fibers is an oxidative treatment, which leads to the formation of carbonyl and carboxyl groups on the surface, rather than finishing, as in the case of glass fibers.

It was found that the adhesive strength of systems composed of binders and carbon fibers with a thoroughly treated surface is no lower than that in the case of glass fibers, although the initial surface of these fibers is inert and the adhesion to it is low.

Quite soon, a lot of actual data on the adhesive strength of carbon fiber-polymer joints were obtained, and, as for glass fibers, it became possible to plot the  $\sigma_c$ - $\tau_{adh}$  curves.

In the end of the 1970s, high-strength super-high-modulus organic aramid fibers (SVM, Kevlar, Terlon) and organoplastics based on them came into operation, and the adhesion to these fibers and the relationship between the strength of these composites and the adhesive strength of their components were studied.

Aramid fibers are rarely subjected to surface treatment. In general, the adhesion changes with a change in the nature of the binder and/or the temperature-time mode of the formation of the material. Significant issues for these fibers were those associated with the diffusion of a liquid polymer binder into a polymer fiber: diffusion changes the structure, failure mechanism, and strength of the material.

Subsequently, in the late 1980s and the 1990s, other types of aramid fibers, such as Armos, Rusar, and polybenzothiazole organic fibers exhibiting a high heat resistance, were developed. Accordingly, the

adhesion of epoxy and modified epoxy binders and binders exhibiting a high heat resistance and better chemical affinity, for example, bismaleimide binders, to the above fibers was studied.

In the early 1980s, many studies focused on the properties of boron and silicon carbide fibers and composites based on them were reported. The diameter of these fibers is  $\sim 100 \mu\text{m}$ . They are mostly used to design materials and structures that work in compression. The adhesion to the above fibers was studied exploring the same range of issues: the adhesion of binders of different nature and the methods to control it. It was found that, as in the case of using carbon reinforcing fillers, the highest adhesive strength is observed when the fiber surface is modified by an oxidative treatment (with nitric acid). In addition, the effect of the scale factor, the temperature–time conditions for the formation of joints, and the test temperature on interfacial strength was studied.

The first studies of the adhesive strength of polyolefins and other linear polymers date back to the same years.

By the early 1980s, the concept of "local adhesive strength" had been finally formulated.

Initially, the possible causes of the scale effect of adhesive strength were considered in detail. It was shown that the nonuniform distribution of tangential stresses at the fiber–polymer interface, which determines the dependence of  $\tau$  on the area of the joints, is associated both with the nonuniform distribution of tangential stresses arising under the application of an external load and—the key point—with the action of residual (primarily, thermally induced) stresses arising during the formation of the joint and the subsequent cooling of the joint to the test temperature, i.e., the stresses existing in the specimen before loading.

Relationships to relate the thermally induced residual stresses to the specimen size were derived; it was shown that the derived relationships adequately describe the experimental data.

Somewhat later, it was found that the classical static scale factor (increase in the probability of formation of a dangerous defect with an increase in the specimen size) has hardly any effect on polymer–fiber joints, because the localization of a dangerous defect (site of maximum stress concentration) in them does not depend on the specimen size. It is determined by their shape and loading pattern; it is always localized near the end of the joint to which an external force is applied.

Understanding of the fact that the measured value of adhesive strength  $\tau$  is determined not only by physicochemical interactions at the interface, but also by the mechanical properties of the components and the specimen size and, accordingly, characterizes a certain joint of a given interacting

pair, rather than this pair has led to the introduction of a very important concept of local adhesive strength  $\tau_{loc}$  as a measure of adhesive strength:

$$\tau_{loc} = \lim_{S \rightarrow 0} \tau(S)$$

The  $\tau_{loc}$  value does not depend on the nonuniform distribution of tangential stresses at the interface ("free" from the effect of residual stresses); it is determined only by physicochemical interactions across the interface; that is, it characterizes a given pair. A procedure to determine the  $\tau_{loc}$  value from experimental  $\tau$ - $S$  curves was developed. In this case, it was assumed that the joint undergoes failure if the sum of the residual and applied external stresses achieves the value of local adhesive strength  $\tau_{loc}$ .

The discussions of all the subsequently obtained experimental data were based on this pattern of failure.

In the late 1980s and in the 1990s, a relationship between the strength  $\sigma_c$  of unidirectional fibrous composites in different stress states and the adhesive strength  $\tau_{adh}$  of their components was determined.

The importance and significance of the  $\sigma_c$ - $\tau_{adh}$  correlation curves lies in the fact that their shape makes it possible to detect the localization of a "weak link" in the material and, accordingly, propose methods to improve the properties of the composite. However the number of experimental studies focused on the relationship between  $\sigma_c$  and  $\tau_{adh}$  is extremely small.

This fewness is attributed to the fact that, in all types of tests, the strength of composites, in common with the strength of adhesive joints, depends on the preparation procedure and test conditions. Therefore, in plotting each  $\sigma_c$ - $\tau_{adh}$  dependence, it is necessary to use composite specimens and adhesive joints prepared and tested under identical conditions. In general, this objective can be met only in specially designed experiments. It is necessary to be extremely careful in plotting  $\sigma_c$ - $\tau_{adh}$  curves using the published data.

The dependence of the strength of unidirectional fibrous composites on the adhesive strength of the components in their unit cells has been studied quite thoroughly by researcher of our Laboratory, because comprehensive studies of both the production technology and properties of reinforced plastics and their components (fibers, matrices, and the matrix-fiber interface) are conventional for our Laboratory [28].

It was found that the strength of glass, carbon, and boron plastics almost linearly increases with an increase in interfacial strength. This behavior is observed under all loading conditions (shear, compression, bending, and tension). Sometimes, a slight increase (10–20%) in adhesive strength provides a significant increase (50–70%) in the strength of the

material. It was found that the "weak link" in these composites is the interface. An improvement in their properties is associated with an increase in the adhesive strength of their components.

The shape of the  $\sigma_c$ – $\tau_{adh}$  curves for composites based on high-strength super-high-modulus aramid fibers and various thermosetting matrices depends on the nature of the fiber and the type of stress state. In many cases, the strength of the composite does not depend on interfacial strength. In these cases, the "weak link" of the composite is the fibers; the strength is limited to the weak bond of the fiber fibrils in the transverse direction. The methods to improve the physicomaterial characteristics of these plastics are associated with improving the properties of the fibers and the temperature–time conditions for the formation of the composite.

In the 1980s, other methods to determine the adhesion to fibers—the fragmentation method and the droplet method (version of the pull-out method)—were also developed in the world. We also have paid tribute to them. However, in our Laboratory, the pull-out method remains the main method to study the interfacial strength: in the classical version for studying the adhesion to thick fibers (with a diameter of  $d \geq 100 \mu\text{m}$ ) and in the three-fiber version for measuring the adhesion to thin fibers ( $d \leq 40 \mu\text{m}$ ).

The first use of heat-resistant linear polymers as binders dates back to the 1990s. It was expected that the use of these polymers would provide the production of plastics exhibiting not only a high strength and rigidity, but also a high fracture toughness. Adhesion researchers were facing new challenges, primarily, methodological.

First, in the as-received condition, all these polymers are solids (pellets, powders, films). Only their melts or solutions can interact with fibers. However, the use of solutions is undesirable, because solvents generally cause a decrease in adhesion.

Accordingly, it was necessary to develop new versions of methods for the formation of polymer–fiber joints. The preparation of powdered thermoplastic–carbon fiber joints was particularly difficult. However, it was carbon fiber-reinforced plastics based on these binders that seemed to be the most promising.

Second, some of the advantages of thermoplastics should become apparent with an increase in temperature, rather than under normal conditions. Therefore, it was necessary to upgrade the existing adhesion testers to provide adhesive strength measurements up to 400–500°C, rather than up to 200–250°C.

After solving these methodological problems, the adhesion of a number of industrial and specially synthesized thermoplastics (PS, PC,

PES, PEI, PPSR, PEEK, PAEK) was studied. Optimum conditions (providing maximum  $\tau$  values) for the formation of joints were determined; temperature dependences of the adhesive strength of thermoplastics in a wide temperature range were measured. The studies made it possible to select required adhesives. However, the key point is that the studies made it possible to compare the relationships that describe the strength of joints of fibers with thermoplastic (rigid-chain) and thermosetting adhesives (previously studied) with a change in temperature. Subsequently, rigid-chain linear polymers were commonly used as one of the components of multicomponent blend matrices.

Until the 1990s, the development of studies on the adhesion of polymer to fibers stimulated the design of new types of fibers (of a new nature). This was the case with the design of carbon, boron, and silicon carbide fibers and various high-strength organic fibers (SVM, Kevlar, Terlon, Armos). In the 1990s and in the current century, the development of these studies is primarily dictated by the necessity to study the adhesion of new—mostly multicomponent—blend matrices to high-strength super-high-modulus fibrous fillers.

The objective is the preparation of matrices by modifying the existing resins by various methods, rather than the design of polymers of a new nature.

Since the late 1990s, the main studies of the adhesion research group have been focused on the adhesion of modified epoxy binders to fibers.

Three modifying methods are under consideration: modifying with active diluents, heat-resistant thermoplastics, and fine (in particular, nanosized) fillers.

In view of the new requirements for composites—high crack resistance, fairly high post-impact properties, and high fracture toughness—it was necessary to determine the behavior of the interface under impact loading, cyclic loading, etc.

In the 1990s, a dynamic adhesion tester was constructed; the tester made it possible to increase the loading rate by 5–6 orders of magnitude and study the properties of polymer–fiber joints under low-speed impacts. In addition, a special device was designed; it is connected to adhesion testers and provides specimen testing in multiple loading–unloading cycles. The first results supported the thermal fluctuation (kinetic) theory of adhesive strength (mechanism of interfacial bond failure) and made it possible to study the formation and propagation of dangerous defects and the development of the adhesion failure process in more detail.

In studying the adhesion of modified epoxy resins, the main attention was paid to studying the concentration dependences of adhesive strength,

i.e., revealing the effect of the type and amount of the introduced modifier on  $\tau$  values. For many systems, the synergism of adhesive strength was detected and the factors responsible for it were discussed.

Rigid-chain thermoplastics and dispersed fillers significantly increase the viscosity of epoxy binders. Therefore, the viscosity of the compositions and the dependence of it on the curing temperature, time, and kinetics were systematically studied. The results of the viscosity studies were also used to work out process procedures for obtaining composite materials by wet spinning methods.

Attempts to interpret the synergism of adhesive strength in joints where the adhesives are thermoplastic–epoxy resin blends have necessitated studies of the structure of these blends after curing. The fact is that blends that are homogeneous before curing frequently undergo phase separation during curing. The structure of the resulting polymers significantly depends on the amount of the thermoplastic introduced into the epoxy resin. It was shown that it is the evolution of the structure that determines the change in the failure of the joints and the synergism of adhesive strength.

In the same years, it was found that modifying can significantly (severalfold) increase the crack resistance of the matrices and unidirectional fibrous composites based on blend matrices (epoxy resin–PSF, epoxy resin–PEI, epoxy resin–PAEK).

We should also mention another new class of polymers whose adhesion has been studied in recent years, namely, ladder polymers [227, 228]. The glass transition temperature of these polymers, which exhibit a unique heat resistance, is higher than their decomposition temperature. At room temperature, the adhesive strength of ladder polymer–fiber systems is low. To show their advantages, the temperature dependences of interfacial strength in joints with a steel wire in a range of 20–450°C were studied. The interface (in common with the polymer) remains efficient up to 400°C, when all other polymers lose their ability to transfer stresses.

To summarize, we can state the following.

The adhesion research group exists for 60 years. All that time, the researchers of the group have been studying the adhesion of polymers to fibers. Apparently, there is not a single group (in our country or abroad) in which the wide variety of aspects of the strength of the fibrous filler–matrix interface have been studied for such a long time and so systematically. A large amount of actual (experimental) data on the interfacial strength of all kinds of adhesive–fiber pairs has made it possible to subsequently use these results for various generalizations.

It is particularly significant that the group has always worked at the Laboratory of Reinforced Plastics, which is part of an academic institute. Therefore, the cornerstone has always been the elucidation of general physical laws that describe a particular process at the interface and the factors determining these laws, rather than the solution of individual applied problems. This focus is a distinctive feature of the activities of the adhesion research group.

Owing to indefatigable attention of the researchers of the group to the methodological (measuring) base and methods for calculating and processing the measurement results, they are among the researchers who were first involved in solving the emerging problems (applied and theoretical).

The publications of the group represent all stages of the study of adhesive phenomena at the fiber–polymer interface. They significantly contributed to the formation of a new direction in the science of adhesion—adhesion of polymers to fibers.

The studies conducted by the researchers of the group were described in numerous papers (list is attached). In addition, the main results obtained in the 1960s through to the 1980s were reported in two monographs:

1. Yu. A. Gorbatkina, *Adgezionnaya prochnost' v sisteme polimer-volokno*, Moscow, Khimiya, 1987, [Yu. A. Gorbatkina, *Adhesive Strength of Fibre–Polymer Systems*, Moscow, Chemistry, 1987].
2. Yu. A. Gorbatkina, *Adhesive Strength of Fibre–Polymer Systems*, New York–London–Toronto, Ellis Horwood, 1992.

This book summarizes the results of studies of the adhesion of multicomponent epoxy matrices to fibers that were obtained after the 1990s.



# APPENDICES

## A1. Determination of the Adhesive Strength of Joints Composed of an Epoxy Matrix and a Steel Wire with a Diameter of $d \geq 100 \mu\text{m}$

The type of the used specimens is shown in Fig. A1. In each test, a few tens of specimens were tested; their areas  $S$  were varied in a range of 0.1 to 0.9–1.1  $\text{mm}^2$ . The spread of diameters of the used wire does not exceed 1%. Therefore, the spread of  $S$  values observed in the tests is associated with a change in length  $l$  of the joints and with the fact that, during the formation of the joints, different amounts of the polymer were placed in aluminum cups.

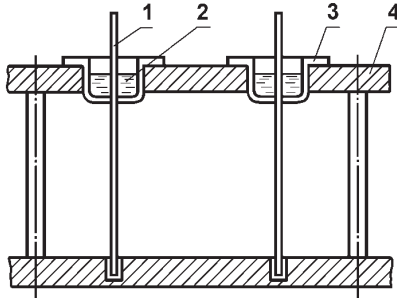


Fig. A1. Schematic of a specimen used to determine the adhesive strength of joints of polymers with fibers with a diameter of  $d \geq 80\text{--}100 \mu\text{m}$  by the pull-out method: (1) fiber, (2) polymer, (3) aluminum cup, and (4) specimen preparation facility.

In a typical procedure of processing the measurement results, the entire range of areas was partitioned into subintervals  $\Delta S$ , each with an area of 0.1  $\text{mm}^2$ , in the same way as in Fig. 1.1. For each subinterval with an area of  $S_m$  to  $S_m + \Delta S$ , the average values of breaking load  $\bar{F}$  and adhesive strength  $\tau$  were calculated. The determined  $\bar{F}$  and  $\tau$  values were assigned to the middle of the respective subinterval  $S_m - S_m + \Delta S$  and used to determine the dependence of the breaking load and adhesive strength (interfacial strength) on the sizes of the joints. In general, at least 40 specimens were tested in a test to plot the  $\tau$ – $S$  ( $F$ – $S$ ) curve.

## A2. Preparation of Epoxy Resin–Heat-Resistant Thermoplastic Compositions

In compositions based on epoxy oligomers ED-20 and ED-22 [84], the following modifiers were used: the PSK-1 PSF, the Ultem 1010 PEI, and PAEK. The modifiers were dissolved in the epoxy oligomer under continuous stirring without adding any solvents. The miscibility conditions (until complete dissolution) are shown in Table A2-1.

The resulting mixtures do not undergo phase separation during storage under normal conditions. As required, a curing agent was added to them to prepare specimens for all types of tests. The curing agents were TEAT and DADPS; they were introduced in an amount of 10 and 30 weight fractions, respectively, of the weight of the epoxy oligomer. The curing conditions are shown in Table A2-2.

**Table A2-1. Miscibility conditions for blends**

Modifier	Amount of modifier, wt %	Blend preparation conditions	
		Time, h	Temperature, °C
PSK-1	5–20	24–72	110
		2–14	120
		5	140
PEI	5–20	5	140
PAEK*	5–30	2–24	120–130

\*The maximum amount of PAEK introduced into the epoxy resin depended on the chemical structure of PAEK.

**Table A2-2. Curing conditions for blends**

Modifier	Curing agent TEAT	Curing agent DADPS
PSK-1	160°C, 8 h	180°C, 6 h
PEI	160°C, 8 h	180°C, 6 h
PAEK	–	180°C, 5.5 h

### **A3. Preparation of Epoxy Resin–Fine Filler Compositions**

Epoxy oligomer ED-20 [84], nanopowders (Aerosil A-380 [93] and aluminas [94]), industrial carbon black nos. 66 and 76 (electroconductive carbon material UM-66 and technical carbon UM-76 [95-97]), and CNTs (MWNTs L-MWNT 40-60 manufactured by Shenzhen Nanotech Port Co., China) were used for the measurements. See also Table 1-5.

A required amount of schungite and alumina powders was added to the ED-20 oligomer with a curing agent introduced into it under continuous stirring.

To provide a uniform distribution of Aerosil and carbon black particles in ED-20, filled compositions were prepared using a high-speed mixer (~2000 rpm); the mixing temperature was ~50°C; the mixing time was 5–10 min.

In the case of using a filler, the nanotubes were initially disaggregated using an ultrasonic emitter (100-W Volna M instrument) in chloroform for 30 min [98]. After that, the epoxy oligomer was added to the resulting suspension of nanotubes in a solvent; the mixture was sonicated for some time (~2 h) and then evacuated to remove the solvent (at a residual pressure of 15–20 mmHg at a temperature of 60–65°C for 15–30 min (until the cessation of foaming)).

#### **A4. Measurement of the Surface Tension of Liquid Epoxy Resins**

The surface tension of the original epoxy resin and the epoxy resin modified with fluorine-containing surfactants was measured by the method developed by P.A. Reh binder (maximum gas bubble pressure method) [128]. The method is based on measuring the critical pressure at which a gas bubble breaks off from a capillary brought into contact with a liquid whose surface tension is determined. In the case of introducing compound no. 1 into ED-20, measurements were conducted at room temperature; tests with compounds nos. 2 and 3 were conducted at 50°C (to reduce the viscosity of ED-20 and prepare true solutions of these compounds in ED-20 at surfactant concentrations exceeding 0.02 mol/L).

### **A5. Determination of the Wettability of Cured Epoxy Resins Modified with Fluorine Compounds**

To prepare cured resin specimens, the original composition was evacuated at 60°C at a residual pressure of 0.01 mmHg for 2.5 h to remove low-molecular-weight compounds. In this case, 0.07 equivalent of telomeric alcohol and 0.07 equivalent of tertiary amine per epoxy equivalent of ED-20 were taken. Curing was run at 80–110°C for 120 min. The cured compositions were 25 × 15 × 3 mm plates, on the surface of which the values of contact angles  $\theta$  were determined using an MBS-2 microscope equipped with a goniometric attachment. The measurements were conducted at room temperature.

## A6. Measurement of Viscosity and Contact Angles

The viscosity of the studied compositions was measured on a Reotest 2.1 rotational cone-and-plane viscometer at different curing temperatures.

To conduct tests at temperatures above room temperature, the measuring device was thermostatted using a liquid circulation thermostat.

Tangential stress  $\tau$  and viscosity  $\eta$  were calculated by the formulas

$$\tau = 3M/2\pi R^3;$$

$$\eta = \tau/\dot{\gamma},$$

where  $M$  is the torque,  $R$  is the cone radius,  $\dot{\gamma}$  is the shear rate,  $\dot{\gamma} = \omega/\tan\varphi$ ,  $\omega$  is the angular velocity of the cone, and  $\varphi$  is the angle of the wedge-shaped gap between the fixed plate and the cone,  $\varphi = 0.3^\circ$  [129-131].

Binders with and without a curing agent were studied.

The wettability of the compositions was characterized by the value of contact angle  $\theta$ , which was measured by the sessile drop method and calculated from droplet height  $h$  and droplet base diameter  $d$ :

$$\cos \theta = ((d/2)^2 - h^2) / ((d/2)^2 + h^2);$$

the  $h$  and  $d$  values were determined using a cathetometer.

The test composition was deposited on a glass plate; the plate was placed in a heat chamber with transparent side walls, which was heated to the curing temperature. The droplet parameters were measured directly during curing (at  $180^\circ\text{C}$ ).

## A7. Curing Process Investigation Procedure

The curing process was studied by DMA on an MK-3 torsional pendulum in the mode of free-damped vibrations with the determination of the mechanical loss angle tangent  $\text{tg}\delta$  and the dynamic modulus of elasticity  $G'$  and by the DSC method on a Mettler Toledo 822e differential calorimeter with determination of the heat of the chemical reaction. Conversion  $\beta$  was calculated by the formula

$$\beta = Q/Q_{\max},$$

where  $Q$  is the heat of the process in the isothermal mode of curing and  $Q_{\max}$  is the maximum heat of the process in the scanning mode of curing at a rate of 1 deg/min.

Glass transition temperature  $T_g$  was determined by the DMA method from the maximum  $\text{tg}\delta$  value and on a Heppler consistometer. In the latter case, the specimen had the form of a pellet with a height of 10 mm and a diameter of 10 mm; the heating rate of the specimen was 1 deg/min.

## A8. Measurement of Residual Stresses

"Internal" (residual) stresses arising at the polymer–solid interface were measured by the cantilever beam deflection method [132].

The test composition was deposited on a glass substrate, which was fixed in a special clamp parallel to an iron (or steel) plate of the clamp. The clamp not only provides the fixation of the glass substrate, but also prevents it from skewing. Using a microscope, the initial distance between the glass substrate and the metal plate of the clamp was measured. The clamp with the glass plate fixed on it was placed in a heating cabinet for 30 min; after that, it was cooled and the distance between the glass substrate and the metal plate of the clamp was measured again. The process was repeated until the test composition was completely cured (with a 30-min interval during the first 2 h and a 1-h interval during up to 8 h).

Residual stresses  $\sigma_{\text{res}}$  were determined from the deflection of the glass plate and calculated by the formula

$$\sigma_{\text{res}} = hE\delta_1^3/[3l^2(1 - \mu^2)(\delta_1 + \delta_2) \delta_2],$$

where  $E$  is the elastic modulus of glass (73 200 MPa),  $\delta_1$  is the glass plate thickness ( $\sim 0.1$  mm),  $\delta_2$  is the binder film thickness ( $\sim 0.3$  mm),  $\mu$  is the Poisson's ratio of glass ( $\sim 0.2$ ),  $l$  is the length of the free end of the specimen ( $\sim 70$  mm), and  $h$  is the deflection of the free end of the plate.



### **A9. Measurement of the Temperature Dependence of the Adhesive Strength of Joints Composed of an Epoxy Matrix and a Steel Wire with a Diameter of $d \geq 100 \mu\text{m}$**

Adhesive joints were formed in air at atmospheric pressure.

Breaking loads were determined using an improved model of the adhesion tester (tensile microtester) developed at Semenov Institute of Chemical Physics of the Russian Academy of Sciences [30, 31]. In all tests, the loading rate remained constant at a level of 1 N/s. The temperature in the chamber was recorded using a thermocouple and automatically controlled at an accuracy of  $\pm 2^\circ\text{C}$ .

## A10. Impact Loading

To determine the strength of fiber-polymer joints under impact loading, a setup was constructed; the setup makes it possible to record impact pulse oscillograms, while pulling out the fiber from the matrix (pull-out method). In this case, the rate of increase in load  $F$  on the specimen is  $10^3$ – $10^4$  N/s.

The main components of the setup are shown in the schematic diagram (Fig. A10-1). Adhesion tester 1 is based on a KPS-2 spring-operated impact testing machine. The setup also includes the following: photosensor 2 designed to synchronize the triggering of the oscilloscope sweep with the start time of the pulsed loading of the specimen, piezoelectric transducer 3 combined with a clamping member for fixing the test specimen, and electronic storage oscilloscope 4 of the C9-16 type (Figure A10-2) shows schematic fixation of a specimen. Specimen 1 is installed in clamping member 2 combined with a piezoelectric transducer. The fiber is fixed in clamp 3. Loading is implemented by pulse impacts of striker 5 on the clamp via transferring an impact pulse from the striker through bar 4 to clamp 3.

The design of the setup makes it possible to control the loading rate by tightening or loosening additional springs that slow down the movement of bar 4 at the instant of loading. The number of possible loading rates was determined by the number of steps of tightening of the accelerating springs.

The setup for impact pulse recording includes a piezoelectric transducer that makes it possible to record a signal of a significantly higher frequency than that in the case of using a strain gauge, and, therefore, conduct measurements at higher rates.

The design of the clamp provides the use of a wide variety of reinforcing fibers. The measuring complex of the setup provides a computerized readout and processing of test results.

The signal of the piezoelectric transducer is recorded by a storage oscilloscope and simultaneously transmitted to a computer in digital form. The breaking force value is determined from the maximum pulse value using a calibration chart.

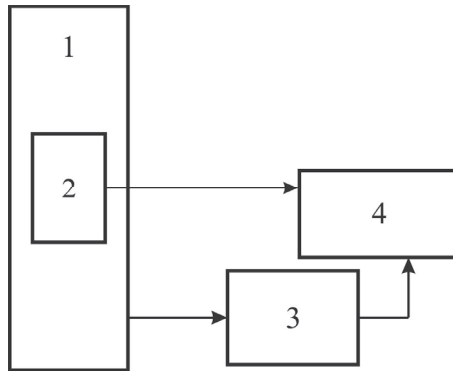


Fig. A10-1. Schematic diagram of the setup for testing model adhesive systems under impact loading: (1) dynamic adhesion tester, (2) photosensor, (3) piezoelectric transducer, and (4) oscilloscope [142].

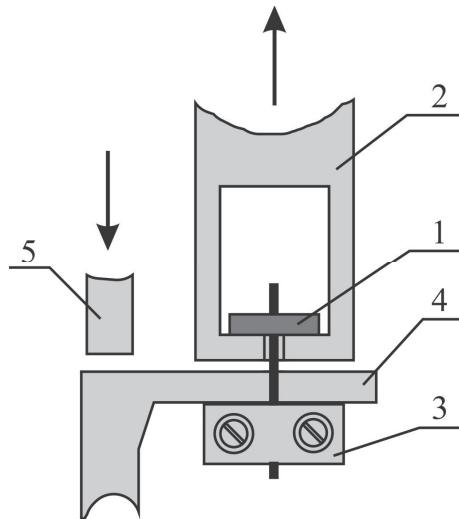


Fig. A10-2. Schematic fixation of a specimen in a dynamic adhesion tester: (1) specimen, (2) guide member for clamping, (3) clamp, (4) transfer bar, and (5) striker [142].

## REFERENCES LIST

1. Hunston D.L., and W.D. Bascom. 1984. Failure behavior of rubber-toughened epoxies in bulk, adhesive, and composite geometries. *Rubber-modified thermoset resins*. Ed. Riew C.K., J.K. Gillham. American Chemical Society. 208(7):83-99.
2. Yamanaka K., T. Inoue. 1990. Phase separation mechanism of rubber-modified epoxy. *J. Mater. Sci.* 25(Part 1A):241-245.
3. Kozii V.V., and B.A. Rozenberg. 1992. Mechanisms of energy dissipation in elastomer-modified thermosetting polymer matrices and composites based on such polymers. *Polym. Sci. Ser. A.* 34919-951.
4. Kochnova Z.A., E.S. Zhavoronok, and A.V. Kotova. 1998. Osobennosti polucheniya epoksidno-kauchukovykh kompozitsyy na osnove zhidkikh butadiennitril'nykh kauchukov i epoksidnykh oligomerov [Features of obtaining epoxy-rubber compositions based on liquid nitrile butadiene rubbers and epoxy oligomers]. *Lakokrasochnie materialy i ikh primenenie*. [Paints and varnishes and their application]. 11:27-28.
5. Bologov D.V., A.M. Kuperman, and M.G. Karpman. 1999. Vliyanie modifikatsii epoksidnogo svyazuyuschego nitril'nykh kauchukom na fiziko-mehaniicheskie svoystva odnonapravlenno ugleplastika [The effect of modification of an epoxy binder with nitrile rubber on the physical and mechanical properties of unidirectional CFRP]. *Mekhanika kompozitsionnykh materialov i konstruksii* [Mechanics of composite materials and structure]. 5(4):33-41.
6. Kochnova Z.A., and E.S. Zhavoronok. 1999. Socondensaty zhidkikh karboksilsoderzhaschikh butadiennitril'nykh kauchukov i nizkomolekulyarnykh epoksidnykh oligomerov [Co-condensates of liquid carboxyl-containing nitrile butadiene rubbers and low molecular weight epoxy oligomers]. *Lakokrasochnie materialy i ikh primenenie*. [Paints and varnishes and their application]. (1):30-33.
7. Ratna D. 2001. Phase separation in liquid rubber modified epoxy mixture. *Polymer*. 42(6):4209-4218.
8. Hourston D.J., and J.M. Lane. 1992. The toughening of epoxy resins with thermoplastics: 1. Trifunctional epoxy resin-polyetherimide blends. *Polymer*. 33(7):1379-1383.

9. Javadyan E.A., V.G. Ivanova-Mumzhieva, Yu.A. Gorbatkina, et al. 1994. Vliyanie razbavitelya na fiziko-mehaniicheskie svoistva epoksidnykh svyazuyuschikh i kompozitov na ikh osnove [Influence of a thinner on the physical and mechanical properties of epoxy binders and composites based on them]. *Vysokomolek. Soedin.* 36A(8): 1349-1352.
10. Chen M.C., D.J. Hourston, and W.B. Sun. 1995. The morphology and fracture behavior of miscible epoxy resin-polyetherimide blend. *Eur. Polym. J.* 31(2):199-201.
11. Yoon T.H., Jr.D.B. Priddy, G.D. Lyle, and J.E. McGrath. 1995. Mechanism and morphological investigation of reactive polysulfone toughened epoxy networks. *Macromol. Symp.* 68:673-686.
12. Kim B.S., T. Chiba, and T. Inoue. 1995. Morphology development via reaction-induced phase separation in epoxy/poly(ether sulfone) with functional end-groups. *Polymer.* 36:43-47.
13. Pisanova E.V., S.F. Zhandarov, and O.R. Yurkevich. 1997. Epoxy-polysulphone networks as advanced matrices for composite materials. *J. Adhesion.* 64:111-129.
14. Ratna D., M. Patri, B.C. Chakraborty, and P.C. Deb. 1997. Amine-terminated polysulfone as modifier of epoxy resin. *J. Appl. Polym. Sci.* 65(5):901-907.
15. Hayes B.S., and J.C. Sefelus. 1998. Variable temperature cure polyetherimide epoxy-based prepreg systems. *Polym. Eng. Sci.* 38(2): 357-370.
16. Robertson J.E., T.C. Ward, and A.J. Hill. 2000. Thermal, mechanical, physical, and transport properties of blends of novel oligomer and thermoplastic polysulfone. *Polymer.* 41:6251-6262.
17. Chalykh A.E., V.K. Gerasimov, A.E. Bukhteev, et al. 2003. Compatibility and phase structure evolution in polysulfone-curable epoxy oligomers blends. *Polym. Sci.* 45(7):676-685.
18. Zheng S., Q. Guo., and Y. Mi. 2003. Miscibility and phase behavior in blends of phenolphthalein poly(ether sulfone) and poly(hydroxyether of bisphenol A). *Polymer.* 44: 867-876.
19. Gojny F.H., and K. Schulte 2004. Functionalization effect on the thermomechanical behavior of multi-wall carbon nanotubes/epoxy composites. *Compos. Sci. Technol.* 64:2303-2308.
20. Lui L., and H.D. Wagner. 2005. Rubbery and glass epoxy resins reinforced with carbon nanotubes. *Compos. Sci. Technol.* 65:1861-1868.

21. Song Y.S., and J.R. Youn. 2005. Influence of dispersion states of carbon nanotubes on physical properties of epoxy nanocomposites. *Carbon*.43: 1378-1385.
22. Fidelus J.D., E. Wiesel, F.H. Gojny, et al. 2005. Thermomechanical properties of randomly oriented carbon/epoxy nanocomposites. *Compos. Part A: Appl. Sci.* 36:1555-1561.
23. Tjong S.C. 2006. Structural and mechanical properties of polymer nanocomposites. *Mat. Sci. Eng. R.* 53:73-197.
24. Borodulin A.S. 2012. Nanomodifikatory dlya polimernykh kompozitsionnykh materialov [Nanomodifiers for polymer composite materials]. *Vse materialy. Entsiklopedicheskii Spravochnik*. [All Materials. Encyclopedic Directory]. 6:51-57.
25. Sopotov R.I., S.V. Zyukin, I. Yu. Gorbunova, et al. 2015. Reokinetika otverzheniya epoksidnogo oligomera ED-20, modifitsirovannogo polisulfonom i poliefirimidom [Rheokinetics of curing of epoxy oligomer ED-20 modified with polysulfone and polyetherimide]. *Plast. Massy*. [Plastics]. 11-12:7-9.
26. Arinina M.P., S.O. Il'in., V.V. Makarova, et al. 2015. Sovmestimost' i reologicheskie svoystva smesei epoksidianovogo oligomera s aromaticshekimi poliefirami [Compatibility and rheological properties of mixtures of epoxydian oligomer with aromatic polyesters]. *Vysokomolek. Soedin.* [Macromolecular compounds], 57A(2):152-161.
27. Sopotov R.I., I.Yu. Gorbunova, M.L. Kerber, et al. 2016. Issledovanie vliyaniya polisulfona i poliefirsulfona na reokineticheskie zakonomernosti protsesa otverzheniya epoxiaminnogo svyazuyushchego [Investigation of the influence of polysulfone and polyethersulfone on rheokinetic patterns of the curing process of an epoxyamine binder]. *Khimicheskaya Promyshlennost' segodnya*. 4:30-39.
28. Gorbatkina Yu.A. 2000. Correlation between the strength of fiber-reinforced plastics and the adhesive strength of fiber-matrix joints. *Mech. Compos. Mater.* 36(3):169-176.
29. *Polimernye kompozitsionnye materialy: struktura, svoystva, tekhnologiya* [Polymer composite materials: structure, properties, technology]. 2014. Ed. A.A. Berlin. Izd-vo «Professiya». Sankt-Peterburg.
30. Gorbatkina Yu.A. 1987. *Adgezionnaya prochnost' v sistemakh polimer-volokno* [Adhesive strength of fibre-polymer systems]. Moscow: Khimiya. 192 p.
31. Gorbatkina Yu.A. 1992. *Adhesive strength of fibre-polymer systems*. N.Y., London: Ellis Horwood. 264 p.

32. Gorbatkina Yu.A. 2004. Vliyanie modifikatorov na adgezionnye svoistva polimernykh kompozitsii. Ch. 1. Obschie predstavleniya [Influence of modifiers on the adhesive properties of polymer compositions. Part 1. General concepts]. *Klei. Germetiki. Tekhnologii*. {Adhesives, sealants, technologies} 4:18-23.
33. Gorbatkina Yu.A., V.G. Ivanova-Mumzhieva, and A.M. Kuperman. 2016. Adhesion of modified epoxy matrices to reinforcing fibers. *Polym. Sci. Ser. A* 5:659-666.
34. Khromov M.K. 1974. Sposob opredeleniya prochnosti svyazi reziny s kordom pri staticheskom nagruzhении [Method for determining the bond strength of rubber with a cord under static loading]. *Kauchuk i rezina*. 12: 42-44.
35. Jarvela P., K.W. Laitinen, J. Purola, and P. Tormala. 1983. The three-fibre method for measuring glass fibre resin bond strength. *Int. J. Adhes. Adhes.* 3(3):141-147.
36. Piggott M.R., P.S. Chua, and D. Andison. 1985. The interface between glass and carbon fibers and thermosetting polymers. *Polym. Composites*. 6: 242-248.
37. Piggott M.R., A. Sanadi, P.S. Chua, and D. Andison. 1986. Mechanical interactions in the interfacial region of fiber reinforced thermosets. *Composite interfaces*. Eds. H. Isida, J.L. Koenig. Amsterdam: Elsevier, P. 109.
38. Miller B., P. Muri, and L. Rebenfeld. 1989. A microbond method for determination of the shear strength of a fiber/resin interface. *Compos. Sci. Technol.* 28:17-32.
39. Gaur U., and B. Miller. 1989. Microbond method for determination of the shear strength of a fiber/resin interface: Evolution of experimental parameters. *Compos. Sci. Technol.* 34:35-51.
40. Dovgyalo V.A., S.F. Zhandarov, and E.V. Pisanova. 1990. Opredelenie adgezionnoi prochnosti v sisteme termoplast-tonkoe volokno [Determination of adhesive strength in the thermoplastic – thin fiber system]. *Mekh. Kompozit. Mater.* [Mech. Compos. Mater.]. 26(1):9-12.
41. Shul' G.S., and J.A. Gorbatkina. 1991. Effect of temperature on the adhesion strength of fiber/ROLIVSAN joints. *3rd Symposium (International) of Mechanics of Polymer Composites Proceedings*. Prague, P.183.
42. Desarmot G., and J.P. Favre. 1991. Advances in pull-out testing and data analysis. *Compos. Sci. Technol.* 42(2):151.
43. Chou C.T., U. Gaur, and B. Miller. 1994. The effect of microvisc gap width on microbond pull-out test. *Compos. Sci. Technol.* 51(2):111-116.

44. Qian L.L., F.A. Bruce, J.J. Kellar, and Winter R.M. 1995. An instrument for testing interfacial shear strength in polymer matrix composites. *Meas. Sci. Technol.* 6:1009-1016.
45. Ivanova-Mumzhieva V.G., Yu.A. Gorbatkina., G.S. Shul', et al. 1995. Adgezionnaya prochnost; soedinenii aramidnykh b polibenzotiazol'nykh volokon s termoreaktivnymi matritsami [Adhesion strength of aramid and polybenzothiazole fiber joints with thermosetting matrices] *Mekh. Kompozit. Mater.* 31(2):147-155.
46. Gorbatkina Yu.A., and V.G. Ivanova-Mumjjeva. 1997. Adhesive strength of fibre/polymer joints upon loading in liquids: Effect of liquid surface tension. *Int. J. Adhes. Adhes.* 17(4):329-332.
47. Shcherbakov L.M., and P.P. Ryazantsev. 1965. Ob odnom metode izmereniya kraevykh uglov. [One method for measuring contact angles]. *Surface phenomena in melts and solid phases arising from them.* Nalchik: Kabard.-Balk. Book. publishing house. P. 230-234.
48. Baibakov V.S., P.P. Ryazantsev, V.P. Safronov, and L.M. Shcherbakov. 1967. *Issledovaniya v oblasti poverkhnostnykh sil* [Research in the field of surface forces]. Moscow: Nauka. 154 p.
49. Volkova N.N., V.P. Tarasov, L.N. Erofeev, and Yu.A. Gorbatkina. 2006. Kinetic Regularities of Thermal Destruction and Structure of an Epoxy Binder Modified with an Active Plasticizer. *Polym. Sci. Ser. B.* 48(3-4): 96-100.
50. Haung P., S. Zheng, J. Huang, et al. 1997. Miscibility and mechanical properties of epoxy resin/polysulfone blends. *Polymer.* 38(2):5565-5571.
51. Taesung Y., K.B. Sup, and D.S. Lee. 1997. Structure development via reaction induced phase separation in tetrafunctional epoxy/polysulfone blends. *J. Appl. Polym. Sci.* 66(12):2233-2242.
52. Pisanova E.V., S.F. Zhandarov, and O.R. Yurkevich. 1997. Epoxy-polysulfone networks as advanced matrices for composite materials. *J. Adhesion.* 64(1-4):111-129.
53. Oyanguren P.A., C.C. Riccardi, and R.J. Williams. 1998. Mondragon phase separation induced by a chain polymerization: Polysulfone-modified epoxy/anhydride systems. *J. Polym. Sci. Polym. Phys.* 36(8):1349-1359.
54. Min H.S., and S.C. Kim. 1999. Fracture toughness of polysulfone/epoxy semi-IPN with morphology spectrum. *Polym. Bull.* 42(2):221-227.
55. Oyanguren P.A., M.J. Galante, K. Andromaque, et al. 1999. Development of bicontinuous morphologies in polysulfone-epoxy blends. *Polymer.* 40(19):5249-5255.



56. Martinez I., M.D. Martin, F. Eceiza, et al. 2000. Phase separation in polysulfone-modified epoxy mixtures. Relation between curing conditions, morphology and ultimate behavior. *Polymer*. 41:1027-1035.
57. Lobanov M.V., A.I. Gulyaev, and A.N. Babin. 2016. Improvement of the impact and crack resistance of epoxy thermosets and thermoset-based composites with the use of thermoplastics as modifiers. *Polym. Sci. Ser. B*. Issue 1:3-15.
58. Breach C.D., M.J. Folkes, and J.M. Barton. 1992. Physical ageing an epoxy resin/polyethersulfone blend. *Polymer*. 33(14):3080-3082.
59. Kishi H., Y.-B. Shi, J. Huang, and A.F. Yee. 1997. Shear ductility and toughenability study of highly cross-linked epoxy/polyethersulfone. *J. Mater. Sci*. 32:761-771.
60. Mimura K., H. Ito, H. Fujioka. 2000. Improvement of thermal and mechanical properties by control of morphologies in PES-modified epoxy resin. *Polymer*. 41:4451-4459.
61. Zhong Z., S. Zheng, J. Huang, et al. 1998. Phase behaviour and mechanical properties of epoxy resin containing phenolphthalein poly(ether ether ketone). *Polymer*. 39:1075-1080.
62. Francis B., G.V. Poel, F. Posada, et al. 2003. Cure kinetics and morphology of blends of epoxy resin with poly(ether ether ketone) containing pendant tertiary butyl groups. *Polymer*. 44(13):3687-3699.
63. Bucknall C.B., and A.H. Gilbert. 1989. Toughening tetrafunctional epoxy resins using polyetherimide. *Polymer*. 30:213-217.
64. Jang J., and W. Lee. 1994. Polyetherimide-modified high performance epoxy resin. *Polym. J*. 26:513-525.
65. Jang J., and S. Shin. 1995. Toughness improvement of tetrafunctional epoxy resin by using hydrolysed poly(ether imide). *Polymer*. 36(6):1199-1207.
66. Chen C., D.J. Hourston, and F.-U. Schafer. 1995. Miscibility and fracture behavior of epoxy resin – nitrated polyetherimide blends. *Polymer*. 36(17): 3287-3293.
67. Kimoto M., and K. Mizutani. 1997. Blends of thermoplastic polyimide with epoxy resin. *J. Mater. Sci*. 32:2479-2483.
68. Barral L., J. Cano, J. Lopez, et al. 2000. Cure kinetics of amino-cured diglycidil ether of bisphenol A epoxy-blended poly(ether imide). *Thermochim. Acta*. 344:127-136.
69. Sidhammali S.K. 2000. Phase separation behavior in poly(ether imide) – modified epoxy blends. *Polym. Plast. Technol*. 39(4):699-710.

70. Min B.-G., Z.H. Stachurski, and J.H. Hodgkin. 1993. Microstructural effects and the toughening of thermoplastic modified epoxy resin. *J. Appl. Polym. Sci.* 50(9):1551-1518.
71. Bong S.K., T. Chiba, and T. Inoue. 1995. Phase separation and apparent phase dissolution during cure process of thermoset/thermoplastic blend. *Polymer.* 36(1):67-71.
72. Teng K.-C., and F.-C. Chang. 1996. Single-phase and multi-phase thermoplastic/thermoset polyblends: 2. Morphologies and mechanical properties of phenoxy/epoxy blends. *Polymer.* 37(12):2385-2394.
73. Ijima T., S. Miura, M. Fujumaki, and Tagushi T. 1996. Toughening of aromatic diamine-cured epoxy resin by poly(butylene phthalate)s and related copolesters. *J. Appl. Polym. Sci.* 6:163-175.
74. Kuperman A.M., E.S. Zelenskii, and M.L. Kerber. 1996. Glass-reinforced plastics based on matrices combining thermoplastics and thermosetting plastics. *Mech. Compos. Mater.* 32(1):81-85.
75. Venderbosch R.W., A.A.J.M. Peijs, H.E.H. Meijer, and P.J. Lemstra. 1996. Fibre-reinforced composites with tailored interphases using PPE/epoxy blends as a matrix system. *Compos. Part A: Appl. Sci.* 27:895-905.
76. Saalbrink A., M. Mureau, and A.A.J.M. Peijs. 1997. Blends of poly(ethylene terephthalate) and epoxy resin as matrix material for continuous fibre-reinforced composites. *11<sup>th</sup> International conference on Composite Materials Proceedings (ICCM-11)*. Gold Coast, Queensland, Australia. Ed. M.L. Scott. – Cambridge: Woodhead. 4:263-270.
77. Rong M., and H. Zeng. 1997. Polycarbonate-epoxy semi-interpenetrating polymer network: 2. Phase separation and morphology. *Polymer.* 38(2): 269-277.
78. Di Pasquale G., O. Motta, A. Rocca, et al. 1997. New high-performance thermoplastic toughened epoxy thermosets. *Polymer.* 38(17):4345-4348.
79. Girard-Reydet E., H. Sautereau, J.P. Pascault et al. 1998. Reaction-induced phase separation mechanisms in modified thermosets. *Polymer.* 39(11): 2269-2280.
80. Bonnaud L., J.P. Pascault, and H. Sautereau. 1999. Thermoplastic modified epoxy networks and their composites: Relationship between morphology and mechanical properties. *Int. SAMPE Students Conf.* – 10-15 April, 1999, Paris.
81. Li S., B.-I. Hsu, F. Li, C.Y. Li, et al. 1999. A study of polyimide thermoplastics used as tougheners in epoxy resins – structure and solubility relationships. *Thermochim. Acta.* 340(1):221.

82. Varley R.J., J.H. Hodgkin, D.G. Hawthorne, et al. 2000. Toughening of a trifunctional epoxy system. Part III. Kinetic and morphological study of the thermoplastic modified cure process. *Polymer*. 41:3425-3436.
83. Polymer blends / Eds. D.R. Paul, K.B. Bucknell. – Wiley. – 2000. Vol. 1. 608 p.
84. GOST 10587-84. Smoly epoksi-dianovyie neotverzhdonnyie. Tekhnicheskiye usloviya (GOST 10587-84. Uncured epoxy-diane resins. Specifications).
85. Gorbatkina Yu.A., V.G. Ivanova-Mumzhieva, and M.L. Kerber. 1997. Adhesion of polysulfone - liquid crystalline polymer blends to fibers. *Mech. Compos. Mater.* 33(4):303-309.
86. Gorbatkina Yu.A. 2004. Vliyanie modifikatorov na adgesionnyie svoistva polimernykh kompozitsii. Ch. 2. Epoksidianovyie oligomery. [Influence of modifiers on the adhesive properties of polymer compositions. Part 2. Epoxydian oligomers]. *Klei, germetiki,ologii*. 5:24-29.
87. Gorbatkina Yu.A., V.G. Ivanova-Mumjjeva, and O.V. Lebedeva. 2009. Adhesion of modified polymers to fibres: Maxima on adhesive strength-modifier amount curves and the causes of their appearance. *Int. J. Adhes. Adhes.* 29(1):9-17.
88. Shaposhnikova V.V., S.N. Salazkin, K.I. Donetskii, et al. 1999. Synthesis and properties of cardo poly(arylene ether ketones). *Polym. Sci. Ser. A* 41(2):124-131.
89. Shaposhnikova V.V., S.N. Salazkin, K.I. Donetskii, et al. 2002. Synthesis and properties of cardo copoly(arylene ether ketones). *Polym. Sci. Ser. A* 44(6):563-569.
90. Salazkin S.N., and K.I. Donetskii. 1998. Aromatichekise prostye poliefiry s bokovymi reaktsionnosposobnymi gruppami vo ftalimidinovykh tsiklakh [Aromatic polyethers with side reactive groups in phthalimidine rings]. *Doklady RAN* (Proceedings of the Academy of Sciences). 362(6):789-790.
91. Donetskii K.I., S.N. Salazkin, G.V. Gorshkov, and V.V. Shaposhnikova. 1996. Aromatichekise prostye poliefiry (gikiarilene-firsulfony i poliariilene-firketony), soderzhaschie bokovye karboksil'nye gruppy [Aromatic polyethers (polyarylene ether sulfones and polyarylene ether ketones) containing pendant carboxyl groups]. *Doklady RAN* (Proceedings of the Academy of Sciences). 350(2):213.
92. Volkov A.S., Yu.A. Gorbatkina, I.Yu. Gorbunova, et al. 2007. Effect of poly(arylene ether ketone)s of different chemical constructions on adhesion properties of an epoxyamine binder // *Polymer Science. Ser. A*. 49(5):559-564.

93. GOST 14922-77. Aerosil. Tekhnicheskiye usloviya (GOST 14922-77. Aerosil. Specifications).
94. Gorbatkina Yu.A., V.G. Ivanova-Mumzhieva, and T.M. Ul'yanova. 2006. Adgezionnaya sposobnost' epoksidianovogo oligomera, napolnennogo poroshkami oksida alyuminiya [Adhesion of epoxydian oligomer filled with aluminum oxide powders]. *Klei, germetiki, tekhnologii*. 11:18-23.
95. Gorbatkina Yu.A. 2008. O nekotorykh parametrokh, opredelyayuschikh prochnost' granitsy razdela v sistemakh polimer-volokno [Some parameters that determine the strength of the interface in polymer-fiber systems] *Klei, germetiki, tekhnologii*. 10:17-19.
96. TU 38 10001-94. Elektroprovodnyy tekhnicheskiy uglerod UM-66 (U 38 10001-Conductive carbon black UM-66).
97. TU 38 10002-94 Elektroprovodnyy tekhnicheskiy uglerod UM-76 (TU 38 10002-Conductive carbon black UM-76).
98. Khmelyov V.N., G.V. Leonov, R.V. Barsukov, et al. 2007. Ul'trazvukovye mnogofunktsional'nye i spetsilizirovannye apparaty dlya intensivatsii tekhnologicheskikh protsessov v promyshlennosti, sel'skom i domashnem khozyaistve [Ultrasonic multifunctional and specialized devices for the intensification of technological processes in industry]. *Barnaul: AltSTU*. 416 P.
99. Budylin N.Yu., A.V. Shapagin, and A.E. Chalykh. 2012. Sravnitel'nye issledovaniya vzaimodiffuzii i fazovykh sostoyanii v smesakh epoksidnykh oligomerov s polisulfonami i poliefirsul'fonami [Comparative studies of interdiffusion and phase states in mixtures of epoxy oligomers with polysulfones and polyethersulfones] *Digests of XIX All-Russia. Conf. "Structure and dynamics of molecular systems"*. Moscow: IPCE RAS. 2:192-195.
100. Perminov V.P., A.G. Modyanova, Yu.N. Ryabkov., et al. 2002. Modifikatsiya epoksidnogo kompozitsionnogo materiala nanodispersnyimi napolnitelyami [Modification of an epoxy composite material with nanodispersed fillers] *Zhurnal prikladnoi khimii (Journal of Applied Chemistry)*. 75(4):650-654.
101. Zelenkova-Myshkova M., Yu. Zelenka, V. Shpachek, and F. Socha. 2003. Svoistva epoksidnykh sistem s glinocoderzhaschimi nanokompozitami [Properties of epoxy systems with clay-containing nanocomposites] *Mekh. Kompozit. Mater.* 39(2):177-182.
102. Ganguli S., M. Bhuyan, and I. Allie. 2005. Effect of multi-walled carbon nanotube reinforcement on the fracture behavior of a tetrafunctional epoxy. *J. Mater. Sci.* 40:3593-3595.

103. Gauthier C., I. Chazeau, T. Prasse, et al. 2005. Reinforcement effects of vapor grown carbon nanofibers as fillers in rubbery matrices. *Compos. Sci. Technol.* 65:335-343.
104. Lau K.-T., C.-K. Lam, H.-Y. Cheung, et al. 2005. Thermal and mechanical properties of single-walled carbon nanotubes bundle-reinforced epoxy nanocomposites: the role of solvent for nanotube dispersion. *Compos. Sci. Technol.* 65:719-725.
105. Liu W., S.V. Hoa, and M. Pugh. 2005. Fracture toughness and water uptake of high performance epoxy/nanoclay nanocomposites. *Compos. Sci. Technol.* 65:2364-2373.
106. Fiedler B., F.H. Gojny, M.H.G. Wichmann, et al. 2006. Fundamental aspect of nano-reinforced composites. *Compos. Sci. Technol.* 66:3115-3125.
107. Wichmann M.H.G., J. Sumfleth, B. Fiedler, et al. 2006. Multiwall carbon nanotube/epoxy composites produced by a masterbatch process. *Mech. Compos. Mater.* 42:395-406.
108. Faulkner S.D., Y.W. Kwon, S. Bartlett, et al. 2009. Study of composite joint strength with carbon nanotube reinforcement. *J. Mater. Sci.* 44: 2858-2864.
109. Nikje M.M.A., A.B. Garmarudi, and M. Haghshenas. 2012. Nanosilica reinforced epoxy floor coating composites: Preparation and thermophysical characterization. *Curr. Chem. Lett.* 1:13-20.
110. Kheladze N.D., Yu.A. Gorbatkina, M.S. Batiashvili, et al. 1990. Issledovanie adgezii v sistemakh napolnennyi polyolefin-volokno [Study of adhesion in systems filled polyolefin – fiber]. *Mekh. Kompozit. Mater.* 2:343-346.
111. Gorbatkina Yu.A., V.G. Ivanova-Mumzhieva, A.B. Solov'yova, et al. 2001. Adgezionnyye svoistva polipropilena, napolnennogo shungitom [Shungite-filled polypropylene adhesion properties]. *Russ. J. Phys. Chem.* 75(12):2027-2031.
112. Gorbatkina Yu.A., T.Yu. Zakharova, V.G. Ivanova-Mumzhieva, and V.I. Solodilov. 2005. Regulirovanie adgezionnykh svoistv epoksidnogo oligomera shungitovym napolnitelem [Regulation of adhesion properties of epoxy oligomer with shungite filler]. *Klei, germetiki, tekhnologii.* 4:10-13.
113. Gorbatkina Yu.A., V.G. Ivanova-Mumzhieva, A.S. Putyatina, et al. 2007. Interfacial strength of joints between fibers and dispersedly filled epoxy matrices. *Mech. Compos. Mater.* 43(1):1-8.
114. Ul'yanova T.M., N.P. Krut'ko, P.A. Vityaz', et al. 2004. Osobennosti formirovaniya struktury tugoplavkikh soedinenii na osnove ZrO<sub>2</sub>, Al<sub>2</sub>O<sub>3</sub> [Features of the formation of the structure of refractory

- compounds based on  $ZrO_2$ ,  $Al_2O_3$ . *Dokl. NAN Belarusi (Reports of the NAS of Belarus)*. 48: 103-108.
115. Ul'yanova T.M., N.P. Krut'ko, L.V. Titova, et al. 2005. Volokna tugoplavkikh oksidov: poluchenie, svoistva, primenenie [Refractory oxide fibers: preparation, properties, application]. *Khim. Volokna*. 5:16-20.
  116. Gorbatkina Yu.A., and V.G. Ivanova-Mumzhieva. 2008. Adgezionnaya sposobnost' sazhenapolnennykh epoksidov [Adhesion of soot-filled epoxies]. *Klei, germetiki, tekhnologii*. 11:2-5.
  117. Gorbatkina Yu.A., and V.G. Ivanova-Mumzhieva. 2012. Adhesion of dispersedly filled epoxides to solids. *Mech. Composite Materials*. 48(2): 161-170.
  118. Shungity – novoye uglerodistoye syr'yo. 1984. Pod red. YU.K. Kalinina. Petrozavodsk: Kareliya. (Shungite – a new carbonaceous raw material. Ed. Yu.K. Kalinin. Petrozavodsk: Karelia). 182 p.
  119. Kalinin Yu.K. 1990. Shungitovye porody: struktura, svoistva i oblasti prakticheskogo ispol'zovaniya [Shungite rocks: structure, properties and areas of practical use]. *Zapiski Vsesoyuznogo mineralogicheskogo obshchestva*. 119(5):1-8. (Kalinin Yu.K. Notes of the All-Union Mineralogical Society). 119(5):1-8.
  120. Buseck P.R., I.P. Goldobina, V.V. Kovalevski, et al. 1997. Shungits: The C-rich rocks of Karelia, Russia. *Can. Mineral*. 35(6):P. 1363-1378.
  121. Gojny F.H., M.H.G. Wichmann, U. Köpke, et al. 2004. Carbon nanotube reinforced epoxy-composites – enhanced stiffness and fracture toughness at low nanotube contents. *Compos. Sci. Technol*. 64:2363-2371.
  122. Rebinder P.A. 1959. Poverkhnostno-aktivnye veschestva [Surfactants]. *Zhurnal Vsesoyuznogo khimicheskogo obshchestva im. D.I. Mendeleeva*. 4(5):554-565.
  123. Michael J. 1975. Industrial applications of surface activity of polydimethylsiloxanes. *Brit. Polym. J.* 7:235-245.
  124. Hare E.F., E.G. Shafrin, and W.A. Zisman. 1954. Properties of films of adsorbed fluorinated acids. *J. Phys. Chem.* 58:236-239.
  125. Pittman A.G. 1972. Surface properties of fluorocarbon polymers. *Fluoropolymers*. Ed. L.A. Wall. – New York, NY, USA: John Wiley & Sons, Inc. P. 419-449.
  126. Poverkhnostno-aktivnyye veshchestva. Spravochnik. [Surfactants. Reference book]. Leningrad: Khimiya. 1979. P. 258.
  127. Bekhli L.S., Yu.A. Gorbatkina, V.G. Ivanova-Mumzhieva, and Lyapunov A.Ya. 2007. Fluorine-containing compounds improving

- adhesion of epoxy oligomers to materials with low surface energy. *Polymer Sci. Ser. C.* 49(3):264-268.
128. Rebinder method (method for determining the maximum pressure in a bubble). 1984. <http://fizportal.ru/>. Surface phenomena and surfactants. Reference book Eds. A.A. Abramzon and E.D. Shchukin. Publishing house "Chemistry", L-d, P. 168.
  129. Malkin A.Ya., and A.E. Chalykh. 1979. Diffuziya i vyazkost' polimerov. Metody izmereniya. [Diffusion and viscosity of polymers. Measurement methods]. M., Chemistry, 1979, 281 p.
  130. Shramm G. 2003. Osnovy prakticheskoi reologii i reometrii. [Fundamentals of Practical Rheology and Rheometry]. M.: KolosS, 312 p.
  131. Malkin A.Ya., and A.I. Isaev. 2009. Reologiya. Kontseptsii, metody, prilozheniya. [Rheology. Concepts, methods, applications].– Spb. – Profession. 560 p.
  132. Sanzharovskii A.T., and G.I. Epifanov. 1960. Vnutrenie napryazheniya d pokrytiyakh. [Internal stresses in coatings]. *Vysokomolek. Soedin.* 2(11):1703-1708.
  133. Gorbatkina Yu.A., I.Yu. Gorbunova, V.G. Ivanova-Mumzhieva, et al. 2014. Adgezionnye svoistva kompozitsii na osnove epoksidnoi smoly, modifitsirovannoi poliefirimidom ili polisulfonom. [Adhesion properties of compositions based on epoxy resin modified with polyetherimide or polysulfone]. *Mekhanika kompozitsionnykh materialov i konstruksii* (Mechanics of composite materials and structure). 20(2):207-218.
  134. Gorbatkina Yu.A., I.Yu. Gorbunova, M.L. Kerber, and M.V. Shustov. 2005. Changes in the adhesion properties of epoxy-polysulfone mixtures during the curing process. *Polym. Sci. Ser.A.* 47(7):716-722.
  135. Gorbatkina Yu.A., I.Yu. Gorbunova, and M.L. Kerber. 2011. Change of adhesion properties of epoxide oligomer modified by polyarylene ether ketone in the process of hardening. *Polym. Sci. Ser. D.* 4(2):95-101.
  136. Wisanrakkit G., and J.K. Gillham. 1990. The glass transition temperature ( $T_g$ ) as an index of chemical conversion for a high- $T_g$  amine/epoxysystems: Chemical and diffusion-controlled reaction kinetics. *J. Coating Technology.* 62(783):35-50.
  137. Wisanrakkit G., and J.K. Gillham. 1990. Continuous heating transformation (CHT) cure diagram of an aromatic amine/epoxy system at constant heating rates. *Am. Chem. Soc. Polym. Prepr.* 31(1):293-295.

138. Wang X., and J.K. Gillham. 1992. Analysis of crosslinking in amine-cured epoxy systems: The one-to-one relationship between  $T_g$  and conversion. *J. Appl. Polym. Sci.* 46(10): 2127-2143.
139. Gorbunova I.Yu., M.V. Shustov, and M.L. Kerber. 2003. Vliyanie termoplastichnykh modifikatorov na svoistva i protsess otverzhdeniya epoksidnykh polimerov [The influence of thermoplastic modifiers on the properties and curing process of epoxy polymers]. *Inzhenerno-fizicheskiy zhurnal.* 76(3):84-87.
140. Gorbatkina Yu.A., V.G. Ivanova-Mumzhieva, and A.Ya. Gorenberg. 1999. Adgezionnaya prochnost' soedinenii polimerov s uglerodnymi voloknami pri razlichnykh skorostyakh nagruzheniya [Adhesion strength of polymer-carbon fiber bonds at different loading rates]. *Khim. volokna.* 5:54-57.
141. Gorbatkina Yu.A., V.I. Solodilov. 2003. Vliyanie skorosti nagruzheniya i kontsentratsii aktivnogo razbavatelya na prochnost' epoksidnykh kompozitov i model'nykh adgezionnykh soedinenii [Influence of loading rate and active diluent concentration on the strength of epoxy composites and model adhesive joints]. *Inzhenerno-fizicheskiy zhurnal.* 76(3):106-111.
142. Brantseva T.V. 2003. Adgezionnoe vzaimodeistvie v sisteme modifitsirovannaya epoksidnaya matritsa/volokno pri razlichnykh rezhimakh nagruzheniya [Adhesion interaction in the modified epoxy matrix/fiber system under various loading conditions]. Diss ... Cand. Chem. Sci. – Moscow.
143. Regel' V.R., A.I. Slutsker, and E.E. Tomashevskii. 1974. *Kineticheskaya priroda prochnosti tverdykh tel* [The kinetic nature of the strength of solids]. Moscow: Nauka. 560 p.
144. Gorbatkina J.A., and N.K. Shaidurova. 1991. The effect of aging in water on the strength of fiber-polymer systems. *J. Adhesion.* 35:203-215.
145. Novikova O.A., and V.P. Sergeev. 1989. Modifikatsiya poverkhnosti armiruyuschikh volokon v kompozitsionnykh materialakh [Modification of the surface of reinforcing fibers in composite materials]. Kiev: Naukova Dumka. 217 p.
146. Manevich L.I., and A.V. Pavlenko. 1982. Ob uchete strukturnoi neodnorodnosti kompozita pri otsenke adgezionnoi prochnosti [Taking into account the structural heterogeneity of the composite when assessing the adhesive strength]. *Zhurnal prikladnoy mekhaniki i tekhnicheskoy fiziki (Journal of Applied Mechanics and Technical Physics).* 3(133): 140-145.



147. McKague E.L., J.D. Reynolds, and J.E. Halkais. 1978. Swelling and glass transition relations for epoxy matrix material in humid environments. *J. Appl. Polym. Sci.* 22:1643.
148. Morgan R.J., J.E. O'Neal, and D.I. Fanter. 1980. The effect of moisture on the physical and mechanical integrity of epoxies. *J. Mater. Sci.* 15:751.
149. Startseva L.T., and I.I. Perepechko. 1984. Vyazkoupругie svoystva I struktura sistemy polimernyi kompozit-voda [Viscoelastic properties and structure of the polymer composite-water system]. *Mekh. Kompozit. Mater.* 1:145-148.
150. Kulik T.A., and A.F. Pryadko. 1985. Mekhanizm vliyaniya vody na svoystva epoksipolimerov [The mechanism of the effect of water on the properties of epoxy polymers]. *Plast. Massy.* 11:29-31.
151. Aminabhavi T.M. 1988. Liquid diffusion into epoxy resin composites. *J. Appl. Polym. Sci.* 35:1251-1256.
152. Brewis D.M., J. Comyn, A.C. Moloney, et al. 1981. The use of isotopically labeled water to monitor the ingress of water into adhesive joints. *Eur. Polym. J.* 17(2):127-130.
153. Rebinder P.A. 1973. *Uspekhi kolloidnoi khimii* [Advances in colloidal chemistry]. M.: Nauka. 362 p.
154. Rebinder P.A. 1979. *Poverkhnostnye yavleniya v dispersnykh sistemakh. Fiziko-khimiicheskaya mekhanika* [Surface phenomena in dispersed systems. Physicochemical mechanics]. M.: Nauka. 381 p.
155. Gorbatkina Yu.A., V.G. Ivanova-Mumzhieva, L.V. Puchkov, et al. 1995. Prochnost' soedinenii polimer-tvyerdoe telo pri ispytaniyakh v zhidkosti [Strength of polymer-solid joints when tested in liquid]. *Mechanics of composite materials and structure.* 1(1):116-124.
156. Gorbatkina Yu.A., V.G. Ivanova-Mumzhieva, L.V. Puchkov, et al. 1996. Vliyanie okruzhayushey zhidkosti na prochnost' granitsy razdela polimer-volokno [Influence of the surrounding liquid on the strength of the polymer-fiber interface]. *Dokl. RAN.* 347(4):486-488.
157. Gorbatkina Yu.A., and V.G. Ivanova-Mumzhieva. 1997. Adhesive strength of fiber/polymer joints upon loading in liquids: Effect of liquid surface tension. *Int. J. Adhes. Adhes.* 17(4):329-332.
158. Gorbatkina Yu.A. 1994. Study of adhesion between thermoplastics and fibers. *Adhesion science and technology. Adhesion Symposium (International). Proceedings.* Ed.H. Mizumachi. Gordon and Breach Science Publs. P. 589-606.
159. Gorbatkina Yu.A., V.G. Ivanova-Mumzhieva, and G.S. Shul'. 1995. Adgeziya termoplastichnykh matriks k uglerodnym voloknam

- [Adhesion of thermoplastic matrices to carbon fibers]. *Khim. Volokna*. 4:33-37.
160. Favre J.P., and J. Perrin. 1972. Carbon fibre adhesion to organic matrices. *J. Mater. Sci.* 7(10):1113-1118.
  161. Sabramanian R.V., T.J.Y. Wang, and H.E. Austin. 1977. Reinforcement of polymers by basalt fibers. *SAMPE Quart.* 2:1-10.
  162. Sabramanian R.V., J.J. Jakubowski, and F.D. Williams. 1978. Interfacial aspects of polymer coating by electropolymerization. *J. Adhesion.* 9:185-195.
  163. Piggott M.R. 1980. *Load-bearing fibre composites*. – Oxford, England: Pergamon Press. 277 p.
  164. Drzal L.T., M.J. Rich, and P.F. Lloyd. 1983. Adhesion of graphite fibers to epoxy matrix: 1. The role of fiber surface treatment. *J. Adhesion.* 16(1): 1-30.
  165. Narkis M., E.J.H. Chen, and R.B. Pipes. 1988. Review of methods for characterization of interfacial fiber-matrix polymer composites. *Polym.Composites.* 9(4):254-261.
  166. Hampe A., Y. Boro, and K. Schumacher. 1990. Bestimmung der haftung zwischenfaser und matrix. *Forsch. Aktuell.* 27-29:21-23.
  167. Miller B., U. Gaur, and D.E. Hirt. 1991. Measurement and mechanical aspects of the microbond pull-out technique for obtaining fiber/resin interfacial shear strength. *Compos. Sci. Technol.* 42(3):207-219.
  168. Rao V., P.J. Herrera-Franco, A.D. Ozzello, and L.T. Drzal. 1991. A direct comparison of the fragmentation test and the microbond pull-out test for determining the interfacial shear strength. *J. Adhesion.* 34(1):65-77.
  169. Herrera-Franco P.J., and L.T. Drzal. 1992. Comparison of methods for the measurement of fibre/matrix adhesion in composites. *Composites.* 23(6):2-27.
  170. Chua P.S., S.R. Dai, and M.R. Piggott. 1992. The glass fibre-polymer interface. II. Work of fracture and shear stresses. *J. Mater. Sci.* 27:913-918.
  171. Pisanova E.V., S.F. Zhandarov, and V.A. Dovgyalo. 1993. Adhesive strength in thermoplastic polymer – thin fiber systems. Measured value as a function of the testing method. *Mech. Compos. Mater.* 29(2):175-180.
  172. Gorbatkina Yu.A., V.G. Ivanova-Mumzhieva, and G.S. Shul'. 1995. Adhesion of thermoplastic matrices to carbon fibers. *Fibre Chem.* 27(4): 259-263.

173. Pisanova E.V., and S.F. Zhandarov. 1997. On the mechanism of failure in microcomposites consisting of single glass fibres in a thermoplastic matrix. *Compos. Sci. Technol.* 57(11):937-943.
174. Zhandarov S.F., and E.V. Pisanova. 1997. The local bond strength and its determination by fragmentation and pull-out tests. *Compos. Sci. Technol.* 57(11):957-964.
175. Shul' G.S., Yu.A. Gorbatkina, and G.P. Mashinskaya. 1998. Effect of chemical nature of matrix on the strength of bonds with Armos aramid fibers. *Mech. Compos. Mater.* 34(3):285-294.
176. Duschk V., E. Pisanova, S. Zhandarov, et al. 1998. "Fundamental" and "practical" adhesion in polymer-fiber systems. *Mech. Compos. Mater.* 34(6):309-320.
177. Zhandarov S., E. Pisanova, E. Mäder, et al. 2000. Investigation of load transfer between the fiber and the matrix in pull-out tests with fibers having different diameters. *J. Adhes. Sci. Technol.* 15:205-222.
178. Zhandarov S., and E. Mäder. 2005. Characterization of fiber/matrix interface strength: Applicability of different tests, approaches and parameters. *Compos. Sci. Technol.* 65:149-160.
179. Ohsava T., A. Nakayama, M. Miwa, et al. 1978. Temperature dependence of critical fiber length for glass fiber-reinforced thermosetting resins. *J. Appl. Polym. Sci.* 22(11):3202-3212.
180. Drzal L.T., M.J. Rich, J.D. Camping, et al. 1982. Interfacial shear strength and failure mechanisms in graphite fiber composites. *35<sup>th</sup> Annual Technical Conference on Reinforced Plastics /Composites Proceedings*. Paper No. 20C.
181. Drzal L.T., M.J. Rich, M.F. Koenig, et al. 1983. Adhesion of graphite fibers to epoxy matrices. II. Effect of fiber finish. *J. Adhesion.* 16(2):133-152.
182. Narisawa N., and H. Oba. 1984. An evolution of acoustic emission from fibre-reinforced composites. *J. Mater. Sci.* 19(11):1777-1786.
183. Di Benedetto A.T. 1985. Evolution of fiber surface treatments in composite materials. *Pure Appl. Chem.* 57(11):1659-1666.
184. Drzal L.T., M.J. Rich, and M.F. Koenig. 1985. Adhesion of graphite fibers to epoxy matrices. III. The effect of hydrothermal exposure. *J. Adhesion.* 18(1):49-72.
185. Clarke D.A., and M.G. Bader. 1986. Direct observation of fibre fracture in a model composite. *J. Mater. Sci. Lett.* 5(9):903-904.
186. Baskom W.D., and R.M. Jensen. 1986. Stress transfer in single fiber/resin tensile test. *J. Adhesion.* 19(3-4):219-226.
187. Di Benedetto A.T., L. Nicolais, L. Ambrosio, et al. 1986. Stress transfer and fracture in single fiber/epoxy composites. *First*

- Conference (International) on Composite Interfaces Proceedings (ICCI-1)*, New York, NY. – USA. P. 47-54.
188. Di Landro L., and M. Pegorato. 1987. Carbon fibre-thermoplastic matrix adhesion. *J. Mater. Sci.* 22:1980-1986.
  189. Baskom W.D., R.M. Jensen, and L.W. Corder. 1987. The adhesion of carbon fibers to thermoplastic polymers. *6th Conference (International) on Composite Materials combined 2nd European Conference on Composite Materials Proceedings.* – London – New York. 5:424-438.
  190. Jacques D., and J.P. Favre. 1987. Determination of the interfacial shear strength by fibre fragmentation in resin systems with a small rupture strain. *6th Conference (International) on Composite Materials combined 2nd European Conference on Composite Materials Proceedings.* – London – New York. 5:471-480.
  191. Crasto A.S., S.H. Own, and R.V. Subramanian. 1988. The influence of the interphase on composite properties: Poly(ethylene-co-acrylic acid) and poly(methyl vinyl ether-co-maleic anhydride) electrodeposited on graphite fibers. *J. Polym. Composite.* 9(1):78-82.
  192. Di Landro L., A.T. Di Benedetto, and J. Groeger. 1988. The effect of fiber-matrix stress transfer on the strength of fiber-reinforced composite materials. *J. Polym. Composite.* 9(3):209.
  193. Di Landro L., and M. Pegorato. 1988. Interfacial adhesion between carbon fibers and PEEK thermoplastic matrix. *Chim. Ind. (Ital).* 70(6):86-89.
  194. Folkes M.J., W.K. Wong, and R.W. Ward. 1988. Determination of interfacial bond strength in fibre thermoplastic composites. *Physics Conference (International) Proceeding.* – Bristol, PA, USA. P. 111-116.
  195. Jacques D., and J.P. Favre. 1988. Modelisation statistique du processus defragmentation dans les composites modeles a monofilament. *Comptes Rendusdes Journees Nationales sur les Composites Proceedings.* Paris. P.169-182.
  196. Rouby D. 1988. Application de l'emissionacoustique a la caracterisation micromecanique de l'interface fibre-matrice. *Comptes Rendus des Journees Nationales sur les Composites Proceedings.* Paris. P. 183-194.
  197. Asloun E.M., M. Nardin, and J. Schultz. 1989. Stress transfer in single-fibre composites: Effect of adhesion, elastic modulus of fibre and matrix and polymer chain mobility. *J. Mater. Sci.* 24(3):1835-1844.

198. Wagner H.D., and L.W. Steenbakkers. 1989. Microdamage analysis of fibrous composite microlayers under tensile stress. *Mater. Sci.* 24:3956-3975.
199. Wimolkiatisak A.S., and J.P. Bell. 1989. Interfacial shear strength and failure modes of interfase-modified graphite/epoxy composites. *Polym. Composite.* 10(3):162-172.
200. Netravali A.N., R.B. Henstenburg, S.L. Phoenix, et al. 1989. Interfacial shear strength studies using the single-filament-composite test. I. Experiments on graphite fibers in epoxy. *Polym. Composite.* 10(4):226-241.
201. Netravali A.N., P. Schwartz, and S.L. Phoenix. 1989. Study of interfaces of high performance glass fibres and DGEBA based epoxy resins using single-fibre composite test. *Polym. Composite.* 10(6):385-388.
202. Yavin B., H.E. Gallis, J. Scherif, et al. 1991. Continuous monitoring of the fragmentation phenomenon in single fiber composite materials. *Polym. Composite.* 12(6):436-446.
203. Tamuzh V.P., Y.G. Korabel'nikov, I.A. Rashkovan, et al. 1992. Determination of the scale dependence of strength of fibrous fillers and evaluation of their adhesion to the matrix based on results of tests of elementary fibers in a polymer block. *Mech. Compos. Mater.* 27(4):413-418.
204. Favre J.-P., P. Sigety, and D. Jacques. 1991. Stress transfer by shear in carbon fibre model composites. Pt. II: Computer simulation of the fragmentation test. *J. Mater. Sci.* 26:189-195.
205. Zhandarov S.F., E.V. Pisanova, and V.A. Dovgyalo. 1992. Fragmentation of a single filament during tension in a matrix as a method of determining adhesion. *Mech. Compos. Mater.* 28(3):270-286.
206. Feillard P., G. Desarmot, and J.P. Favre. 1993. A critical assessment of the fragmentation test for glass/epoxy systems. *Compos. Sci. Technol.* 49: 109-119.
207. Gorbatkina Yu.A., Yu.G. Korabel'nikov, V.P. Tamuzh, et al. 1994. Some characteristics of the use of acoustic emission method in the study of the fragmentation of single fibers in a polymer matrix. *Mech. Compos. Mater.* 29(6):540-545.
208. Cho K., T. Kong, and D. Lee. 1997. Interfacial adhesion strength between fibers of liquid crystalline polymer and thermoplastic matrix. *Polymer J.* 29(1):904-909.

209. Zhandarov S.F., and E.V. Pisanova. 1996. Two interfacial shear strength calculations on the single fiber composite test. *Mech. Compos. Mater.* 31(4):325-336.
210. Mandeli J.F., D.H. Grande, T.-H. Tsiang, and F.G. McGarry. 1986. Microbonding test for direct in situ fiber/matrix bond strength determination in fiber composites. *7th Conference on Composite Materials: Testing and Design Proceedings*. Philadelphia, PA, USA. P. 87-107.
211. Cox H.I. 1952. The elasticity and strength of paper and other fibrous materials. *Brit. J. Appl. Phys.* 3:72-85.
212. Kelly A., and N.H. Macmillan. 1986. *Strong Solids*. 3-rd ed. Oxford: Clarendon Press. 437 p.
213. Freidin A.S., and R.A. Turusov. 1990. *Svoistva i passchyot adgezionnykh soedinenii* [The properties and calculation of adhesive joints]. Moscow: Khimiya. 256 p.
214. Turusov R.A. 2016. *Adgezionnaya mekhanika* [Adhesive mechanics]. Moscow: NRU MGSSU. 232 p.
215. Gorenberg A.Ya. 2008. *Issledovanie deformatsii i razrusheniya polimernykh matrits, volokon i kompozitov elektronno-mikroskopicheskimi metodami* [Investigation of deformation and destruction of polymer matrices, fibers and composites by electron microscopic methods]. Dissertation for the degree of candidate of physical and mathematical sciences. 149 p.
216. Gorbatkina Yu.A., A.Ya. Gorenberg, D.A. Gorenberg, and V.G. Ivanova-Mumzhieva. 2009. Pryamoe nablyudenie razrusheniya poverkhnosti kontakta volokno-matritsa [Direct observation of fiber/matrix interface failure]. *Proceedings of the conference "Modern problems of chemical and radiation physics"*, Moscow – Chernogolovka. P. 364-367.
217. Gorenberg A.Ya, Yu.A. Gorbatkina, and V.G. Ivanova-Mumzhieva. 2021. An Electronic Microscopy Study of the Destruction of Polymer-Fiber Adhesion Compounds. *Polymer Sci. Ser.D.* 14(3):370-375.
218. Gorbatkina Yu.A., and V.G. Ivanova-Mumjjeva. 2001. Variance of adhesive strength and fracture mechanism of fibre/matrix joints. *Int. J. Adhes. Adhes.* 21(1):41-48.
219. Gorbatkina Yu.A., and V.G. Ivanova-Mumjjeva. 2000. Analysis of the adhesive strength variance in epoxy matrix-boron fiber joints. *Mech. Compos. Mater.* 36(4):255-260.
220. Van-der-Waerden B.L. 1957. *Mathematische statistik*. – Berlin: Springer. 369 p.

221. Smirnov N., and I. Dunin-Barkowski. 1961. *Mathematische statistik in der Technik*. Berlin. Verlag Technik.
222. Smirnov N.V., and I.V. Dunin-Barkowski. 1969. *Kurs teorii veroyatnostei i matematicheskoi statistiki dlya tekhnicheskikh prilozhenii* [Course in Probability Theory and Mathematical Statistics for Technical Applications]. Moscow:Nauka. 512 p.
223. McGarry F.I. 1959. Resin-glass bond characteristics. *ASTM Bull.* 235:63-68.
224. Shiryaeva G.V., and G.D. Andreevskaya. 1962. Metod opredeleniya adgezii smol k poverhknosti steklyannogo volokna [Method for determining the adhesion of resins to a glass fiber surface]. *Plast. Massy.* 4:42-43.
225. Andreevskaya G.D., G.V. Shiryaeva, and V.G. Ivanova-Mumzhieva. 1963. Vliyanie obrabotki steklyannykh volokon appreturami na adgeziyu epoksidno-fenol'noi smoly [Effect of processing glass fibers with finishing agents on the adhesion of epoxy-phenolic resin]. *Vysokomolek. Soedin., sb. «Adgeziya polimerov»* [Adhesion of Polymers]. P. 99-102.
226. Andreevskaya G.D., G.V. Shiryaeva, and A.M. Il'inskii. 1964. Obraztzy dlya massovogo ispytaniya pri opredelenii adgezii polimerov [ Samples for mass testing in determining the adhesion of polymers]. *Standartizatsiya.* 11:13-16.
227. Gorbatkina Yu.A., V.G. Ivanova-Mumzhieva, A.M. Kuperman, et al. 2008. Adhesive ability of heat-resistant double-chain polymer and strength of CFRP based on it. *Mech. Compos. Mater.* 44(4):371-378.
228. Gorbatkina Yu.A., V.G. Ivanova-Mumzhieva, A.M. Kuperman, et al. 2010. Effect of thermal aging on the adhesive strength of joints of double-chain polymers with fibers and on the properties of unidirectional CFRPs based on them. *Mech. Compos. Mater.* 46(1):69-76.

## AUTHORS PREVIOUS PUBLICATIONS

### Gorbatkina Yulia Arkadievna

1. Gorbatkina Yu.A. 1992. *Adhesive strength of fibre-polymer systems*. N.Y., London: Ellis Horwood. 264 p.
2. Gorbatkina Yu.A. 1987. *Adgezionnaya prochnost' v sistemakh polimer-volokno* [Adhesive strength of fibre-polymer systems]. Moscow: Khimiya. 192 p. (in Russian).
3. Gorbatkina Yu.A., and V.G. Ivanova-Mumzhieva. 2018. *Adgeziya modifitsirovannykh epoksidov k voloknam* [Adhesion of modified epoxides to fibers]. Moscow: TORUS PRESS. 216 p.
4. Gorbatkina J.A., and N.K. Shaidurova. 1991. The effect of aging in water on the strength of fiber-polymer systems. *J. Adhesion*. 35:203-215.
5. Gorbatkina Yu.A. 1994. Study of adhesion between thermoplastics and fibers. *Adhesion science and technology. Adhesion Symposium (International). Proceedings* / Ed. H. Mizumachi. Gordon and Breach Science Publs. :589-606.
6. Gorbatkina Yu.A. 2000. Correlation between the strength of fiber-reinforced plastics and the adhesive strength of fiber-matrix joints. *Mechanics of composite materials*. 36(3):169-176.
7. Chalykh A.E., V.K. Gerasimov, Yu.A. Gorbatkina, et al. 2003. Compatibility and phase structure evolution in polysulfone-curable epoxy oligomers blends. *Polym. Sci.* 45(7):676-685.
8. Gorbatkina Yu.A., I.Yu. Gorbunova, M.L. Kerber, et al. 2005. Changes in the adhesion properties of epoxy-polysulfone mixtures during the curing process. *Polym. Sci. Ser. A*. 47(7):716-722.
9. Volkov A.S., Yu.A. Gorbatkina, I.Yu. Gorbunova, et al. 2007. Effect of poly(arylene ether ketone)s of different chemical constructions on adhesion properties of epoxyamine binder. *Polym. Sci. Ser. A*. 49(5):559-564.
10. Gorbatkina Yu.A., V.G. Ivanova-Mumzhieva, A.M. Kuperman, et al. 2010. Effect of thermal aging of the adhesive strength of joints of double-chain polymer with fibers and the unidirectional CFRPs based on them. *Mech. Composite Materials*. 46(1):69-76.



11. Gorbatkina Yu.A., I.Yu. Gorbunova, and M.L. Kerber. 2011. Change of adhesion properties of epoxide oligomer modified by polyarylene ether ketone in the process of hardening. *Polym. Sci. Ser. D.* 4(2):95-101.
12. Gorenberg A.Y., Y.A. Gorbatkina, and V.G. Ivanova-Mumzhieva. 2021. An Electron Microscopy Study of the Kinetics of the Destruction of Polymer–Fiber Adhesion Joints. *Polym. Sci. Ser. D.* 14(3):370–375.

### **Ivanova-Mumzhieva Viktoria Georgievna**

1. Gorbatkina Yu.A., and V.G. Ivanova-Mumzhieva. 2018. *Adgeziya modifitsirovannykh epoksidov k voloknam* [Adhesion of modified epoxides to fibers]. Moscow: TORUS PRESS. 216 p.
2. Gorbatkina Yu.A., V.G. Ivanova-Mumzhieva, and G.S. Shul'. 1995. Adhesion of thermoplastic matrices to carbon fibers. *Fibre Chem.* 27(4): 259-263.
3. Ivanova-Mumzhieva V.G., Yu.A. Gorbatkina, G.S. Shul', et al. 1995. Adhesive strength of bonds between aramide and polybenzothiazole fibers and thermoset matrices. *Mech. Composite Materials.* 31(2):103-108.
4. Gorbatkina Yu.A., and V.G. Ivanova-Mumzhieva. 1997. Adhesive strength of fibre/polymer joints upon loading in liquids: Effect of liquid surface tension. *Int. J. Adhes. Adhes.* 17(4):329-332.
5. Gorbatkina Yu.A., and V.G. Ivanova-Mumzhieva. 2001. Variance of adhesive strength and fracture mechanism of fibre/matrix joints. *Int. J. Adhes. Adhes.* 21(1):41-48.
6. Gorbatkina Yu.A., V.G. Ivanova-Mumzhieva, A.S. Putyatina, et al. 2007. Interfacial strength of joints between fibers and dispersedly filled epoxy binders. *Mech. Composite Materials.* 43(1):1-8.
7. Gorbatkina Yu.A., V.G. Ivanova-Mumzhieva, A.M. Kuperman, et al. 2008. Adhesive ability of heat-resistant double-chain polymer and strength of CFRP based on it. *Mech. Composite Materials.* 44(4):371-378.
8. Gorbatkina Yu.A., V.G. Ivanova-Mumzhieva, and O.V. Lebedeva. 2009. Adhesion of modified polymers to fibres: Maxima on adhesive strength-modifier amount curves and the causes of their appearance. *Int. J. Adhes. Adhes.* 29(1):9-17.
9. Gorbatkina Yu.A., and V.G. Ivanova-Mumzhieva. 2009. Adhesion of Polymers to Fibers: Further Elaboration of Pull-Out Method. *Polym. Sci. Ser. D.* 2(4):214-216.

10. Gorbatkina Yu.A., and V.G. Ivanova-Mumzhieva. 2012. Adhesion of dispersedly filled epoxides to solids. *Mech. Composite Materials*. 48(2): 161-170.
11. Gorbatkina Yu.A., V.G. Ivanova-Mumzhieva, and V.I. Solodilov. 2019. The influence of multiple curing on the strength of fiber-matrix interface. *Polym. Sci. Ser. D*. 12(2):133-136.